DISSERTATION

CANDIDATE GENE IDENTIFICATION FOR GLYPHOSATE RESISTANCE AND RAPID CELL DEATH IN *AMBROSIA TRIFIDA*

Submitted by

Crystal Devona Sparks

Department of Agricultural Biology

In partial fulfillment of the requirements

For the Degree of Doctor of Philosophy

Colorado State University

Fort Collins, Colorado

Spring 2024

Doctoral Committee:

Advisor: Todd Gaines

Franck Dayan
Roland Beffa
Marc Nishimura
Phil Westra

ABSTRACT

CANDIDATE GENE IDENTIFICATION FOR GLYPHOSATE RESISTANCE AND RAPID CELL DEATH IN *AMBROSIA TRIFIDA*

Glyphosate is one of the most widely used herbicides worldwide due to favorable chemical characteristics and availability of compatible transgenic biotechnology in crops. Resistance to glyphosate has evolved in many weed species capable of significant yield reduction in top production systems globally. One such species is *Ambrosia trifida* (giant ragweed), a monoecious broadleaf with imperfect flowers native to North America where it is highly competitive in corn, soybean, and cotton production. Some glyphosate resistant populations of *A. trifida* also display a rapid response with cell death in the mature leaves within 24-48 hours after treatment with glyphosate. Transcriptomic analysis revealed differential expression of multiple gene families associated with known glyphosate resistance mechanisms such as ATP-binding cassette (ABC) transporters and aldo-keto reductases. Gene ontology analysis showed an enrichment of many genes related to phytohormone response to biotic and abiotic stress in the differentially expressed genes. This could be related to a novel glyphosate resistance mechanism or a signaling cascade involved in the rapid cell death response. The *A. trifida* genome contains two loci of the glyphosate target site gene 5-enolpyruvylshikimate-3-phosphate-synthase (*EPSPS*), with a previously reported Pro106Ser mutation in *EPSPS2*. This locus showed up-regulation by three hours after treatment. Trait mapping revealed three genomic regions associated with glyphosate resistance and a single interval associated with the

rapid response. Along with phenotypic segregation ratios, this indicates that resistance and rapid response traits are genetically independent and multiple genes likely contribute to resistance.

ACKNOWLEDGEMENTS

My deepest gratitude goes to everyone who believed in me enough to provide the opportunities and support that have allowed me to explore my potential and develop as a scientist and human being. Starting with instructors at AIMS community college who continuously encouraged me to raise the bar of my academic career goals. I would especially like to thank Eric Patterson for introducing me to the CSU weed lab and to molecular biology, and for his guidance and encouragement that set the foundation of my academic experience.

To my advisor, Todd Gaines, I cannot express how thankful I am for your support which enabled my personal and scientific growth over the course of this program. While traversing a graduate degree is inevitably challenging, I am profoundly thankful for the privilege of having a highly knowledgeable, but more importantly empathetic mentor. I must also mention my gratitude to Franck Dayan for being a de facto co-advisor and source of wisdom and guidance over the past few years.

To my other committee members, I am forever thankful for your feedback, input, and your belief in me and the project. Roland Beffa, your high-level ideas, and suggestions inspired me to think about things differently and your thoughtful feedback and acknowledgement of my growth provided invaluable encouragement. To Marc Nishimura, thank you for believing in the project enough to dedicate your time and provide a viewpoint from outside of the weed science sphere. To Phil Westra, your career speaks for your impact on all the work we do in the CSU weed lab and on the field of weed science, thank you for your enthusiasm which inspires us to pursue knowledge that will drive our work to have a vast impact on agriculture.

To Bayer CropScience, thank you for providing financial support and intellectual feedback for the project. Your input made this work possible and provided me a perspective at the interface of industry and academia.

To my dearest friend, Emily Lawrence, thank you for your unyielding interest and support throughout my entire academic journey, for keeping me grounded outside of academia, and always letting me comfortably be my truest self. To my colleagues, or more truthfully-friends, in the CSU weed lab, thank you for all the support, comradery, and exchange of skills and knowledge over the years. Especially, thank you William Kramer and Catherine Traxler for our natural understanding of each other, exchange of niche humor, and continuous support.

To my father, Ronny, your support sustained me through many years of uncertainty such that I am now able to celebrate a life of happiness and fulfillment. I am a first-generation student due to hurdles and sacrifices made by my parents. I am a non-traditional student as a consequence of these generational struggles. With the support of many people, I made a narrow escape from these cycles. My greatest hope is that my completion of this degree and the person I have grown into may inspire and facilitate endless possibilities to our future generations including my niece and nephew, Chad and Priscilla. Though much time and distance has separated us, you are in my heart, and I am here for you always.

TABLE OF CONTENTS

CHAPTER 1 - GLYPHOSATE HISTORY AND RESISTANCE MECHANISMS

1.1 INTRODUCTION

The Herbicide Glyphosate:

The molecule that would eventually become the most widely used herbicide around the globe was originally discovered by a Swiss pharmaceutical company, who discovered its utility as a chelating agent. The usefulness of glyphosate [*N*-(phosphonomethyl)glycine] would begin to be realized by a Monsanto Co. chemist in 1970 who discovered its non-selective herbicidal activity and patented it as an active ingredient in 1974 (Duke and Powles 2008).

During the first two decades of commercialization the systemic, non-selective, and broad-spectrum activity of glyphosate limited applications to scenarios that avoided contact with foliage intended for survival. In most crops this consisted of a complete burn-down of weeds that emerged prior to planting. Glyphosate was also successfully adopted into tree and vine systems with sufficient space to safely target weeds without application to the cultivated foliage. Glyphosate has been used to control unwanted weeds outside of agricultural systems such as along roadsides, in residential lawns and gardens, in urban areas, and public recreation areas (Powles 2008).

The commercialization of transgenic glyphosate-resistant crops (GRCs) in the mid to late 1990's commenced a new era of glyphosate usage and weed management in agricultural systems (Dill et al. 2008). The rapid adoption of glyphosate-resistant soybean, maize, cotton, and canola permitted season-long control of weeds without damage to crops. This provided convenient and efficient weed management while reducing usage of other pesticides and conventional tillage (Dill et al. 2008).

Absorption and Translocation

Physiochemical properties that confer efficient up-take and transport throughout a plant are required for a compound to be an effective systemic herbicide. Glyphosate [*N*-(phosphonomethyl)glycine] is a zwitterion consisting of a carboxylic, phosphonic, and amino groups with pKa of approximately 2.2, 5.4, and 10.2, respectively (figure 1.1). At physiological pH the deprotonated carboxylic and phosphonic groups balance the positive charges of the amino group making glyphosate hydrophilic and water soluble, capable of systemic transport through the phloem and xylem.

The first barrier that glyphosate must overcome is the cuticle of the leaf. Two concentration-dependent mechanisms of glyphosate uptake may exist. A linear relationship between uptake and concentration at higher glyphosate levels suggests passive diffusion into the leaves (Gougler and Geiger 1981). Passive diffusion through membranes would likely favor a less-charged form of glyphosate. However, in *Conyza canadensis,* or a three-phase synthetic membrane system, uptake of glyphosate was equivalent regardless of delivery pH being above or below the pKa of the phosphonic group (Ge et al. 2013; Takano et al. 2019) Rates of glyphosate uptake may be subject to endogenous phosphate status, possibly due to regulation of a phosphate transporter (Pereira et al. 2019).

After uptake into the leaves, glyphosate must translocate to the site of inhibition in the chloroplast. Further, it must reach growth points to effectively kill the plant. Phloem loading has been observed within two hours of treatment and is maintained for at least 24 hours (Bromilow and Chamberlain 2000; Feng et al. 2003). Glyphosate may enter the phloem by diffusion through the symplast and plasmodesmata or through active uptake, possibly by phosphate transporters (Shaner 2009). The hydrophobicity of glyphosate in phloem sap pH likely facilitates effective

transport to sink tissues alongside photosynthates. Glyphosate may have a self-limiting effect on translocation. As more glyphosate reaches the target site the resulting dysregulation of carbon metabolism and photosynthetic activity results in reduced photosynthate flow from source to sink leaves (Geiger et al. 1999).

Mode of Action

The shikimate pathway, a metabolic pathway exclusively found in plants and micro-organisms, was proposed as a hypothetical source of ideal candidates for herbicidal target sites that would be non-toxic to animals (Baillie et al. 1972). Screening programs at the time were not successfully at identifying inhibitors of the shikimate pathway. Simultaneously, work was being done to characterize the recently discovered herbicidal activity of glyphosate. It was discovered that phenylalanine and tyrosine reversed glyphosate-induced growth inhibition in some species of plant and microbes (Jaworski 1972). Tryptophan was not effective in reducing growth inhibition leading to the hypothesis that glyphosate inhibited the synthesis of these aromatic amino acids at a step that channels chorismite metabolism toward tyrosine and phenylalanine synthesis. Specifically chorismite mutase and/or prephenate dehydratase were proposed as potential glyphosate target sites (Jaworski 1972). However, later studies with C^{14} radiolabeled shikimic acid showed that glyphosate inhibited incorporation of shikimic acid into all three aromatic amino acids, and also lead to accumulation of shikimic acid, pointing to a target site upstream of chorismate formation (figure 1.2) (Holländer and Amrhein 1980). Further work to identify the metabolites accumulating after glyphosate treatment revealed that shikimate-3-phosphate (S3P) was forming after glyphosate treatment while 5-enolpyruvylshikimate (EPSP) was not, revealing that the toxic effect of glyphosate on plants is due to inhibition of the sixth enzymatic step of the shikimate pathway 5-enolpyruvylshikimic acid-3-phosphate synthase

(EPSPS) (Steinrücken and Amrhein 1980). Thus, the shikimate pathway inhibitor hypothesized by Baillie et al, already existed as the non-selective herbicidal molecule rejected by the pharmaceutical industry: glyphosate.

The target site of glyphosate had been identified but it was still unclear exactly how glyphosate inhibits EPSPS and ultimately results in plant death. EPSPS catalyzes the transfer of the enol pyruvyl side chain from 2-phosphoenolpyruvate (PEP) to position 5 of S3P via a reversible addition-elimination mechanism (Herrmann and Weaver 1999). Investigation of the kinetics of EPSPS inhibition by glyphosate revealed that it acts as a competitive inhibitor with regard to PEP and an uncompetitive inhibitor with respect to S3P (Steinrücken and Amrhein 1984). It was later confirmed by the analysis of the crystal structure of EPSPS that glyphosate binds near the S3P binding cavity of EPSPS but does not perturb the structure, and that similar ionic interactions are present when either glyphosate or PEP interact with EPSPS. Additionally, the mechanism of inhibition is ordered such that S3P must first bind to EPSPS inducing a transition from an open to closed state, revealing the positively charged active site in which either PEP or glyphosate interact (Schönbrunn et al. 2001).

Since the initial discovery that glyphosate inhibits aromatic amino acid biosynthesis, this has been proposed as the mode of action by which plant death occurs (Jaworski 1972). The products downstream to EPSPS inhibition, including phenylalanine, tyrosine, tryptophan, and even chorismate are precursors to a suite of secondary metabolites required for normal development, growth, and defense. Phenylalanine and tyrosine formation from chorismate is facilitated by prephenate aminotransferase and arogenate dehydratase (Tzin and Galili 2010). These two aromatic amino acids are precursors for compounds such as phenylpropanoids, flavonoids, and plastoquinone such as coumarins, chalcones, cinnamic acid and lignans. These

compounds have crucial roles as antioxidants, pathogen inhibitors, and cell wall components (Norma Francenia et al. 2019). The phenolic phytohormone salicylic acid has a multifaceted set of established roles in both biotic and abiotic defense and is also synthesized from these precursors by phenylalanine ammonia lyase (PAL) or directly from chorismate by isochorismate synthase (ICS) (Ullah et al. 2023). Tryptophan metabolisms branches away from that of phenylalanine and tyrosine as its formation is facilitated by the conversion of chorismate to anthranilate by anthranilate synthase. Tryptophan is catabolized to form a variety of indole compounds such as terpenoids and phytoalexins that act in defense against herbivores and pathogens (Tzin and Galili 2010). Auxins, a class of phytohormones, are synthesized through the conversion of tryptophan to indole-3-pyruvic acid by tryptophan aminotransferases followed by conversion to auxin compounds by flavin monooxygenases such as the YUCCA family (Brumos et al. 2018). Auxins have roles across all of plant growth and development from differentiation and organogenesis to cell division and elongation as well as signaling in response to environmental stimuli and pathogen perception. Chorismate itself is a precursor to tetrahydrofolate and phylloquinone, vitamins with roles in nucleotide and protein synthesis and electron transport, as well as the ICS-mediated salicylic acid biosynthetic pathway.

In addition to being the link between carbon and aromatic amino acid synthesis it is often stated that more than 30% of total fixed carbon passes through the shikimate pathway making it a major metabolic pathway. Inhibition of such a high magnitude of carbon flux could lead to lethal consequences upstream of EPSPS inhibition due to reallocation of carbon from other metabolic pathways, such as draining it into the shikimate pathway (Siehl 1997).

Inhibition of the shikimate pathway at the glyphosate target site EPSPS results in a large accumulation of the precursor metabolite, shikimate acid (Servaites et al. 1987). The carbon

redirected to facilitate this formation shikimate acid is potentially channeled into a metabolic dead end. Reduced photosynthetic carbon intermediates ribulose-1,5-biphosphate and 3-phosphoglyceric acid occurred after glyphosate treatment (Servaites et al. 1987). Reduced stomatal conductance could also lead to a reduced capacity to assimilate CO_2 into new carbon (Shaner and Lyon 1979). Impaired carbon metabolism was also noted in treated garden peas (*Pisum sativum)* as accumulation of carbon was observed in leaves and roots due to diminished carbon utilization, suggesting that this contributes to glyphosate inhibiting plant growth (Orcaray et al. 2012).

While the exact mechanism of plant death remains unknown, several widespread physiological effects of glyphosate treatment have been observed that may be due to upstream or downstream consequences of EPSPS inhibition or potential off-target effects. Decreased photosynthetic activity and oxidative stress are among notable physiological changes induced by glyphosate (Gomes et al. 2014).

Inhibition of Photosynthesis

Though some results were contradictory early evidence indicated that glyphosate has an inhibitory effect of on photosynthesis (Van Rensen 1974; Sprankle et al. 1975; Brecke and Duke 1980; Richard et al. 1979; Muñoz-Rueda et al. 1986). It was unclear if inhibition of photosynthesis was directly related to the glyphosate mode of action or an indirect consequence of glyphosate activity. Several mechanisms were proposed: (1) Inhibition of the electron transport chain (ETC) of PSII and PSI by direct glyphosate inhibition of the complexes, or some effect that indirectly disrupts the quantum yield, (2) the phosphate moiety of glyphosate interfering with the phosphorylation of adenine diphosphate to adenine triphosphate, or (3) generalized disruption of the thylakoid membranes (Richard et al. 1979).

In green algae (*Chlorophyta sensu*) and isolated chloroplast of spinach (*Spinacia oleracea*) inhibition of the ETC of PSII and overall reduction of photosynthetic O_2 evolution was observed in a time-dependent manner beginning 15 minutes after glyphosate treatment (Van Rensen 1974). Studies on bean (*Phaseolus vulgaris*) leaf discs and in wheat (*Triticium aestivum*) found a more delayed inhibition of photosynthetic activity and CO_2 assimilation into photosynthates that was measurable 7 or 72 hours after treatment, respectively. These delayed effects lead to the conclusion that glyphosate was indirectly affecting photosynthesis rather than directly inhibiting the photosynthesis machinery or molecular interactions (Sprankle et al. 1975; Brecke and Duke 1980). Assays evaluating changes in electron transport, phosphorylation, and light harvesting capacity in isolated chloroplast thylakoids of garden peas (*Pisum sativum)* indicated that glyphosate did not affect the ETC of the PSII as previously reported, and no disruption of thylakoid pigments were observed within two hours of incubation (Richard et al. 1979). This further supported an indirect mechanism by which glyphosate interferes with photosynthesis. The authors proposed that the apparent contradiction to previous studies could be due to glyphosate acidifying the assay solution below the optimal pH, which they accounted for in subsequent work. Another study in bean reported simultaneous changes in stomatal conductance and photosynthesis within 6 hours after treatment with glyphosate and asserted the decrease in photosynthetic rate was likely due to the inability to assimilate CO_2 (Shaner and Lyon 1979). Studies on red clover (*Trifolium pratense*) and alfalfa (*Medicago sativa*) revealed that chlorophyll a and b and carotenoids were being significantly reduced as early as 24 hours after treatment, the photosynthetic ETCs were inhibited, and the stomatal conductance was reduced (Muñoz-Rueda et al. 1986). Therefore, chlorophyll biosynthesis and/or damage to chlorophyll in the absents of carotenoids could be a mechanism through which glyphosate

inhibits photosynthesis, an idea supported by modern studies (Gomes et al. 2016). Glyphosate could inhibit chlorophyll biosynthesis by the chelation and depletion of Mg^{2+}, or by inhibition of δ-Aminolaevulinic acid, precursors to chlorophyll biosynthesis (Cakmak et al. 2009; Kitchen et al. 1981). The decrease in protective carotenoids could be directly related to shikimate pathway inhibition through the loss of plastoquinone (PQ), a co-factor of carotenoid biosynthesis(Sandmann et al. 2006). Glyphosate not only decreased the PQ pool, but shifted it and the PSII reaction centers to a more reduced state as shown by an increase in unquenched fluorescence and decrease of photochemical quenching (Gomes et al. 2017). This could indicate that reduced photosynthetic activity was a consequence of lower PQ content caused by inhibition of the shikimate pathway. Further evidence for inhibition of the shikimate pathway having a direct role in decreased photosynthetic activity was shown by a significant decrease in CO_2 assimilation and shifts in chlorophyll *a* fluorescence quenching parameters within 24 hours of treatment in a glyphosate susceptible line of soybean and not in soybean engineered to have an insensitive glyphosate target site (Vivancos et al. 2011). Taken together, past studies suggest that glyphosate may have an inhibitory effect on photosynthesis through various mechanisms, both direct and indirect to the glyphosate mode of action.

Oxidative Stress

Reactive oxygen species (ROS) have important roles in signaling, development, and stress response, but if left unchecked they can quickly become molecules of mass cellular destruction (Mittler 2017). Reactions that generate ROS are specific to cellular compartments and are accompanied by a system of compartmentalized antioxidant systems which regulate ROS to maintain an appropriate cellular redox state (Janků et al. 2019). Disruption of redox status in glyphosate-treated plants has been observed to varying magnitudes in different species. This

often begins as an accumulation of ROS such as hydrogen peroxide (H_2O_2) and a corresponding attempt to quench the oxidative burst with an increase in antioxidant enzymes or molecules such as catalase and ascorbate (Traxler et al. 2023). Though the primary mechanism is not fully clarified, multiple sources of ROS evolution have been associated with response to glyphosate including inhibition of photosynthetic and mitochondrial electron transport chains and increased peroxisomal glycolate oxidase activity (Vivancos et al. 2011; Gomes et al. 2017; Gomes and Juneau 2016; de Freitas-Silva et al. 2017). Currently, there are no studies indicating that glyphosate induced ROS Reactive oxygen species is generated by NADPH oxidates. These enzymes such as respiratory burst oxidase homologues (rboh) produce ROS in the cell wall, apoplastic space, and plasma membrane (Janků et al. 2019)

In the case of glyphosate-induced photosystem inhibition, ROS could be causative, consequential, or a combination of cause and consequence (Gomes et al. 2017). Photosynthesis forms the basis of energy acquisition for most life on earth, when the energy of a photon is harvested by chlorophyll and transferred to PSII where it is used to split water molecules into protons, oxygen molecules, and electrons that are carried along the photosynthetic electron transport chain (PETC), through PSI, and then to ferredoxin where they ultimately reduce $NADP^+$. The inevitable interaction of O_2 with this electron transport chain leads to the formation of a superoxide anion radical and subsequent H_2O_2 (Ivanov et al. 2022). H_2O_2 also forms in the thylakoid membrane, though not likely via dismutation, due to the electrostatic repulsion of the charged superoxide anions in the membrane (Ivanov et al. 2022). The reduced form of plastoquinone, plastohydroquinone (PQH_2) is believed to be the only electron carrier in the PETC capable of both protonating and reducing superoxide anions to H_2O_2. Through these mechanisms, ROS are produced as a by-product of photosynthesis and have been harnessed by

evolution as signaling molecules. Chloroplast ROS levels increase in response to stress, and are scavenged effectively by tocopherols and carotenoids (Janků et al. 2019). When H_2O_2 levels exceed the chloroplast antioxidant capabilities photosynthetic activity is inhibited, partially due to oxidation of thiol group of enzymes in the Calvin cycle, and further by oxidative damage within the chloroplast (Foyer 2018). Photoinhibition, whether caused by excess ROS, light, heat, or other stress imposes a limitation on electron transport which in turn can lead to ROS formation the reduction of O_2 to superoxide anion radical by triplet chlorophyll (Pospíšil 2016). Glyphosate inhibits photosynthesis, potentially triggering ROS formation, concurrently other physiological effects of glyphosate, including but not limited to some processes believed to drive photoinhibition such as depletion of chlorophyll and carotenoids, and decreased stomatal conductance can independently result in ROS production which would in turn inhibit photosynthesis (Gomes et al. 2017; Vivancos et al. 2011). In this way ROS may be either a cause or effect of decreased photosynthesis.

Just as electrons in photosynthetic ETCs can reduce oxygen leading to production of ROS, oxygen reduction by electrons moving through the complexes of the mitochondrial ETC also serve as a major source of ROS. Though a by-product of cellular respiration, mitochondrial ROS are associated with regulation of development and stress response that are somewhat dependent on the mitochondrial complex of origin (Huang et al. 2016). Inhibition of cellular respiration leads to an increase in mitochondrial generated ROS which can mediate signaling cascades effecting cell wide processes such as programmed cell death, hormone responsive signaling, and pathogen defense (Janků et al. 2019). In addition to antioxidant enzymes such as superoxide dismutase (SOD), glutathione-S-transferases (GST) and ascorbate peroxidases (APX), alternative oxidase (AOX) and uncoupling proteins are mitochondrial proteins that

regulate ROS by minimizing reduction of the ubiquinol pool by channeling electrons to NAD(P)H dehydrogenase as an alternative electron acceptor, or by promoting proton leak across the inner mitochondrial membrane (Rhoads et al. 2006).

A series of experiments involving glyphosate and inhibitors of mitochondrial complexes in duckweed *(Lemna minor)* indicated that ROS produced in response to glyphosate may be partially generated in the mitochondria, before complex IV (Gomes and Juneau 2016). Glyphosate had the strongest inhibition on complex III, where further inhibition at the Q0 site showed a reduction in glyphosate induced ROS while inhibition at the Q1 site did not, indicating that ROS acted similarly to complex inhibitor antimycin A. Though chlorophyll and photosynthetic activity decreased in these treatments, florescence imaging indicating that ROS initially accumulates outside of the chloroplast followed by gradual overlap with chloroplast (Gomes and Juneau 2016). This provides evidence that initial oxidative burst caused by glyphosate may originate in the mitochondria. Glyphosate also induced ROS production in mitochondrial mouse leydif cells, suggesting that glyphosate could induce ROS evolution independent of chloroplasts or the shikimate pathway (Lu et al. 2022).

In addition to ROS generation, glyphosate perturbs antioxidant systems that hold cellular redox status in balance by the quenching of ROS. Proteomic analysis of rice leaves revealed upregulation of a handful of antioxidant enzymes in response to glyphosate treatment including tau class GST, APX, thioredoxin, peroxiredoxin, and Cu/Zn-SOD (Ahsan et al. 2008). Another GST of the phi class was downregulated. It was confirmed that the glyphosate treated rice leaves accumulated H_2O_2 and thiobarbituric acid reactive substance (TBARS), a marker for lipid peroxidation. In glyphosate sensitive soybean it was found that five days after glyphosate

treatment the ratio of reduced to oxidized redox pools was comparable to untreated controls and GSH was increased, while Round-up Ready soybean containing an insensitive form of the glyphosate target site presented with a sustained oxidation of the ascorbate and GSH pools, but no increase in GSH (Vivancos et al. 2011). This was attributed to a transient increase of ROS that was quenched by an increased abundance of antioxidants Cu/Zn-SOD and GSH observed only in the sensitive soybean, implicating inhibition of the shikimate pathway and associated changes in amino acid metabolism in upregulation of detoxification pathways. The ascorbate pool of sensitive soybean was assessed 5 days after treatment and was maintained in a reduced state, similar to control plants; however, a study in willow suggests an earlier shift in redox state of ascorbate pool may occur and be resolved by 72 hours (Vivancos et al. 2011). In willow H_2O_2 accumulated within 24 hours of glyphosate treatment and further increased over the 72-hour study, total ascorbate, and the activity of antioxidant enzymes SOD, APX, catalase (CAT), GPX, and GR (glutathione reductase) occurred within six hours of treatment (Gomes et al. 2017). The redox state of the ascorbate pools shifted in a time-dependent manner, the oxidized form was greater in glyphosate treated plants up to 24 hours, at which time the reduced form became dominant through 72 hours, while untreated controls had a consistently reduced pool of ascorbate. An increase in carotenoids was observed six hours after treatment, followed by a decrease by 24 hours. Similar to glyphosate sensitive soybean, it was concluded that the early increase of antioxidant enzymes, ascorbate and carotenoids was attributed to regulation in response to early ROS evolution (Vivancos et al. 2011; Gomes et al. 2014). In Arabidopsis seedlings grown in the presence of 20 μM glyphosate, oxidative stress was implied by increased protein oxidation, however reduced levels of H_2O_2 compared to a 0 μM glyphosate control was

attributed to increased GSH and activity of catalase, glycolate oxidase, APX, GR and two other enzymes related to ascorbate-glutathione cycling (de Freitas-Silva et al. 2017).

Glyphosate has been reported to induce activity in the oxidative pentose phosphate pathway (OxPPP). Activity of glucose-6-phosphate dehydrogenase (G6PD) and 6-phosphogluconate dehydrogenase (6PGDH) were upregulated in Arabidopsis seedlings grown in the presence of glyphosate (de Freitas-Silva et al. 2017). These enzymes can regenerate NADPH which is necessary for antioxidant processes including GSH generation by glutathione reductase (GR). Increased GSH pool and GR activity were also significantly higher in plants grown on media containing glyphosate, supporting a role of OxPPP in the regulation of oxidative stress response to glyphosate. This is also supported by glyphosate induced reduction of $NADP^+$/NADPH ration and accumulation of proline, an NADPH dependent response to oxidative stress (Gomes and Juneau 2016; Vivancos et al. 2011). The introductory molecule to the shikimate pathway, erythrose-4-phosphate, is also produced by the OxPPP pathway; therefore, upregulation of this pathway may be related to unregulated changes in carbon flux associated with inhibition of the shikimate pathway (Siehl 1997; Gomes and Juneau 2016).

Induction of ROS by glyphosate appears to trigger a transient antioxidative burst in sensitive plants, perhaps due to decreasing levels of compounds secondary to the shikimate pathway, or by deactivating carbonylation of antioxidant enzymes as ROS levels breach capacity (Gomes et al. 2017; Tola et al. 2021). Similar to inhibition of photosynthesis, glyphosate may induce oxidative stress and reduce antioxidant capacity through a combination of indirect consequences such as mitochondrial electron transport chain inhibition through an unknown mechanism, or directly through shikimate inhibition depleting photosynthetic activity and

antioxidant molecules. Accumulation of ROS in one or more cellular compartments may positively regulate further ROS evolution in the same or other compartments through inhibition of electron transport, loss of antioxidant capacity, or through signaling cascades. There is limited evidence for glyphosate induced ROS evolution in the peroxisomes and additional work is needed to investigate oxidative response to glyphosate in this compartment as well as in NADPH-oxidase mediated ROS evolution in the cell wall, apoplast, and cytoplasmic membrane.

Resistance in Agronomic Weeds

The necessity of non-selective applications in row crops imposed a limitation on recurrent glyphosate usage across much cultivated acreage. This limited use coupled with alternative management practices such as application of different herbicides, tilling, or hand weeding helped mitigate selection pressure for glyphosate resistance. Across the hectares used only used for row-crops the weeds that emerged prior to planting may have been the only individuals exposed to glyphosate each season. Heavier selection pressure was potentially being placed on weeds in systems where recurrent usage was possible such as orchards, vineyards, fallow land, and non-agricultural areas (Powles 2008).

In 1996, soybean was the first glyphosate-resistant crop (GRCs) approved and commercialized in the United States (Dill et al. 2008). This transgenic soybean line expressed a glyphosate insensitive version of the glyphosate target site enzyme enolpyruvylshikimate-3-phosphate synthase (EPSPS) from *Agrobacterium* sp. strain CP4 which was had been isolated from a waste disposal column at a glyphosate production facility. The consistent exposure to glyphosate likely selected for the single mutation in the CP4 EPSPS that endowed glyphosate

insensitivity while maintaining sufficient affinity for natural substrates shikimate-3-phosphate and PEP (Funke et al. 2006).

As this groundbreaking advancement was being rapidly adopted by growers, an article was being prepared in which the authors reflected on two decades of effective broad spectrum weed control, with perspectives on why glyphosate resistance had not been selected in the field and was unlikely to become a prominent issue (Bradshaw et al. 1997). Reduced likelihood of selectable resistance was suggested based on lack of evidence for selection for resistance in the field over two decades, with up to six applications a year in orchards, and some roadsides and railways in United States and Australia with 10-15 years of history with multiple yearly applications. The difficulty of developing glyphosate-resistant lines by several techniques was also implied as evidence that evolution of resistance mechanism would be rare in nature. Artificial selection of resistant perennial ryegrass required over a decade of selection pressure. Mutagenesis of two million *Arabidopsis thaliana* seeds did not yield any survivors grown on either 10× or 5× the dose survivable by wild type. Assuming that the experimental conditions were adequate, and the absence of survivors was truly related to rarity of the mutation, this supports that occurrence of resistance alleles would be very rare in nature. An attempt to develop target site amplification in tissue culture was met with difficulty of plant regeneration, reproduction, and maintenance of observed resistance, it was assumed that it would be even more difficult for a healthy, fertile, individual with sufficient resistance to naturally evolve in the field. Lessons from developmental process of the GR soybean were convincing to the authors that resistance was not likely to evolve. A form of EPSPS from *Salmonella* conferred resistance through Pro101Ser mutation but was not targeted to the chloroplast. Using the EPSPS gene from petunia as a template, an expressed construct with a Gly101Ala mutation was insensitive to

glyphosate; however, it had lost some affinity for PEP as well, and catalytic efficiency was reduced to 58% of the wild type. After many iterations of the petunia EPSPS with additional random mutations failed to generate an enzyme with loss of glyphosate binding and sufficient PEP affinity and enzymatic activity, further supporting that selection on random mutations in the field would not result in a resistant weed, and loss of glyphosate interaction in plant EPSPS will result in loss or decrease in PEP affinity and potential decrease in the products of the shikimate pathway in PEP limiting conditions. From these studies it was determined that if an individual with an EPSPS mutation was selected then it would either not survive or have reduced fitness and competitive ability. After the isolation of the CP4 EPSPS with ideal kinetics it was revealed to have only 23 to 41% identity to plant EPSPS, leading to an assumption that an EPSPS form with similar kinetics could not occur in plants due to the quantity and specificity of mutations involved. Metabolism was not considered a risk due to the rare and inefficient observations of glyphosate metabolism in plants. Additionally, the uniqueness of the glyphosate chemical structure, target site and lack of soil activity would reduce selection pressure. Cross-resistance to glyphosate from selection of resistance alleles to other herbicides is low risk compared to target sites with multiple compounds. The lack of resistance seen with historic usage was hypothesized to indicate that usage patterns under the GRC system would not select resistance alleles at a high rate (Bradshaw et al. 1997).

With an anthropomorphic irony, the inevitable processes of evolution were catching up with glyphosate selection pressure as these perspectives on the improbability of glyphosate resistance were being composed. The first report of a weed with field selected glyphosate resistance, rigid ryegrass (*Lolium rigidum*) came out of Victoria, Australia in 1996 (Powles et al. 1998). Though the advent of the GRC technology would become regarded as the harbinger of

glyphosate resistance, the first cases were found in some of the very systems which had boasted up to six applications per year, such as fruit and almond orchards, grapevine production, fence lines, irrigation channels, and buildings.

The remainder of the decade would see more reports in rigid ryegrass in Australia and Malaysia, as well as resistance goosegrass in the United States. GR cotton, maize, and canola varieties were released in the United States. It was after the turn of the millennium when the first case of glyphosate resistance was reported in a broadleaf species, horseweed *(Erigeron Canadensis)*. Unlike previous reports, resistance was selected in a row crop, soybean, a system that would not have experienced recurrent application prior to the adoption of GRCs four years prior. Twenty-one new cases of resistance emerged from 2000-2003, 90% of which were horseweed and annual or perennial ryegrasses, 62% were in the US and all of those were in soybean, maize, cotton, and another 33% were in orchards, vineyards, or along roadsides and fence lines (Heap 2023). Trends were already emerging in that 95% of the new cases were in systems with a capacity for recurrent application, and that certain types of weeds were evolving resistance faster than others. Standing resistance alleles may have existed in some populations of these species from previous selection pressure which then drifted quickly through populations due to the strong selection pressure from more widespread and recurrent glyphosate application.

An increase in diversity of species evolving resistance began to appear starting in the mid 2000's. In the US GR alfalfa and sugar beet lines were launched in 2005 and 2008, respectively. The trend of increased cases in systems receiving repeated applications of glyphosate continued through present day. Currently at least 359 individual cases of glyphosate have been reported, encompassing 58 species in 31 countries across 6 continents (Figure 1.3; Figure 1.4) (Heap 2023)

Mechanisms of Glyphosate Resistance

Mechanisms of herbicide resistance are rooted in molecular and physiological differences evolved in a resistant population compared to a sensitive population. These changes may be related to the target site of the herbicide such as mutations in the genetic sequence conferring direct or indirect changes to the protein binding kinetics, or increased gene copy number can result in increased abundance of the target protein beyond the efficacy of the label application rate. Changes in the sequence of regulatory elements such transcription factors or gene promotors can also lead to increased target site abundance. Resistance mechanisms may otherwise fall under the umbrella of non-target site resistance involving a variety of biochemical, cellular, physiological changes that ultimately prevent a toxic dose of active herbicide from reaching its site of action, often by alterations in how a herbicide is absorbed, translocated, or metabolized (Gaines et al. 2020).

Target Site Resistance

Glyphosate target site resistance has been associated with the increased abundance of the target site enzyme 5-enolpyruvylshikimate-3-phosphate synthase (EPSPS) to levels in which label rates of glyphosate are quenched before enough enzyme is inhibited to the toxic effects of target site inhibition. Target site mutations have been reported that induce changes near the binding site of glyphosate/PEP that specifically decrease the affinity for glyphosate while preserving that of PEP (Sammons and Gaines 2014).

At least nine species have increased gene copy number of EPSPS, including both dicot and monocot species. Copy number variation of EPSPS has been observed as tandem duplications along a chromosome or as multiple copies along extra chromosomal circular DNA

fragments that are tethered to chromosomes (Patterson et al. 2018). These two types of copy number variations have been investigated more closely in kochia and Palmer amaranth.

Glyphosate-resistant kochia was first reported in 2007 in Kansas, United States. Resistance was due to amplification of tandem repeats of the glyphosate target gene, EPSPS (Jugulam et al. 2014). These populations accumulated progressively more copies of EPSPS and increased glyphosate resistance levels over multiple generations, leading to the idea that a duplication event originated from unequal crossing over and was then selected by glyphosate treatment. The sequence homology of the original copy and the first duplicate copy may help facilitate further unequal crossing over resulting in additional gene copies and enhanced glyphosate resistance in the progeny (Jugulam et al. 2014). Genomic analysis resolved the structure of the EPSPS duplication in a resistant population from Colorado, U.S. Two types of repetitive segments of different lengths, with a mobile genetic element (MGE) flanking each repeat. A conserved region of the repeated segments had additional genes including RAD51, a regulator of homologous crossing over. It was proposed that insertion of the MGE on either side of a single copy EPSPS, unequal crossing over produced an additional gene copy. It was proposed that the two types of repeats were generated by a double stranded break at the MGE boundary that underwent inaccurate repaired by alternative non-homologous end joining machinery (Patterson et al. 2019).

The first evidence of EPSPS gene duplication as a mechanisms of glyphosate resistance was in an *Amaranthus palmeri* population from Georgia, U.S. in which some individuals had a greater than 150 fold increase in EPSPS gene copy number that appeared to be dispersed through the genome (Gaines et al. 2010). Rather than insertions throughout the genome it was determined that the unique genetic backdrop of the numerous EPSPS duplications was extra chromosomal

circular DNA (eccDNA) tethered to the chromosomes throughout the genome and containing 72 other putative genes (Molin et al. 2017).

Identification of an extended autonomous replication sequence (EACS) and associated elements related to replication in plants were attributed to replication of the eccDNA (Molin et al. 2020). Interestingly, eccDNA can be transmitted in pollen to related species in which a susceptible F1 with some percentage of meristematic cells containing a high quantity of eccDNA tethered to chromosomes. Though the plant is susceptible, it is hypothesized that the cells with eccDNA would be resistant and capable of regrowing a resistant shoot and produce some proportion of resistant progeny. In this way glyphosate treatment may select for resistance at the cellular level within the life of an individual, leading to rapid evolution of resistance (Koo et al. 2023).

Over-expression of a single copy genomic EPSPS could generate enough target site enzyme to quench glyphosate but there may be some regulatory mechanisms that lead to enhanced transcription of EPSPS in response to glyphosate treatment. Transcript abundance of EPSPS was induced in a population of goosegrass (*Eleusine indica*) from China. Resistant individuals began accumulating EPSPS transcript at 12 hours and peaked at 48 hours (Zhang et al. 2015). An insertion in a Py-rich region of the in the EPSPS promotor in resistant individuals which resulted in loss of transcription factor binding at the Py-rich site, while five other transcription factors predicted to bind the EPSPS promotor were differentially expressed (Zhang et al. 2018; Zhang et al. 2021). Glyphosate treatment up-regulated expression of EPSPS possibly due to regulation by differentially expressed transcription factors and differential binding of transcription factors on an altered sequence moiety of the promotor.

Polymorphisms in the primary sequence of EPSPS translate to changes in the enzyme that may shift the binding capacity for glyphosate, PEP, or S3P. A commonly reported mutation is change of amino acid 106 from proline (Pro^{106}) to Ser, Ala, Thr, Leu, or Arg. In EPSPS of *Escherichia coli (E. coli)* the site analogous to Pro^{106} is located approximately nine angstroms from the glyphosate target site. The carbonyl oxygen of Thr^{102} is held in place by a hydrophobic interaction with Pro^{106}. Loss of this interaction leads to rotation of Thr^{102} and neighboring Gly^{101} toward the active site and narrowing the glyphosate binding site. The degree to which this occurs will depend on the structure of the substituted amino acid. The shorter size of PEP compared to glyphosate likely explains why some Pro^{106} confer a glyphosate insensitive EPSPS that can maintain varying degrees of affinity for PEP (Healy-Fried et al. 2007). The double mutation Thr^{102}Ile and Pro^{106}Ser, known as the TIPs mutation provides higher glyphosate resistance than Pro^{106} Ser or Thr^{102}Ile single mutations while maintaining a higher affinity for PEP than Thr^{102}Ile (Funke et al. 2009). In the TIPs mutation, as with Pro^{106} Ser, the interaction with Pro with position 102 is lost, leading to rotation and of Ile^{102} which pushes Gly^{101} toward the target site in a manner that reduces the affinity for PEP only slightly more than Pro^{106}Ser but drastically reduces the of glyphosate to access the binding site (Funke et al. 2009).

Non-target Site Resistance

Several non-target site glyphosate resistance mechanisms have been observed or proposed and typically related to exclusion of glyphosate from its target site due to reduced absorption or translocation or and metabolism of glyphosate by degradation to aminomethyl phosphonate (Sammons and Gaines 2014). The multiple barriers that glyphosate must cross to reach the target site provide mechanistic opportunities for evolution of differential absorption or translation. At least three mechanisms have been suggested that can result in reduced

translocation of glyphosate: vacuolar sequestration, chloroplast exclusion, and restricted cellular entry (Ge et al. 2013). In glyphosate-resistant populations of horseweed (*Conyza canadensis*) from Delaware, USA, reduced source to sink translocation of glyphosate was due to rapid vacuolar sequestration of up to 90% of source leaf glyphosate within 24 hours of treatment (Ge et al. 2013). In glyphosate-resistance johnsongrass (*Sorghum halepense*) from Arkansas, USA, decreased accumulation of glyphosate into the source leaves was observed compared to glyphosate susceptible. In resistant horseweed, reduction of cytosolic signal and increased vacuolar glyphosate signal were not observed. This indicates that glyphosate was excluded from the source leaves, perhaps remaining in the apoplast (Ge et al. 2013). Similar work on lamb's quarters (*Chenopodium album*) revealed that glyphosate accumulated in the cytoplasm and did not result in shikimate 3-phosphate accumulation, supporting exclusion of glyphosate from the chloroplasts as a mode of reduced translocation (Ge et al. 2013). Though ^{31}P-NMR revealed the varied compartmentalization of glyphosate in these resistant populations it is unclear how glyphosate was differentially transported or excluded. One or more active transporter families were suggested as the "traffic control" of glyphosate transport (Ge et al. 2013). ATP-binding cassette (ABC) transporters, major facilitator superfamily (MFS), multidrug and toxic compound extrusion family (MATE), small multidrug resistance family (SMR), and resistance-nodulation cell division family (RND) have been suggested as candidates of herbicide transport due to location of unique family members on the tonoplast, chloroplast, or plasmas membranes as well as ability to transport a variety of molecules including glutathione conjugates (Conte and Lloyd 2011). Transcription based studies support the potential role of ABC transporters in glyphosate-resistant horseweed, hairy fleabane (*Conyza bonariensis*), and jungle rice (*Echinochloa colona)* (Pan et al. 2021).

Glyphosate metabolism is not generally considered a significant pathway in plants, but does occur at various levels in different species (Reddy et al. 2008). Many microbes have enzymes capable of catabolizing glyphosate by either conversion to sarcosine by a C-P lyase or by a glyphosate oxidoreductase (GOX) splitting the C-N bond to form AMPA (Pizzul et al. 2009). The existence of a GOX-like gene in plants has been theorized (Duke 2011). In glyphosate-resistant jungle rice from Australia expression of an aldo-keto reductase (Liu et al. 2017) was upregulated in conjunction with increased conversion of glyphosate to AMPA and glyoxylate (Pan et al. 2019a). A causal relationship to glyphosate resistance and metabolic activity was validated by expression in AKR in rice calli and *E. coli*. The discovery of a plant enzyme that efficiently converts glyphosate to AMPA necessitates the exploration of these AKRs in other species and elucidation of the downstream metabolism and physiological effects. The main activity of aldo-keto reductases is in the reduction of aldehydes and ketones in an NADPH dependent manner, but they have also had a broad range of substrate recognition including xenobiotics (Penning 2015; Simpson et al. 2009). While these resistance mechanisms may work independently, combinations of mechanisms may work synergistically to confer survival or a higher resistance factor than on its own.

Glyphosate has many qualities that make it a useful agronomic tool. Given the variety of resistance mechanisms and the quantity of cases that have emerged in the past three decades, the future of glyphosate as an effective herbicide relies on our understanding of resistance evolution and how to manage fields that already contain resistance alleles.

1.2 FIGURES

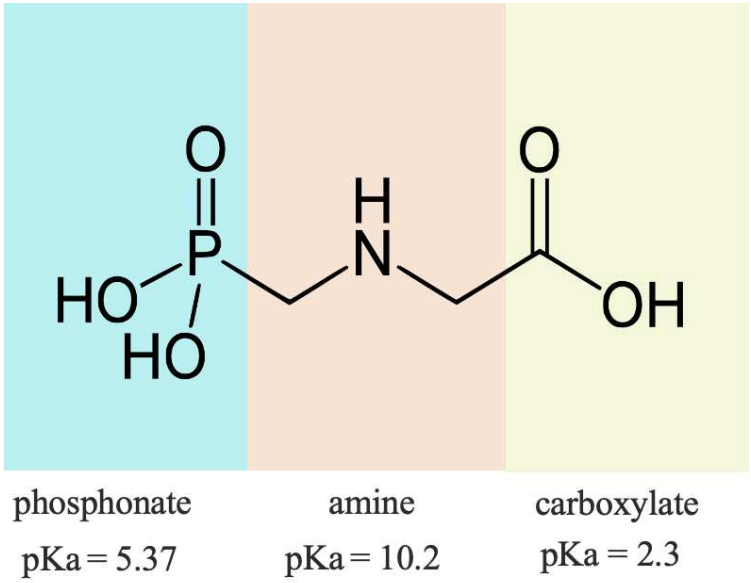

Figure 1.1 Structure of glyphosate and pKa values associated with functional groups.

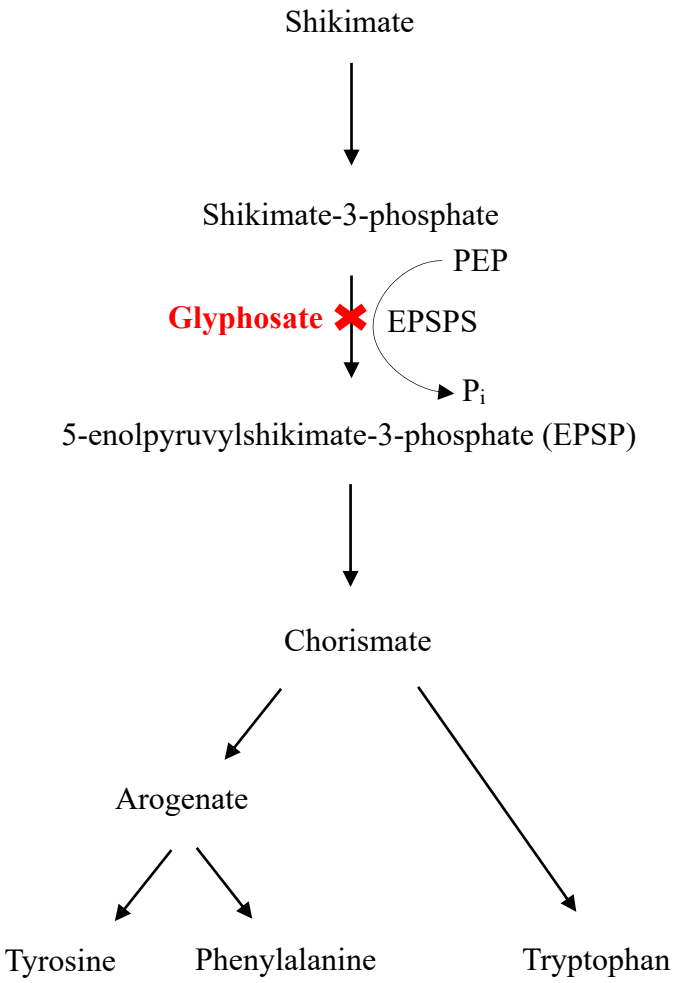

Figure 1.2. Simple schematic of the shikimate pathway from enzymatic step five through formation of aromatic amino acids. The target site of glyphosate is indicated at step six.

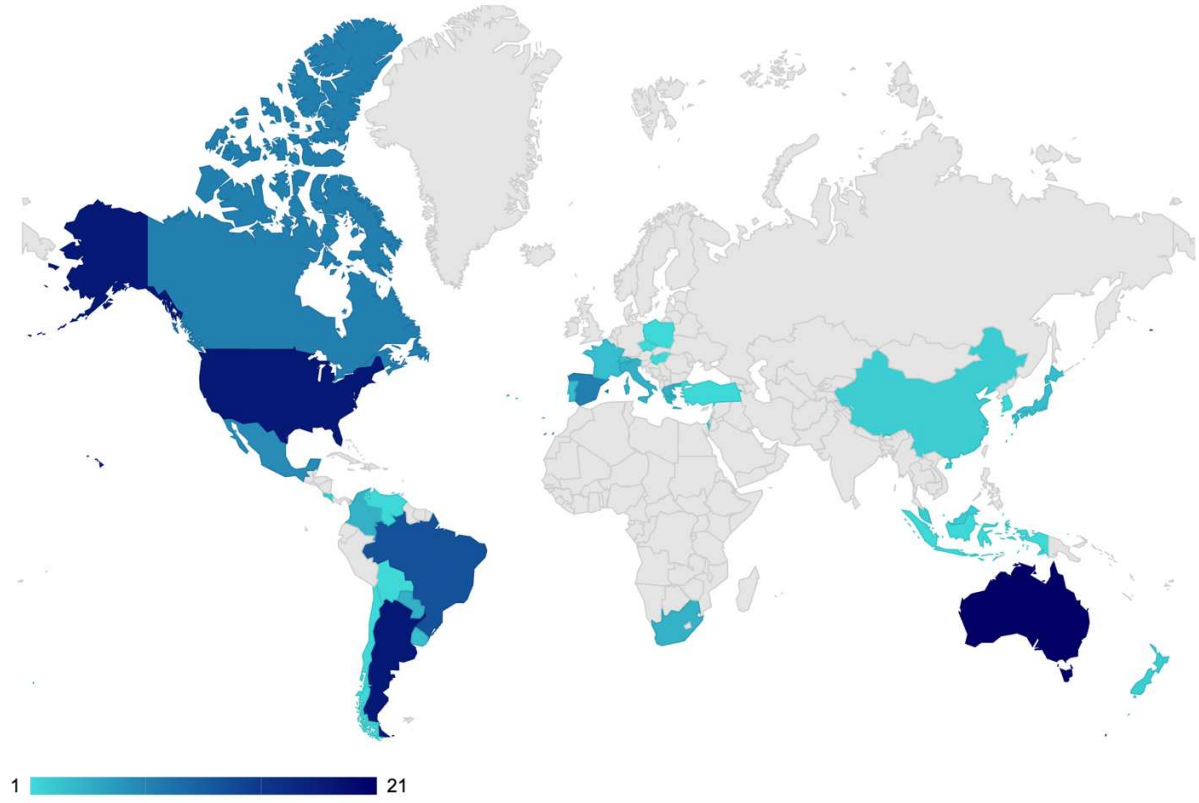

Figure 1.3. Global distribution of glyphosate resistance cases in 2021 (Heap 2023)

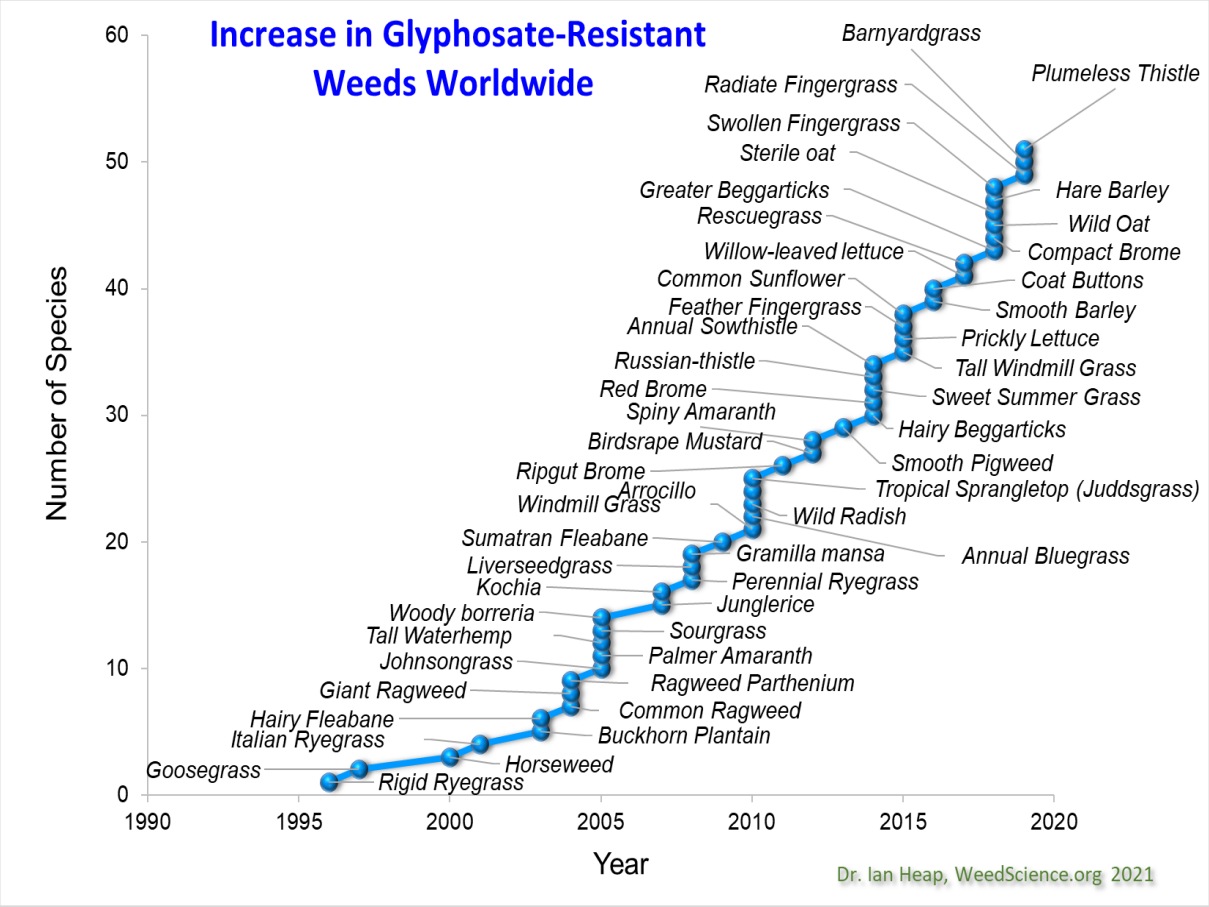

Figure 1.4. Species with reported glyphosate resistance occurrence from initial report in 1996 to 2021 (Heap 2023)

CHAPTER 2: TRANSCRIPTOMIC ANALYSIS OF RAPID RESPONSE *AMBROSIA TRIFIDA*

2.1 INTRODUCTION

Herbicide resistance has posed a threat to agricultural systems since the first case of 2,4-D resistance in 1975, followed by many more cases in the following decades (Beckie 2020). The introduction of glyphosate in the late 1970's provided a highly effective option in systems where treatment of weeds could occur without contacting the crop. When transgenic crops were released in the mid-90s and early 2000's growers of the imminently popular soybean, cotton, and corn were now able to make applications to their row crops. For the first 20 years of glyphosate use there were no reported cases of resistance. The first cases emerged in systems where repeated applications were historically permissible such as orchards, vineyards, roadsides, and railways (Powles 2008). By the 2010s, selection pressure from continuous and repeated and application of glyphosate had selected for a variety of resistance mechanisms in multiple weed species. Resistance is sometimes associated with changes to the glyphosate target site, but a variety of non-target mechanisms involving different families of genes and pathways have been identified (Sammons and Gaines 2014). Transcriptome-wide analysis can drive discovery of novel gene candidates for resistance.

Next generation sequencing (NGS) has rapidly evolved since the first platforms, becoming more accessible to a growing number of researchers. Aside from cost and availably of sequencing core, another barrier to NGS approaches is a lack of genomic resources, such as a reference genome. Improved *de-novo* assembly methods as well as collaborative efforts to generate genomic resources for non-model species will continue to make NGS-based

experiments available to answer complex questions about a variety of species (Montgomery et al. 2023)

Sequencing of mRNA and subsequent quantification of transcript abundance per gene allows researchers to explore transcriptome wide changes in gene expression between multiple groups such as different genotypes, tissue types, or treatment conditions. This approach can be used to understand underlying changes in gene expression for a variety of traits. Plant response to environmental stimuli can be understood by exploring which genes are being induced or repressed. The response may vary between a population that is tolerant to the stimuli compared to one that is sensitive. This could include abiotic stresses such as drought, cold, or osmotic stress, or biotic stress such as presentation of a pathogenic bacterium or fungi, or insect herbivory.

In agronomic weeds, transcriptomic analysis such as RNAseq can lead to discovery of candidate genes with differential expression conferring traits that give weeds an advantage in systems where humans would prefer them to be eradicated. In agronomic systems weeds can cause loss of yield through competition, interference with harvest, hosting of other pests such as insects or pathogens. Herbicide application is the most widely utilized method of weed control giving a major advantage to individuals who have evolved resistance. Finding gene candidates through transcriptomic studies leads to understanding of herbicide resistance mechanisms.

Past transcriptomic studies on model species, crops, and other weeds provide insight to how glyphosate treatment effects specific genes and pathways. A microarray study assessing gene expression in wild-type *Arabidopsis thaliana* accession Lansberg *erecta* (Ler-0) six hours after being submerged in 200 μM glyphosate found that many genes for abiotic and biotic stress

response, detoxification, and programmed cell death were upregulated, while genes associated with photosynthesis and chlorophyll biosynthesis were down-regulated after glyphosate treatment (Faus et al. 2015).

An increasing number of transcriptomic studies have emerged in recent years specifically comparing herbicide-resistant and susceptible biotypes of agronomic weeds. These include monocot species such as *Eleusine indica, Echinochloa colona*, and *Lolium multiflorum*, as well as dicotyledonous *Conyza bonariensis* and *Conyza canadensis* (Zhang et al. 2021; Wright et al. 2018; Piasecki et al. 2019; Yang et al. 2021). Studies such as these have resulted in discovery of genes related to a variety of known resistance mechanisms and candidates of novel or less understood mechanisms.

One such case is *Ambrosia trifida* (giant ragweed), with two distinct biotypes of glyphosate-resistant biotypes (Harre et al. 2017). One type displays little to no initial response to treatment and a gradual continuation of growth. The other is a rapid response biotype characterized by rapid tissue death of mature leaves and an oxidative burst of hydrogen peroxide within hours of treatment (Moretti et al. 2018). Previous work on the rapid response biotype revealed no target site mutations or copy number variations of the glyphosate target site gene 5-enolpyruvylshikimate 3-phosphate synthase (*EPSPS*) (Van Horn et al. 2018). Electron microscopy revealed that by 24-hours the rapid response in mature leaves shares features with programmed cell death progression, while necrotic cell death displayed by susceptible cells occurs weeks after treatment (Lespérance 2015). This would indicate the induction of tightly regulated signaling pathways such as those that evolved in response to plant pathogen infection,

often involving a rapid burst of ROS such as that reported in the mature leaves of A. trifida (Moretti et al. 2018).

To identify genes with differential expression in resistant and susceptible individuals an RNAseq-based transcriptomic analysis was used. The goal of this study was to identify candidate genes for glyphosate resistance in the rapid response biotype of giant ragweed. Early time points, 0, 15, 60, and 180 minutes after treatment, were selected to capture initiation of signaling prior to the rapid cell death observed in the mature leaves and overall differences in gene expression between resistant and susceptible populations.

2.2 MATERIALS AND METHODS

Sample Collection and Sequencing

Individuals from previously reported populations of a glyphosate-resistant rapid response biotype and glyphosate-susceptible biotype of *A. trifida* were self-pollinated for two generations (Van Horn et al. 2018). Seeds were planted in Magenta® boxes in 2-4 cm of moistened soil (Fafard Custom Mix, Sun Gro Horticulture), and cold stratified at 4 °C for 6 weeks to break dormancy. Seedlings were grown under a photoperiod of 14 h light, 25 °C/10h dark, 20 °C. Glyphosate (Roundup PowerMAX®) was applied at 0.84 kg ae ha^{-1}, using a laboratory track sprayer calibrated at 187·L ha^{-1} spray volume with an 8002EVS single even flat-fan nozzle. Leaf disc samples were collected immediately prior to treatment and at 15, 60, and 180 minutes after treatment. Samples were collected from fully expanded mature leaves and from the newest set of young leaves. A total of 48 samples were collected for RNA-seq consisting of three replicates of each of the two tissue types from each of the two biotypes at the four different time points. The

tissue was immediately frozen in liquid nitrogen upon collection and stored at -80 °C until total RNA was extracted. Preparation of mRNA libraries, sequencing, and initial quality control was completed by Fasteris DNA Sequencing Service (Geneva, Switzerland). The 48 libraries were sequenced using Illumina Hiseq2500, producing 125 bp paired end reads.

Alignment of reads to reference genome

The quality of raw reads was assessed using FastQC [v0.11.9] (Andrews 2010). Sequencing adapters and reads with a phred score of less than five were removed and read quality was again confirmed using Fastp [v0.23.3]Chen et al. (2018). The trimmed reads were aligned to a reference genome of *A. trifida* supplied by the International Weed Genomics Consortium, with STAR (version 2.7.10b) using a per-sample two pass alignment with default settings (Dobin et al. 2013; Montgomery et al. 2023). The resulting sequence alignment map (SAM) files, were then compressed to binary alignment map (BAM) format and indexed using Samtools (version 1.17) (Li et al. 2009). The number of reads mapped to each gene was quantified and formatted into a counts matrix using featureCounts from the Subread package (version 2.0.6)(Liao et al. 2013).

Differential Gene Expression Analysis

The gene-level matrix of read counts, a metadata file of per-sample phenotype information, and functional gene annotation parsed from the general feature format (GFF) file of the *A. trifida* reference genome were loaded into RStudio version 2023.03.0+386, (Team 2020). The 16 sample groups for comparison were labeled as follow: RM-0, RM-15, RM-60, RM-180, RY-0, RY-15, RY-60, RY-180, SM-0, SM-15, SM-60, SM-180, SY-0, SY-15, SY-60, SY-180,

with R or S indicating resistant or susceptible phenotype, Y or M indicating young or mature leaves, and 0, 15, 60, or 180 indicating minutes after treatment (MAT). The limma package was used to filter genes with low expression, scale library sizes, and fit the counts to a linear model to test for significant differences in transcript abundance (v3.56.2)(Ritchie et al. 2015). Genes were filtered out as too low expressed if counts were below a count per million (CPM) cutoff corresponding to less than 10 counts in all three replicates of at least one sample group. The counts were normalized to account for differences in library size between samples using trimmed mean of M-values (TMM) library scaling (Robinson and Oshlack 2010). Voom transform method was applied to the TMM scaled counts (Law et al. 2014). The mean-variance relationship and appropriate observation-level weights were estimated and the counts were then fit to a linear model accounting for correlation of paired samples across the treatment time course (Law et al. 2014). Differential expression was assessed by applying empirical bayes statistics to the linear model in sets of pre-determined contrasts to compute moderated t-statistics, F-statistic, and log-odds of differential expression (v3.56.2) (Ritchie et al. 2015). Due to the relatively conservative nature of this method the package authors suggest using a fold change threshold much lower than the desired cutoff. Based on the package information a fold change threshold of 1.25 ($Log_2FC = \sim 0.32$) was selected with a false discovery rate of 5% (adjusted p value < 0.05). Statistical contrasts were applied in pairs to assess glypohsate response by comparing post-treatment time points, 15-MAT, 60-MAT, and 180-MAT, of a given sample with itself at 0-MAT. To assess constitutive differences between resistant and susceptible individuals, and discover genes differentially expressed at all time-points a direct comparison of RM vs SM and RY vs SY was conducted at 0, 15, 60, and 180 MAT. Results of each contrast were both manually processed and used for gene ontology (GO) over representation analysis. Venny 2.1

was used to compare quantities of genes in each set of contrasts and to identify genes exclusive to resistant plants (Oliveros 2015).

Five published housekeeping genes were selected as candidate reference genes for candidate gene validation via reverse transcription quantitative polymerase chain reaction (RT-qPCR). The coding sequences for *ef1-α, eIF-4a, GAPDH, importin*, and *SAND* from *Helianthus annus* and *Arabidopsis thaliana* were obtained from the National Center for Biotechnology Information (NCBI). The reciprocal best hit in *A. trifida* was determined using NCBI BLAST to the coding sequences of the *A. trifida* reference genome. Another nucleotide BLAST found similar genes in *A. trifida* to ensure primer specificity regions of sequence with exact alignments were avoided. Primers for the glyphosate resistance candidate genes were designed by aligning the coding sequence to other genes with high sequence similarity and targeting primer design to regions of specificity toward the candidate gene.

To investigate expression patterns in two known families of genes related to non-target site resistance ATP binding cassette (ABC) transporters and aldo-keto reductases (Liu et al.) gene sequences of these families in *Helianthus annus* and *Arabidopsis thaliana* were obtained from the National Center for Biotechnology Information (NCBI). Reciprocal BLAST was used to find potential orthologous genes in the A. trifida genome. These genes were plotted in R studio to manually examine interesting patterns.

A gene ontology (GO) over-representation analysis was conducted on significant DEGs (Hong et al. 2014). The GO annotations were acquired from the general feature format (GFF) file of the *A. trifida* reference genome, as well as BLAST to the protein sequence of the *Helianthus annus* reference genome. Only those genes that passed the expression threshold filter for DEG

analysis were used as the background gene set for the analysis. A Fisher exact test was used to determine which GO terms were overrepresented in contrasts that had DEG results. The TopGO package was used for the analysis, using the weight01 algorithm which combines the elimination and weight based methods of decision making along the GO graph structure (Alexa et al. 2006).

Exploratory Data Visualization

Principle component analyses (PCA) was used to assess overall trends in sample grouping and variation(Pearson 1901). The prcomp function in R was ran on the Voom normalized counts (Team 2020; Law et al. 2014). A scree plot was generated to visualize the proportion of variation explained by the first 12 principal components. All pairs of the first five principal components were plotted for further exploration. PCAtools (version 2.14.0) was used to identify and plot the top 5% of the loadings of PC3 (Blighe and Lun 2019). A matrix of sample-to-sample distances were calculated on the Voom normalized counts and plotted on a heatmap using the pheatmap package (version 1.0.12) (Kolde 2019).

Phytohormone Analysis

The previously described TMM normalized counts were used to generate heatmaps for genes in the biosynthesis pathways of jasmonic acid (JA), salicylic acid (SA), abscisic acid (ABA), indole-3-acetic-acid (IAA). To quantify phytohormones at the metabolomic level, plants were grown, treated, and collected similarly to methods described for RNAseq; however, the earliest timepoint was adjusted to 30 minutes after treatment to facilitate additional time for metabolomic changes to occur. To avoid measuring phytohormone response to wounding associated with tissue collection, each time point was collected from an individual plant rather

than collecting from a single plant across all time points. Leaf samples were immediately frozen in liquid nitrogen and stored at -80° C until they were lyophilized, homogenized, and extracted with organic solvents. The extracts were analyzed along with standards using UPLC-MS/MS for targeted metabolic profiling of JA, SA, ABA, IAA, and indole-3-carboxylic acid (ICA). Observation of extreme values in S-rep 2 throughout the dataset, as well as lesion development soon after treatment guided the decision to exclude susceptible replicate two from the analysis. A one-way analysis of variance (Brumos et al.) and a-priori contrasts on the linear model were used to determine if phytohormone quantities were significantly different in different samples.

Characterization of two EPSPS loci

Initial exploration of a De Novo transcriptome assembled from the previously described RNAseq reads using Trinity (version 2.14.1) revealed two potential *EPSPS* loci (Grabherr et al. 2011). The trimmed sequencing reads were aligned to a fasta file consisting of the two EPSPS loci in the *A. trifida* reference genome using Hisat2 (Kim et al. 2019). The resulting SAM files were compressed to BAM format and indexed using Samtools (Li et al. 2009). For each individual plant the BAM files for the two tissue types and the four time points were merged into a single BAM file. The BAM files were visualized in Integrative Genome Viewer (IGV) to examine the reads associated with each version of the loci. Consensus sequences from each RNAseq sample were aligned using MUltiple Sequence Comparison by Log- Expectation (version 3.8.155) (Edgar 2004). Expression of each *EPSPS* locus over time was explored in the normalized counts previously described in the DEG analysis.

Oligonucleotide primers were designed for Kompetitive allele specific PCR (KASP) genotyping assay to introduce a HEX fluorophore to amplicons with a proline allele at the

second *EPSPS* loci (5’-GAAGGTCGGAGTCAACGGATTGGAACYGCTATGCGTC-3’) or a FAM fluorophore to those with a serine allele (5-GAAGGTGACCAAGTTCATGCTGGAACYGCTATGCGTT-3), along with a universal reverse primer (5’-CCTTGAGTTTCCACCAGC-3’). Degenerate bases were incorporated to account for variants found by running the GATK variant calling pipeline on the aligned reads (Van der Auwera and O'Connor 2020). Multiple sets of primers for qPCR with specificity to either *EPSPS1* or *EPSPS2* were generated by aligning the two genes and designing primers in areas specific to one or the other, efficiency of these primers will be tested and included in future reports for quantifying gene expression or copy number variation.

2.3 RESULTS AND DISCUSSION

Exploratory Data Visualization

To assess sample grouping and sources of variance in the dataset a principal component analysis (PCA) was conducted, and sample-to-sample distances were calculated and visualized on a heatmap. The PCA revealed that 46.29% of the variance in the data is explained by PC1 (Figure 2.1) 15.45% was explained by PC2, and 8.41% by PC3 (Figure 2.2). Samples grouped by tissue type along PC1, and by biotype along PC3. The loadings for PC3 revealed that six genes made up the top 5% contributing to the variance explained by PC3, these were *Osmotin34* (*OSM34*), an inositol tetrakisphosphate-1-kinase 3-like protein, a subtilisin-like protease, a histone H2A, putative C2 domain-containing protein, and a phosphorylase superfamily protein (Figure 2.2). The heatmap of sample-to-sample distances revealed that sample groups generally shared the lowest sample distances, but tissue type showed a strong influence on the sample distances (Figure 2.3).

Differential Gene Expression Analysis

Of the total 43,884 genes in the *A. trifida* reference genome 15,537 were filtered out as too lowly or not expressed. The DEG analysis and subsequent GO over-representation analysis were conducted on these remaining 28,347 genes. The number of differentially expressed genes from each contrast was relatively low at the early timepoints, 15 and 60 minutes, but dramatically increased by 180 minutes after treatment, more-so in the resistant tissues (Table 2.1).

Some ATP-binding cassette (ABC) transporters and Multidrug and Toxic Compound Extrusion (MATE) transporters were significantly induced in resistant tissue, however transcript abundance was relatively low compared to many other genes (Table2.5; Figure 2.15) Based on previous studies and observed low transcript abundance of other genes that were significantly induced by 180-MAT, it was considered that three hours after treatment may be too early to capture responses in many genes. Previous studies examining expression of ABC transporters in glyphosate resistance reported significant expression at 1-4 days after treatment (Moretti et al. 2017; Tani et al. 2015). This gene family has been implicated in the past studies of glyphosate resistance. If these proteins are important carriers of glyphosate in *A. trifida* either up or down regulation could be important. Downregulation of a carrier required for systemic glyphosate translocation could prevent systemic inhibition of the glyphosate target site. If these transporters facilitate exclusion of glyphosate from sink cells or chloroplast, then upregulation may sequester glyphosate away from the target site. Previously upregulation of ABC transporters conferring glyphosate resistance has been supported by previously studies in *Conyza bonariensis* and *Echinochloa colona* (Moretti et al. 2017; Pan et al. 2021).

An aldo-keto reductase (Liu et al.) was significantly up-regulated in resistant mature tissue by 60-MAT and in both resistant young and mature tissue by 180-MAT (Table 2.5; Figure 2.15). While metabolism of glyphosate has not been as commonly reported as other herbicides, there is strong evidence that a population of *Echinochloa colona* has evolved an aldo-keto reductase capable of metabolizing glyphosate to aminomethyl phosphonic acid (Kanissery et al. ; Pan et al. 2019a). In *E. colona* an aldo-keto reductase was up-regulated compared to susceptible populations, and the ability to confer resistance and metabolize glyphosate was confirmed in transgenic *Oryza sativa* and *Escherichia coli* heterologous expression systems.

In both the susceptible and resistant tissues there were many pathogen defense genes responding to glyphosate. Differences in the response between the susceptible and resistant individuals may reveal how changes in a normal pathogen response could contribute to glyphosate resistance. Differences in phytohormones involved in stress response were explored and discussed in the following section. Many genes related to pathogen perception and response were upregulated in resistant plants. Several types of nucleotide binding leucine rich repeat (NB-LRR) proteins and receptor like kinases (RLKs) were constitutively higher or induced in response to glyphosate. Disease resistance protein RPV1, an NB-LRR was upregulated in both young and mature resistant leaves by 180 minutes after treatment. Malectin-like receptor kinases such as *FERONIA (FER*) were significantly higher in resistant plants. These genes have roles in pathogen perception and response that involve several other proteins that are also transcriptionally upregulated in resistant leaves such as RIN4, RPM1, and RALF33 (Franck et al. 2018). The type of pathogen interaction determines which specific signaling routes are affected, in the case of pathogen associated molecular pattern perception FER activity resulted in a burst of ROS through the activation of RbohD, a process involving proteins FLS2, ERF, and BAK1

(Franck et al. 2018). All of which are transcriptionally up regulated in resistant *A. trifida*. The hypersensitive response (HR) is a plant immune response involving some of these proteins and others that are upregulated in resistant mature leaves such as Heat shock protein 90 (Hsp90), which is upregulated in resistant mature leaves, but down regulated in young leaves, matching the pattern of the rapid cell death response. HR and other cellular response rely on transporters of calcium ions and its interaction with binding protein calmodulin, both of which are upregulated in resistant leaves (Yuan et al. 2022). A key difference in HR and the cell death observed in the rapid response biotype of *A. trifida* is that HR is localized to the site of pathogen infection, while the rapid response resembles a run-away cell death through the entire mature leaf. This could be due to changes in the genes that typically regulate HR. Type one metacaspases are required for HR cell death, while Lesion Stimulating Disease 1 (LSD1) and metacaspase 2 typically antagonize cell death in cells adjacent to infection (Coll et al, 2014). While *metacaspase type 1* is upregulated in mature leaves of resistant *A. trifida*, *LSD1* and *metacaspase 2* are not indicating that other factors are likely contributing to the run-away cell death. A gene annotated as HR-like lesion inducer is up-regulated in young and mature resistant leaves, but slightly more-so in mature. This gene is believed to mediate HR-like cell death against turnip mosaic virus (Wu, 2021). Other genes up regulated in this dataset that are related to HR or other pathogen defense include a variety of map kinases, and several WRKY transcription factors. The top gene from the loadings of PC3, which explained the most variation between resistant and susceptible plants, and a top DEG at all time points for resistant plants was *Osmotin 34 (OSM34).* This pathogenesis-related protein may also have roles in abiotic stress response Anil Kumar et al. (2015). It is believed to have roles in signal transduction for programmed cell death and for activation of antioxidant systems in plants. Ubiquitin ligases were also highly represented in the

DEG results, while though these proteins have roles throughout most processes in plants, they have been cited as a potential bridge between biotic and abiotic stress responses, which could be the case with herbicide response and pathogen response pathways (Stone 2022).

A gene ontology analysis was used to determine what processes and functions are enriched in the full set of significant DEGs by comparing the proportion of genes annotated with a given ontology to the expected occurrence based on the background set of expressed genes. Jasmonic acid (JA) biosynthesis and immune response processes were enriched in the upregulated DEGs from mature resistant plants by 60 (table 2.4). The processes shifted by 180 minutes toward processes that may be related to the rapid cell death, such as vesicular transport (Figure 2.5). Phosphate transport was also among the significantly enriched down regulated processes, perhaps contributing to the reduced translocation attributed to cell death in previous translocation studies (Moretti et al. 2018).

Phytohormone analysis

Transcript abundance revealed trends associated with tissue age in most steps of the JA biosynthesis pathway; however, some differences were observed specifically between resistant and susceptible tissues (Figure 2.6). In resistant mature leaves many genes for JA biosynthesis were strongly upregulated by 180 minutes after treatment. A similar pattern could be observed in mature susceptible leaves but to a lesser degree. Other genes, such as an isoform of *LOX2* were constitutively higher in resistant mature leaves. The gene ontology analysis also revealed that genes involved in JA biosynthesis were highly enriched in resistant mature leaves by 60 minutes after treatment (Figure 2.4). At the metabolomic level a significant increase of JA in the mature

leaves was measured by 180 minutes (Figure 2.11). JA can be rapidly synthesized in response to wounding or pathogen perception (Griffiths 2020).

A decrease in SA was measured in RY tissue at all time points after treatment, and in SM by 180 minutes after treatment. SA levels are lower after treatment in SY, like RY but it is not a significant decrease by 180 MAT (Figure 2.11) There is a slight decrease of SA in RM leaves at 30 and 60 minutes, however by 180 MAT concentrations are very similar to those in RM untreated (Figure 2.11). Rapid signaling for JA biosynthesis could repress SA biosynthesis, however if this is the case it is relieved by 180 minutes in RM tissues. The isochorismate (Williams et al.) pathway is often attributed to synthesizing the majority of salicylic acid in plants. Recent work indicates that the alternative pathway phenylalanine ammonia lysate (PAL) may not generate any SA in *A. thaliana* but is likely involved in pathogen response in other species (Wu et al. 2023). In RM tissue *A. trifida* PAL was significantly upregulated (Figure 2.7). The two known SA biosynthesis pathways both require chorismate from the shikimate pathway, it would not be unexpected for SA precursors to become depleted in populations with a sensitive EPSPS enzyme, however full inhibition would likely occur on a larger time scale. If SA levels are naturally depleted rapidly after glyphosate treatment, antagonistic suppression of JA may be relieved allowing a momentary increase of JA (Caarls et al. 2015). Conversely, biosynthesis of JA, elicited by glyphosate treatment could be causing a repression in SA that is recovered by 180 minutes. Indeed, JA and SA could be undergoing antagonistic regulation with one-another, however JA and SA can also act synergistically. It is believed that SA may antagonize JA through *COI1*-mediated signaling but that *NPR3*, a gene related to the SA receptor *NPR1* may be able to induce JA responsive genes during effector triggered immunity (Liu et al. 2016). *NPR3* is also upregulated in resistant leaves of *A. trifida.* The observations at 180 minutes that JA

increased exclusively in RM, while SA resisted down-regulation indicates that these phytohormones are acting differently in resistant compared to susceptible plants. It is possible that the burst of ROS previously observed in RM leaves is induced through JA signaling or the synergism of JA and SA (Moretti et al. 2018). The rapid cell death associated with the oxidative burst may decrease the amount of glyphosate that reaches the apical meristem by 24 hours, but question remains if JA and SA have further roles in glyphosate resistance. These compounds are often conjugated to sugars, amino acids, or other functional groups to achieve an active form as in the case of JA-Ile, or to be sequestered away for storage (George Thompson et al. 2017). This dynamic should be considered in future discussion and quantification of phytohormones in response to glyphosate.

Abscisic acid has been well characterized in abiotic stress response and in some cases of pathogen defense. ABA dependent regulators of stress response signaling, such as dehydration-responsive element-binding proteins were highly represented in the DEG results. Resistant mature leaves showed increased transcript abundance for steps of ABA biosynthesis (Figure 2.10). However, at the metabolomic level no major changes were observed in ABA in resistant leaves at by 3 hours. ABA did increase in susceptible tissues, perhaps a normal response to glyphosate that was repressed by signaling related to the resistant biotype. Antagonism of SA to ABA has been reported during defense responses (Moeder et al. 2010).

Indole based auxin phytohormones have many roles in plant growth and development and have been observed to decrease in response to glyphosate treatment (Westwood and Biesboer 1985). In *A. trifida* the auxin phytohormones IAA and ICA responded similarly to glyphosate in both biotypes with a complete depletion in all tissues after treatment. Like SA, biosynthesis of

these metabolites is also downstream to the shikimate pathway, however being a derivative of tryptophan, chorismate is the last molecule in common with SA biosynthesis.

Glyphosate target site inhibition consequently inhibits the biosynthesis pathways of phytohormones salicylic acid (SA) and auxins. It has also been suggested that glyphosate elicits effects for other phytohormones such as jasmonic acid (JA), though these are not fully understood (Fuchs et al. 2021). Differential transcriptomic and metabolomic responses presented here in resistant and susceptible *A. trifida*, suggest some direct association between phytohormone signaling and glyphosate resistance and/or the rapid response. Similar to their roles in pathogen or herbivore response, it is plausible that JA and SA signaling are intricately linked to the rapid evolution of ROS observed in the mature leaves of the rapid response biotype of *A. trifida* (Caarls et al. 2015; Moretti et al. 2018). The resulting rapid cell death and consequent reduction of glyphosate translocation from the mature leaves is a conceivable link between phytohormone signaling and increased chance that a plant may survive glyphosate treatment. Other gene candidates could allude to other roles of JA in glyphosate resistance. Genes involved in multiple steps of the JA biosynthesis pathway were up regulated or constitutively higher in resistant mature tissue including multiple lipoxygenases (*LOX*). Interestingly several genes annotated as the receptor for JA, *COI1,* were downregulated in resistant mature tissue after treatment. When levels of the most active form of JA, a conjugate with isoleucine, increase it interacts with *COI1* leading to the formation of a complex that ultimately releases transcriptional repression of JA responsive genes through ubiquitination of repressors for proteasomal degradation (Yan et al. 2018). Several genes annotated as JAZ proteins, the repressors of JA responsive genes, were upregulated in resistant mature leaves. It is possible that *COI1* down regulation and JAZ upregulation were responses to rising JA levels and

part of normal regulatory processes that keep JA responses in check. One of the most abundant gene families throughout the DEG results were members of the transcription factor family AP2/ERF. These transcription factors regulate a variety of genes related to abiotic stress responses including cold, drought, salt, heat, flooding, and are positive regulators of JA-mediated stress responses through *COI1,* such as wounding and pathogen response (Xie et al. 2019; Santner and Estelle 2007). While this large family has members with various expression patterns in the data set, a majority are up regulated in either resistant tissue compared to susceptible.

Characterization of two EPSPS loci

Previous Sanger sequencing of PCR amplicons suggested that GR *A. trifida* did not have any mutations in the glyphosate target site, *EPSPS* (Van Horn et al. 2018). Given the observation that high-coverage Illumina transcriptome sequencing can reveal *EPSPS* mutations not found by direct sequencing of PCR products (McElroy and Hall 2020), the contigs annotated as *EPSPS* a previously *De Novo assembled* transcriptome were examined for differential expression and sequence variants. While multiple contigs existed as likely assembly errors two distinct *EPSPS* genes were characterized by differences in sequence including alternative codons at proline 106 (Pro^{106}). Not only did one contig have reads coding for a serine at this position, a mutation known to confer glyphosate resistance, but the wild-type codon was also varied at the third position (Table 2.2; Figure 2.12). Availability of the *A. trifida* reference genome confirmed that one copy of the *EPSPS* gene is on chromosome 4 and the second copy is on chromosome 12, hereby called *EPSPS1* and *EPSPS2*, respectively. It was determined from the differential expression analysis that *EPSPS2* becomes significantly upregulated in the mature leaves of resistant individuals by three hours after treatment (Figure 2.13). Induction of *EPSPS* is

considered a mechanism of resistance in a population of *E. indica* where induction was observed beginning at 12 hours and peaking at 48 hours (Zhang et al. 2015). It was determined that there are changes in transcription factor binding motifs in the promotor region upstream of *EPSPS*, leading to loss of interaction with some transcription factors while other transcription factors that were found to interact were also differentially regulated after glyphosate treatment (Zhang et al. 2018; Zhang et al. 2021). Validation of the observed up-regulation in *A. trifida* and quantification beyond three hours after treatment can help determine if differential regulation of either *EPSPS* loci is involved in resistance.

One of three GR samples contained the Pro106Ser mutation in *EPSPS2*, while two of three GS samples contained the Pro106Ser mutation in *EPSPS2* (Table 2.2, Figure 2.12). To explore association of the Pro106Ser mutation to resistance, the most resistant and most susceptible individuals of a segregating F2 population were screened using a KASP genotyping assay. In agreement with the RNAseq results, the Pro106Ser mutation was identified in both resistant and susceptible individuals, however, susceptible individuals were only heterozygous for the serine mutation or homozygous for proline, while resistant individuals were sometimes heterozygous and sometimes homozygous for serine (Table 2.3; Figure 2.14). A linear regression of the occurrence of the mutant allele and dry mass 28 days post glyphosate treatment revealed an association of Pro106Ser to increased dry mass (Table 2.3; Figure 2.15). A Fisher's exact test on the observed proportion of each allele and survival also suggested association between the Pro106Ser mutation in *EPSPS2* and resistance (Table 2.4). These Pro106Ser KASP genotyping markers may be used to screen additional individuals and populations to further associate the mutation to resistance and generate a survey of resistance allele frequency. Seed collections with the mutation can be established for a dose response comparing resistance factors in homozygous

mutant and wild-type lines. Activity assays on the EPSPS enzyme could be carried out in vivo on individuals homozygous for the mutation, or in vitro, using the mutant EPSPS from *A. trifida.* Past results from similar experiments varied between populations and environments (Van Horn et al. 2018). The existence of a second *EPSPS* loci with an unknown frequency of resistance alleles may have contributed to the variable results and explain the observation that some populations showed a less sensitive EPSPS enzyme at lower doses of glyphosate but an apparent similar sensitivity to susceptible populations at higher doses as the pool of insensitive enzyme was quenched (Van Horn et al. 2018).

Expression of *EPSPS2* was significantly higher in the mature leaves of resistant replicates by 180MAT (Figure 2.13). Induction of *EPSPS* in response to glyphosate has been observed in a resistant population of *Eleusine indica* beginning around 12 hours after treatment and peaking at 48 hours (Zhang et al. 2021). In *A. trifida* the induction seen at three hours may be due to feed-back into the shikimate pathway in the rapidly dying mature leaves. To investigate if induction of *EPSPS2* has any role in glyphosate resistance, expression beyond the three-hour time point in young and mature leaves should be quantified. These results have confirmed the presence of target site mutation Pro106Ser. Though only some fraction of the total target site enzyme pool would consist of an insensitive form of EPSPS, this could favor survival under conditions that reduce glyphosate efficiently, synergistically endow resistance when other mechanisms are present. Given that these populations were collected over fifteen years ago, the KASP genotyping markers should be used on new collections to determine the abundance of the mutation, assess and monitor gene flow, and to identify seed stocks in which further experiments can characterize any associated resistance factor.

This transcriptomic dataset encompasses differentially expressed gene candidates for glyphosate resistance. Some of these have known roles in glyphosate activity or response, and some are potential candidates for novel mechanisms in resistance. The observed pathways and patterns provide some knowledge of how glyphosate affects signaling pathways in susceptible *A. trifida* as well as the unique resistant biotype. Based on the results, multiple hypotheses can be developed about the mechanism of resistance, including synergistic or additive activity of multiple resistance mechanisms. A subset of genes related to the pathways mentioned were selected as candidate genes of interest to be further validated with qPCR and potential functional validation (Table 2.5; Figure 2.15). This list includes many upregulated genes from resistant leaves such as ABCC and MATE transporters, an aldo-keto reductase (AKR), an NB-LRR related to disease resistant (RPV-1), metacaspase-1 (*MC1*), rapid alkalization factor33(*RALF33*) and its receptor kinase *FERONIA(FER)*, pathogenesis-related gene *osmotin-34* (*OSM34*), an *ethylene-responsive transcription factor* (*AP2/ERF*), an *allene oxide synthase (AOS)* and an *allene oxide cyclase (AOX)* from JA biosynthesis, the JA receptor *COI1*, and *phenylalanine ammonia lyase* (*PAL*) from SA biosynthesis.

The overall results of the transcriptomic analysis identified multiple candidates for glyphosate resistance. Some related to known mechanisms and others pointing to potential novel mechanisms that will require extensive validation. The results of the transcriptomic study widely implicated parallels between glyphosate response and biotic stress such as pathogen or herbivory response, or abiotic stress such as drought. Some stress response genes shared some transcriptional patterns between glyphosate-resistant and susceptible individuals such as many drought response transcription factors related to abscisic acid signaling, however this did not pan out to the metabolic level. Many key genes in well elucidated stress pathways were different in

resistant and susceptible, either constitutively or in response to glyphosate. Transcription of several genes involved in perception of pathogens and response signal relay were significantly higher in resistant tissues, including NB-LRR receptors, RLKs, map kinases, WRKY transcriptions, pathogenesis related proteins and ubiquitin ligases.

Quantification of phytohormones using targeted metabolomics identified patterns of phytohormone response to glyphosate in both resistant and susceptible individuals. In resistant mature leaves JA levels significantly increased by 180 minutes. SA levels decreased in all tissues by 30-60 minutes after treatment but return to pre-treatment quantities by 180 minutes in resistant mature leaves. These phytohormones also have key roles in the pathogen responses previously discussed, providing additional evidence that glyphosate resistance may share similar pathways as pathogen response.

A second locus of the glyphosate target site, EPSPS, was confirmed to contain a mutation known to confer resistance. A Pro106Ser mutation in this second target site gene was associated with increased dry mass after glyphosate treatment and survival. By 180 minutes after treatment EPSPS2 was significantly upregulated in resistant mature individuals.

To further characterize glyphosate resistance and the rapid response in *A. trifida,* future work will validate the differentially expressed genes described here and expand on the time course to explore how transporters, metabolic genes, and even the glyphosate target site *EPSPS*, are being expressed days after treatment. Another transcriptome wide approach or a targeted analysis such as RT-qPCR could be utilized to answer these questions. Phytohormone response may be associated with the rapid response or a novel glyphosate resistance mechanism. The traits could be isolated and studied independently by selectively self-pollinating individuals from a segregating F_2 populations. Generating, or obtaining, lines with more stable phenotypes would

facilitate larger sample sizes and reduced variation in phytohormone analysis and other studies. Utilization of published LCMS and GCMS based phytohormone quantification protocols could allow higher sample processing over time. Enzyme-linked immunosorbent assay (ELISA) is also a higher throughput option for phytohormone quantification in a microplate reader. To understand the role of specific candidate genes, or signaling molecules they interact with, a reverse genetics approach may involve silencing, knocking out, or over-expressing a target gene using a CRISPR cas9 system, virus induced gene-silencing, or similar methods. The amiability of *A. trifida* to stable or transient transformation must be assessed to determine the feasibility of such methods.

Additional genotyping of resistant and susceptible individuals can further validate the association of the Pro106Ser in *EPSPS2* to glyphosate resistance. The genotyping assay could also reveal or guide development of populations with a fixed mutant allele. This would allow further studies on the contribution to resistance. Experiments characterizing resistance can be repeated with the knowledge of the second EPSPS loci and frequency of Pro106Ser allele to better understand its role in resistance and clarify past results such as *EPSPS* activity assay.

2.4 TABLES

Table 2.1. Number of significant differentially expressed genes from each contrast that comparing susceptible young (SY), susceptible mature (SM), resistant young (RY), and resistant mature (RM) at 15, 60, and 180 minutes after treatment compared to 0 minutes after treatment or compared to each other at each time point. Base level of contrast is referenced at end of contrast name.

Contrast	SY 15vs0	SY 60v0	SY 180 vs0	SM 15 vs0	SM 60 vs0	SM 180vs0
Down	0	2	891	10	51	2994
NotSig	28347	28343	25190	28337	28104	22594
Up	0	2	2266	0	192	2759

Contrast	RY 15vs0	RY 60vs0	RY 180vs0	RM 15vs0	RM 60vs0	RM 180vs0
Down	0	2	2080	8	736	5135
NotSig	28335	28334	22035	28315	26195	17485
Up	12	11	4232	24	1416	5727

Contrast	SYvsSM 0	RYvsSY 0	RMvsSM 0	RMvsRY 0
Down	6281	303	358	5949
NotSig	15715	27792	27634	16433
Up	6351	252	355	5965

Contrast	SYvsSM 15	RYvsSY 15	RMvsSM 15	RMvsRY 15
Down	5086	348	286	5136
NotSig	19081	27702	27721	18306
Up	4180	297	340	4905

Contrast	SYvsSM 60	RYvsSY 60	RMvsSM 60	RMvsRY 60
Down	6778	342	392	6381
NotSig	15253	27701	27522	16281
Up	6316	304	433	5685

Contrast	SYvsSM 180	RYvsSY 180	RMvsSM 180	RMvsRY 180
Down	6844	474	1656	6868
NotSig	16745	27101	24177	16304
Up	4758	772	2514	5175

Table 2.2. Reads from glyphosate-resistant (GR) or glyphosate susceptible (GS) RNAseq samples aligning to A. *EPSPS1* or B. *EPSPS2* with either a wild-type (C) or mutant (T) at the first position of the codon for Pro^{106}.

A. EPSPS1

	GR 1	GR 2	GR 3
CCT (Proline)	566	528	324
TCT (Serine)	0	0	0

	GS 1	GS 2	GS 3
CCT (Proline)	544	244	374
TCT (Serine)	0	0	0

B. EPSPS2

	GR 1	GR 2	GR 3
CCG (Proline)	483	244	1
TCG (Serine)	0	245	951

	GS 1	GS 2	GS 3
CCG (Proline)	281	578	0
TCG (Serine)	318	0	550

Table 2.3. Linear regression of Ser^{106} allele frequency to dry mass of 28 days after glyphosate treatment. Model statistics and equation given below.

Predictor	Estimate	Std. Error	t value	Pr (>|t|)
Intercept	1.1867	0.1855	6.398	8.90E-07
Allele	1.3121	0.1823	7.199	1.21E-07

F-statistic: 51.82 adjusted R^2: 0.6531 p-value: 1.206e-07

Dry mass(g) = 1.19 + 1.31 * T Allele

Table 2.4. Contingency table of genotypes and survival of 28 F2 individuals selected to assess association between strong glyphosate survival and the Pro^{106}Ser mutation in *EPSPS2.* Fisher exact test P-value, 95% confidence interval and odds ratio are given.

Genotype	Survive	Dead	Total
CCG (Pro)	0	11	11
TCG (Ser)	10	0	10
CCG /**T**CG	4	3	7
Total	14	14	28

Fisher's Exact Test p-value = 0.0006
95 percent confidence interval: 0.008 - 0.4018
Odds ratio: 0.068

Table 2.5. Differentially expressed genes selected as candidate genes of interest for glyphosate resistance or the rapid response.

			Average TMM scaled CPM							
			Young				Mature			
Gene	Name	Biotype	0	15	60	180	0	15	60	180
AmbTrChr02Ag092180	MATE	GR	0.07	0.20	1.40	1.84	0.85	1.14	24.61	16.64
		GS	0.05	0.10	0.32	0.20	0.57	0.56	3.54	4.59
AmbTrChr05Ag165360	ABCC	GR	0.21	0.33	1.32	22.88	1.56	0.93	2.29	87.79
		GS	0.06	0.15	0.13	0.98	1.61	0.26	1.34	8.56
AmbTrChr02Ag086930	ABCC	GR	0.00	0.01	0.03	0.39	0.07	0.03	0.04	1.90
		GS	0.00	0.03	0.00	0.02	0.02	0.00	0.03	0.15
AmbTrChr05Ag194110	Aldo-keto reductase	GR	34.88	41.02	41.02	324.53	46.50	48.21	133.58	515.16
		GS	41.26	43.34	47.11	90.61	46.42	41.59	69.66	199.23
AmbTrChr10Ag358190	RPV1	GR	12.71	15.94	16.90	75.08	35.70	34.23	25.71	95.24
		GS	0.88	0.93	0.97	4.30	2.07	1.75	2.78	7.84
AmbTrChr01Ag007550	COI1	GR	4.61	4.53	6.06	4.80	7.23	8.86	3.09	1.56
		GS	5.18	5.10	4.63	5.10	9.04	6.46	3.90	5.81
AmbTrChr09Ag320850	AOC	GR	3.42	7.01	11.64	3.03	28.10	31.93	352.20	304.39
		GS	2.50	1.51	1.67	4.37	18.74	10.55	38.71	15.13
AmbTrChr09Ag313240	AOS	GR	0.84	8.85	9.67	3.57	4.56	18.58	164.47	17.93
		GS	0.53	1.10	7.92	1.51	4.75	3.33	49.21	8.24
AmbTrChr04Ag133640	PAL	GR	66.63	44.71	104.49	325.54	64.00	83.16	112.41	1309.12
		GS	84.35	39.81	62.56	244.81	60.19	81.42	98.31	181.08
AmbTrChr12Ag415790	AP2/ERF	GR	2.07	3.72	6.46	5.36	5.68	12.88	204.52	58.10
		GS	2.27	3.80	3.83	6.22	4.54	6.33	57.43	12.51
AmbTrChr01Ag026540	FERONIA	GR	0.37	1.13	2.80	56.62	13.74	6.26	21.12	51.17
		GS	0.34	0.21	1.38	14.46	6.78	1.22	7.86	24.17
AmbTrChr08Ag300380	RALF33	GR	19.72	39.91	26.01	68.18	8.95	48.04	122.34	218.76
		GS	18.72	24.97	14.01	56.22	12.25	22.70	63.11	55.36
AmbTrChr03Ag098360	MC1	GR	4.38	12.40	12.94	118.15	9.72	20.16	64.71	361.51
		GS	4.88	6.03	7.79	63.20	6.93	9.46	62.91	46.48
AmbTrChr05Ag195350	OSM34	GR	104.36	104.37	53.90	6.57	588.36	609.50	371.20	129.12
		GS	0.00	0.00	0.00	0.01	1.18	0.40	0.54	0.45
AmbTrChr10Ag354160	HR-like lesion inducer	GR	20.51	20.41	11.10	16.92	5.52	6.65	9.65	24.24
		GS	15.51	16.06	14.34	10.28	4.37	6.77	9.42	5.49

2.4 FIGURES

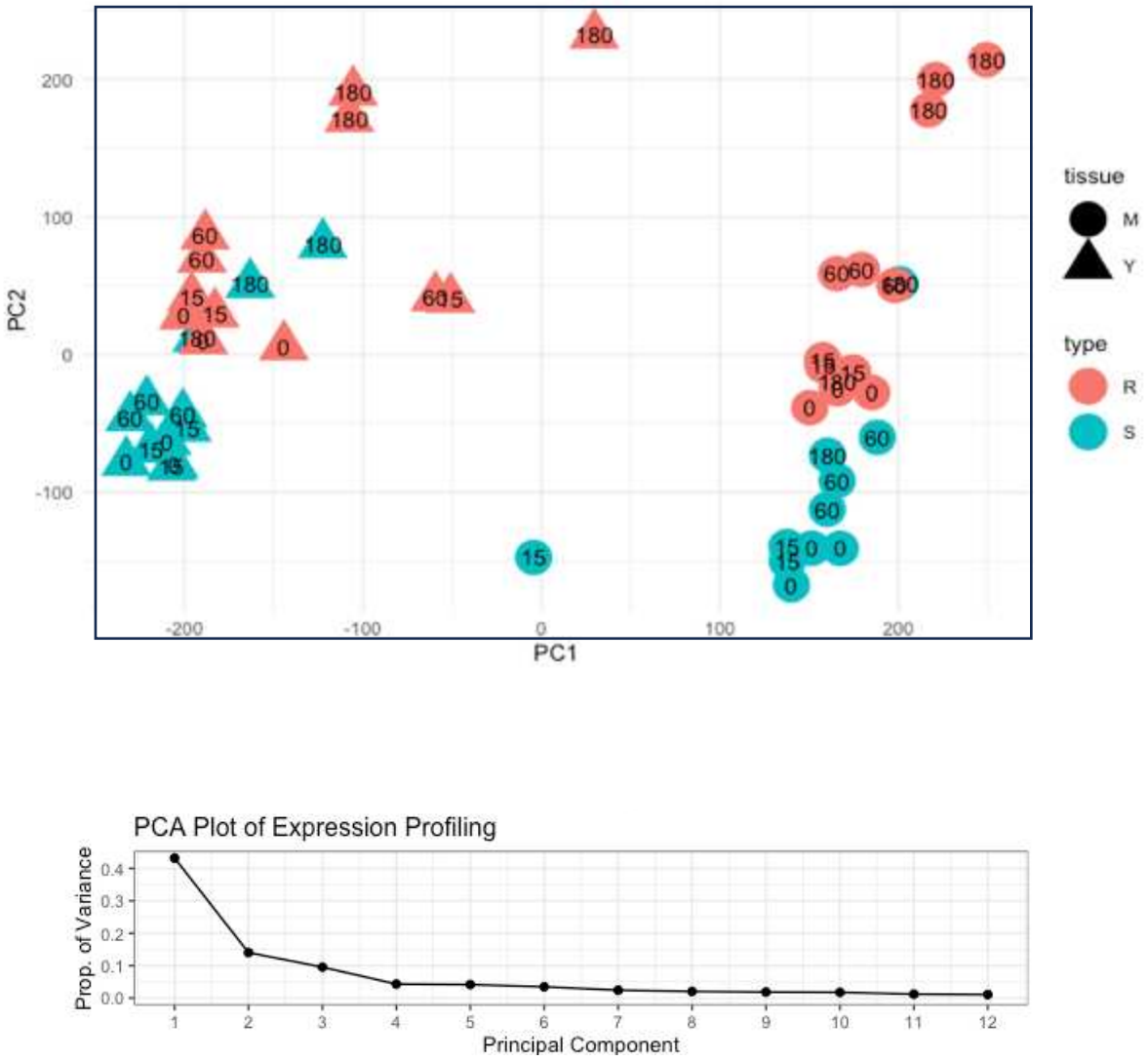

Figure 2.1. PCA plot of PC1 and PC2 and scree plot showing expression profiling across first 12 principal components

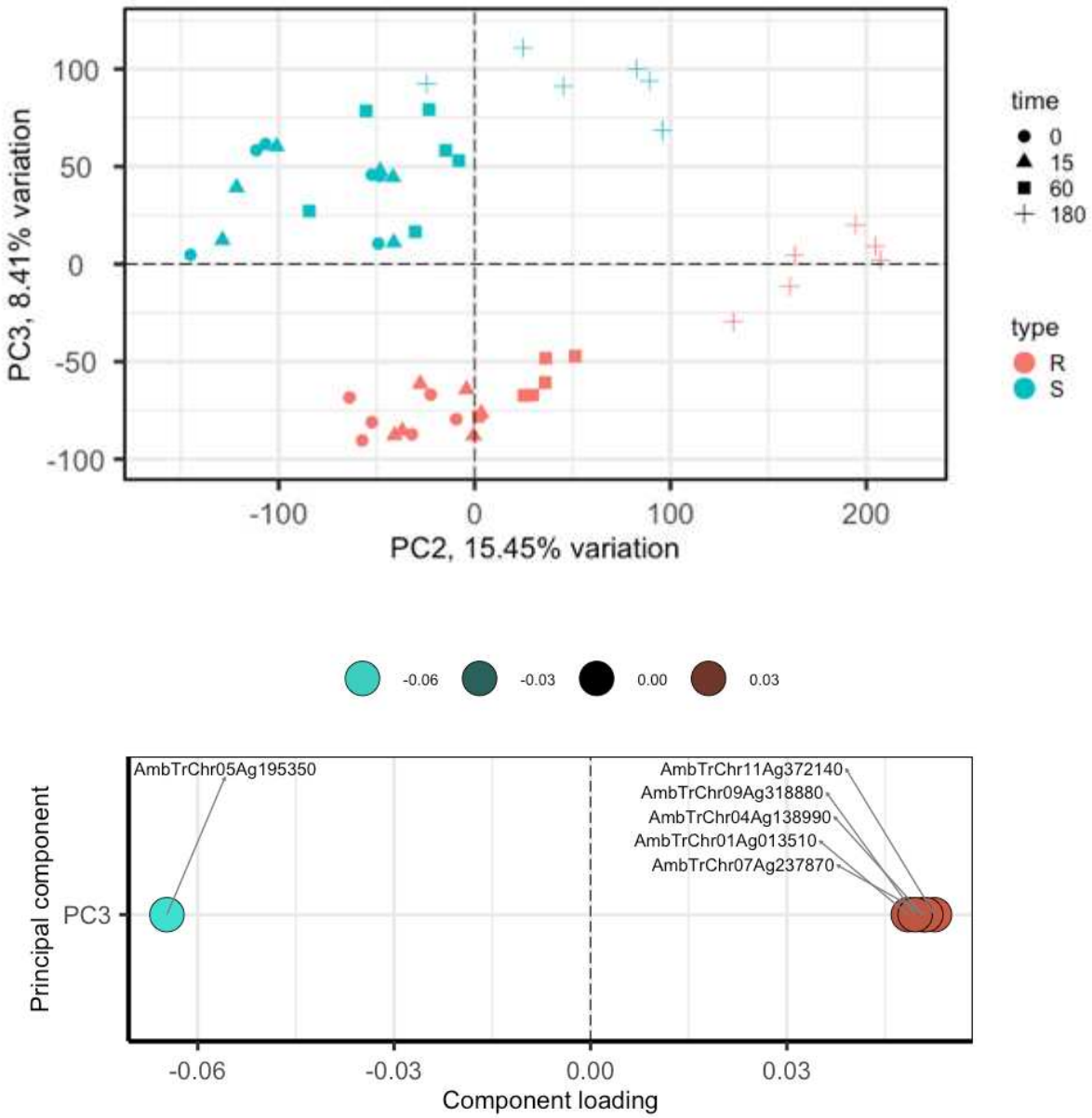

Figure 2.2. Plot of PC2 and PC3 loadings plot for PC3 showing top 5% of genes contributing to variation.

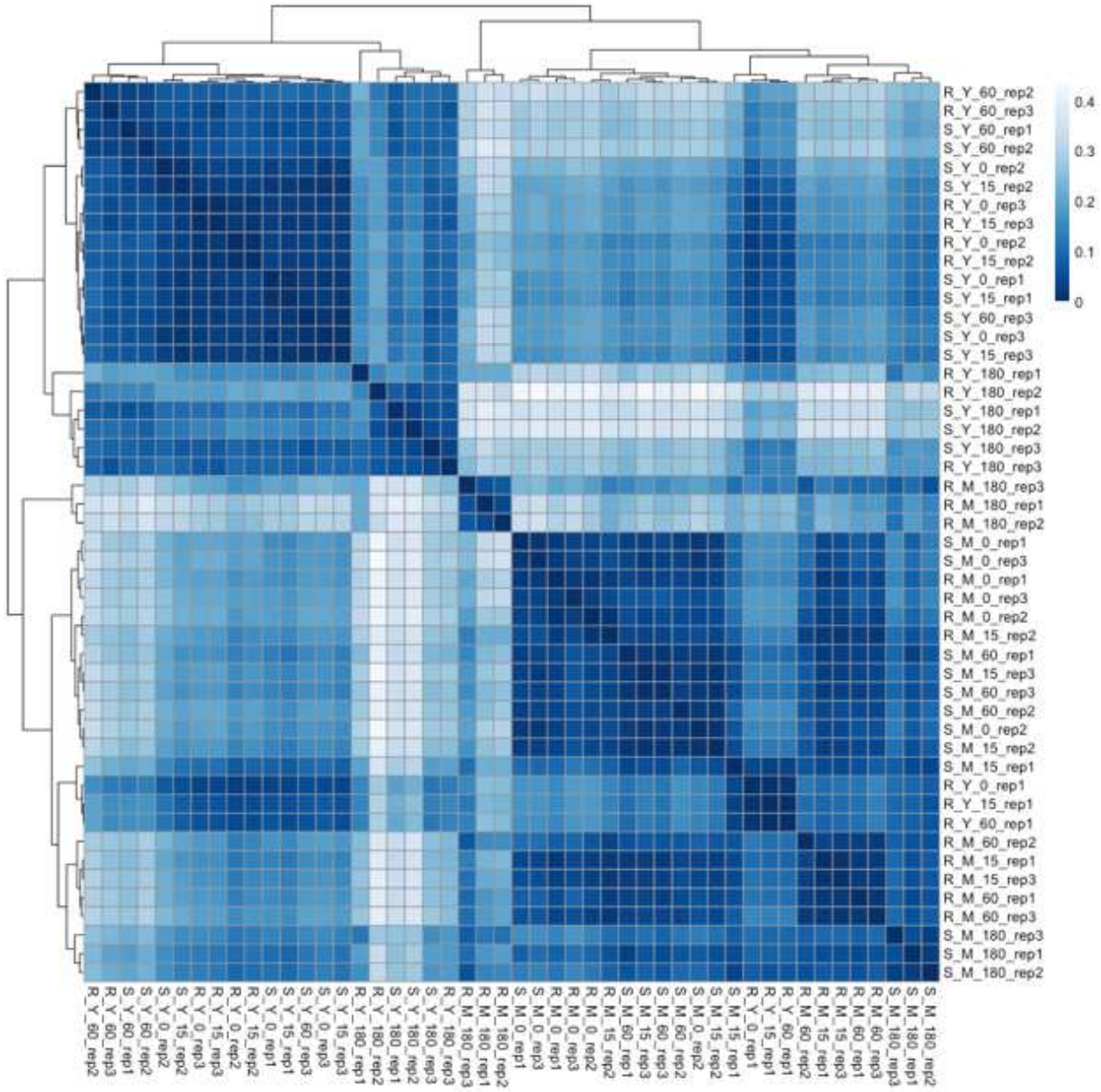

Figure 2.3. Heatmap of sample-to-sample distances for all 48 RNAseq samples.

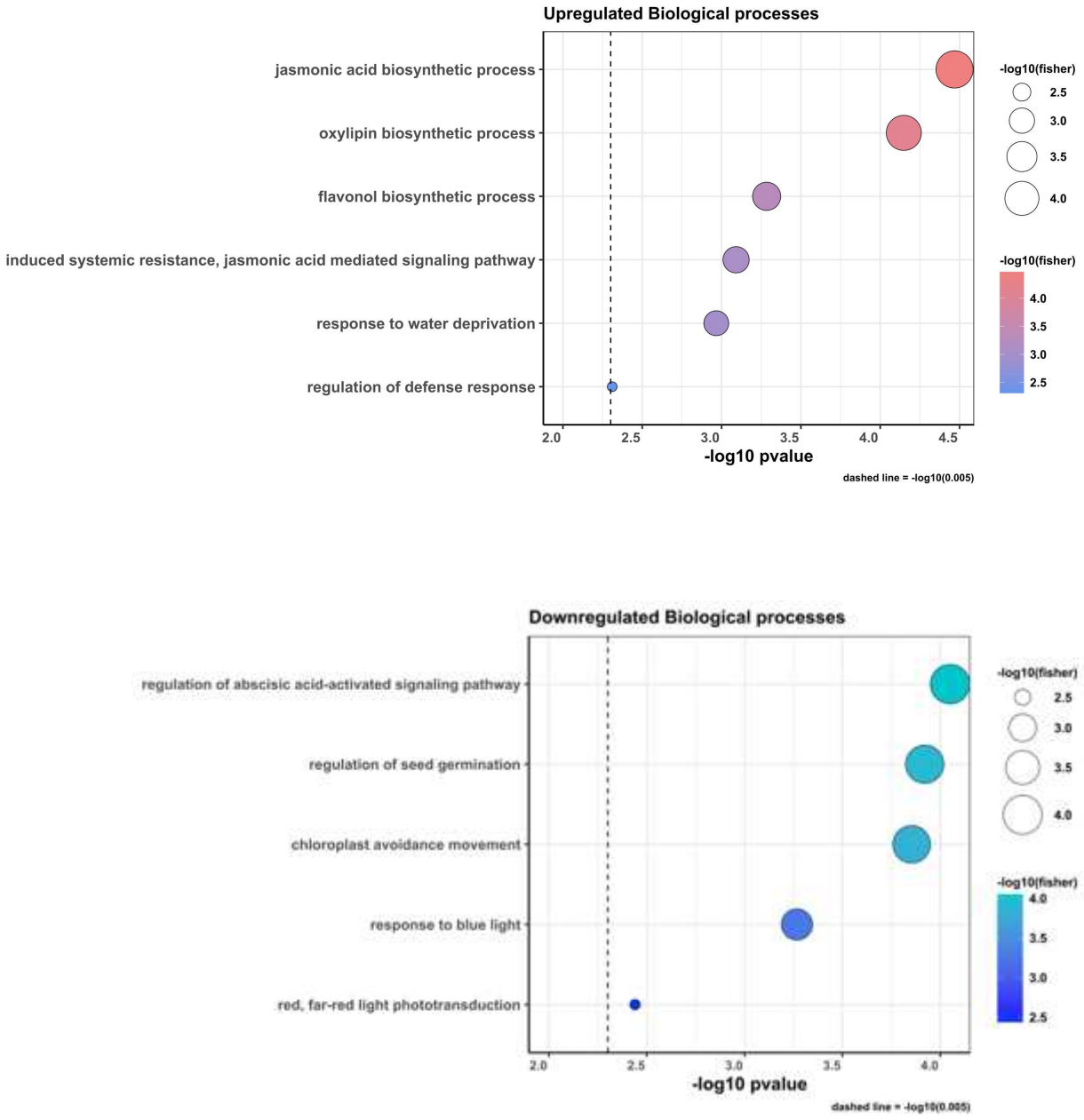

Figure 2.4. Dot plot showing gene ontology (GO) terms enriched in resistant mature tissue at 60 minutes after treatment compared to 0 minutes after treatment. The top panel shows biological processes with upregulated differentially expressed genes, the bottom panel shows biological processes with downregulated differentially expressed genes.

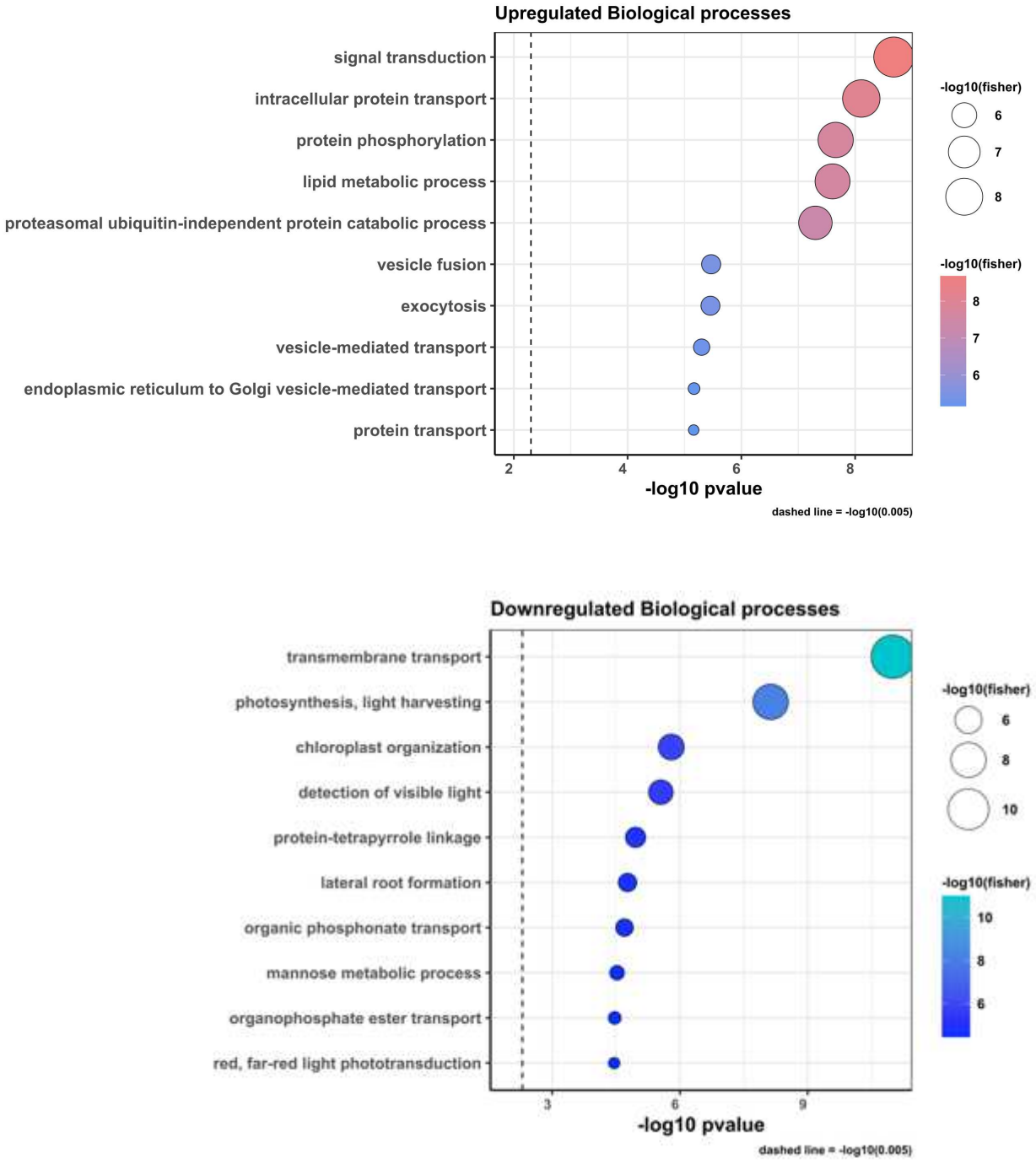

Figure 2.5. Dot plot showing gene ontology (GO) terms enriched in resistant mature tissue at 180 minutes after treatment compared to 0 minutes after treatment. The top panel shows biological processes with upregulated differentially expressed genes, the bottom panel shows biological processes with downregulated differentially expressed genes.

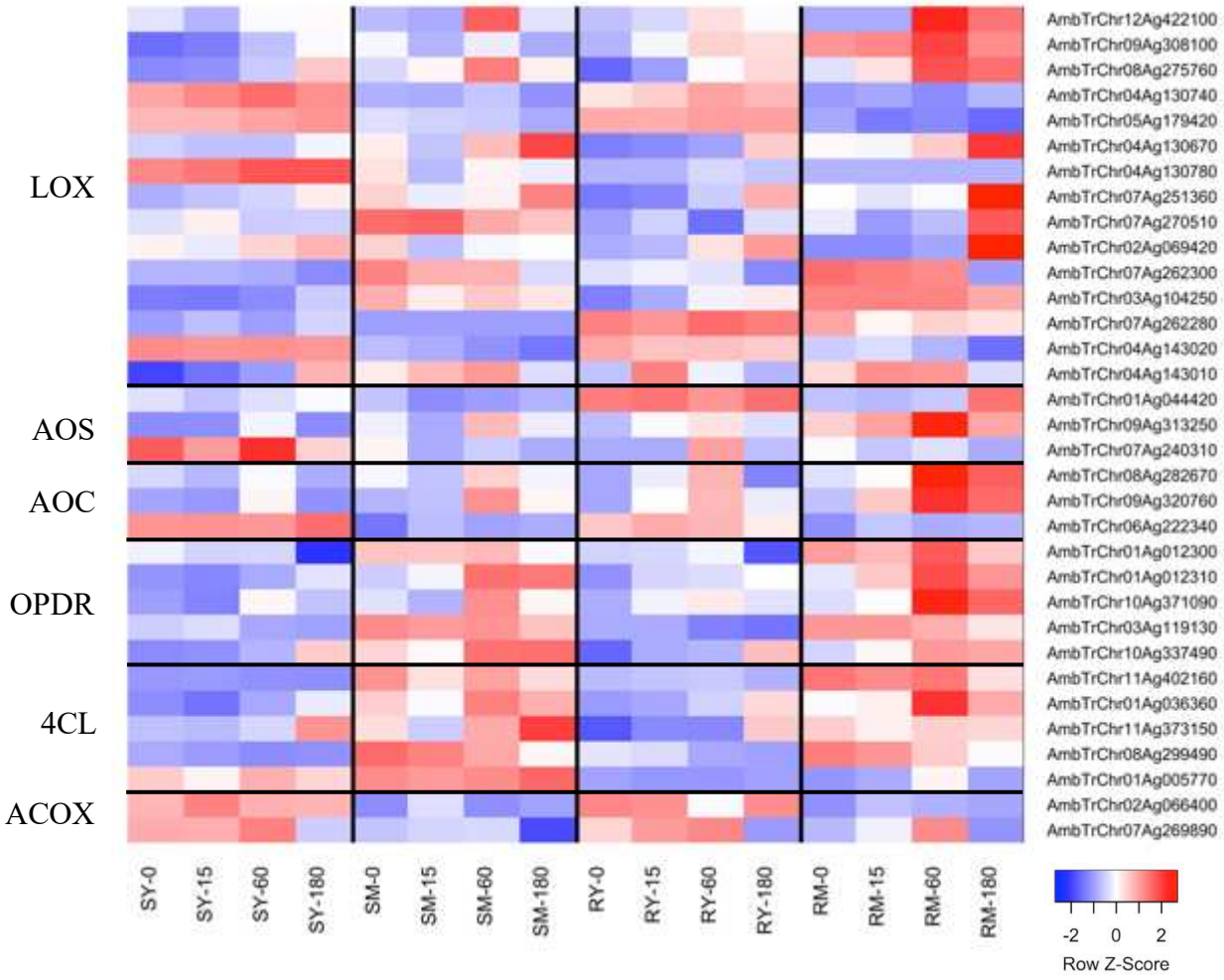

Figure 2.6. Heat map of log transformed TMM scaled CPM values for steps of jasmonic acid biosynthesis: lipoxygenase (LOX), allele oxide synthase (AOS), allele oxide cyclase (AOC), 12-oxophytodienoate reductase (OPDR), 4-coumarate-CoA ligase-like (4CL), peroxisomal acyl-coenzyme A oxidase (ACOX), averaged across biological replicates in all samples.

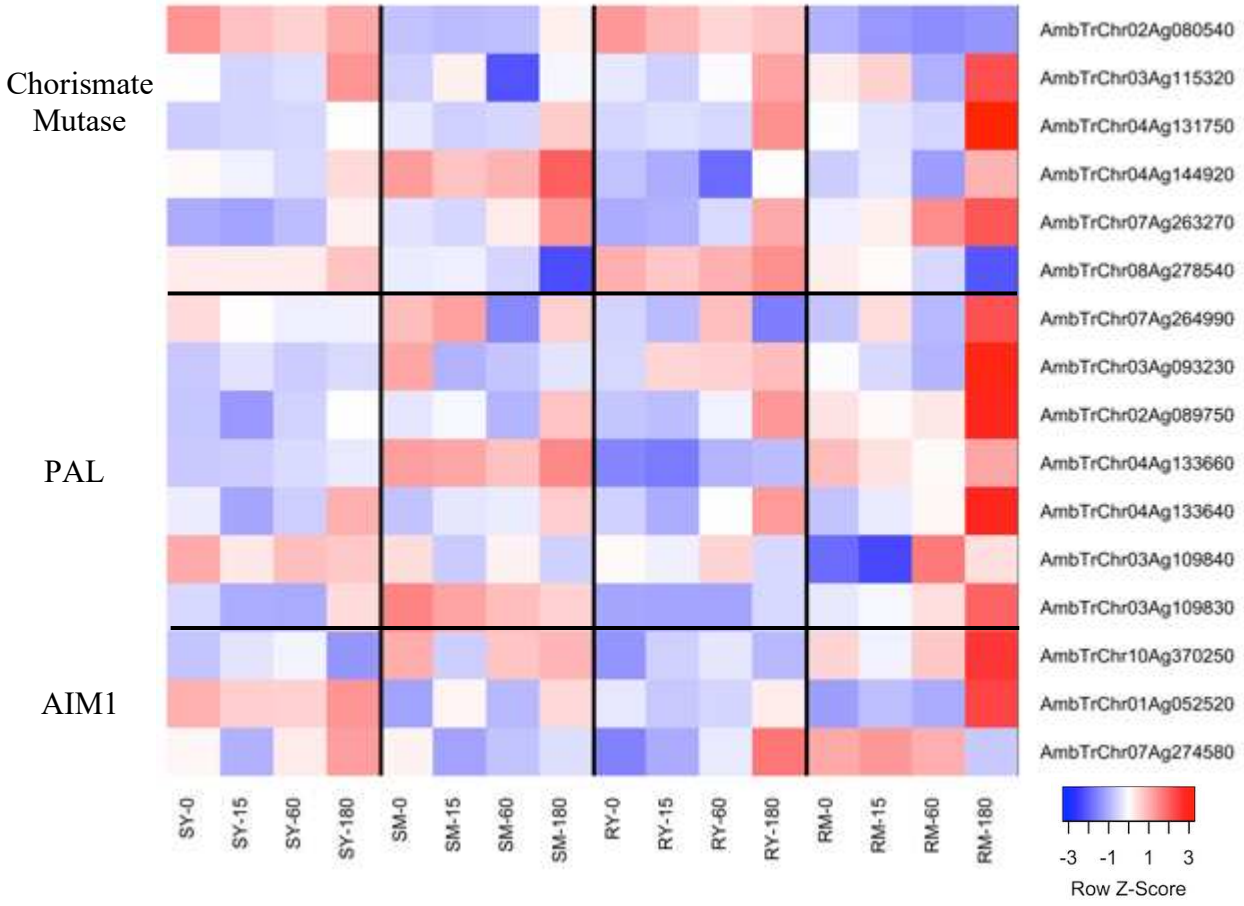

Figure 2.7. Heat map of log transformed TMM scaled CPM values for steps of the phenylalanine ammonia lyase pathway of salicylic biosynthesis: Chorismate mutase, phenylalanine ammonia lyase (PAL), ABNORMAL INFLORESCENCE MERISTEM (AIM1), averaged across biological replicates in all samples.

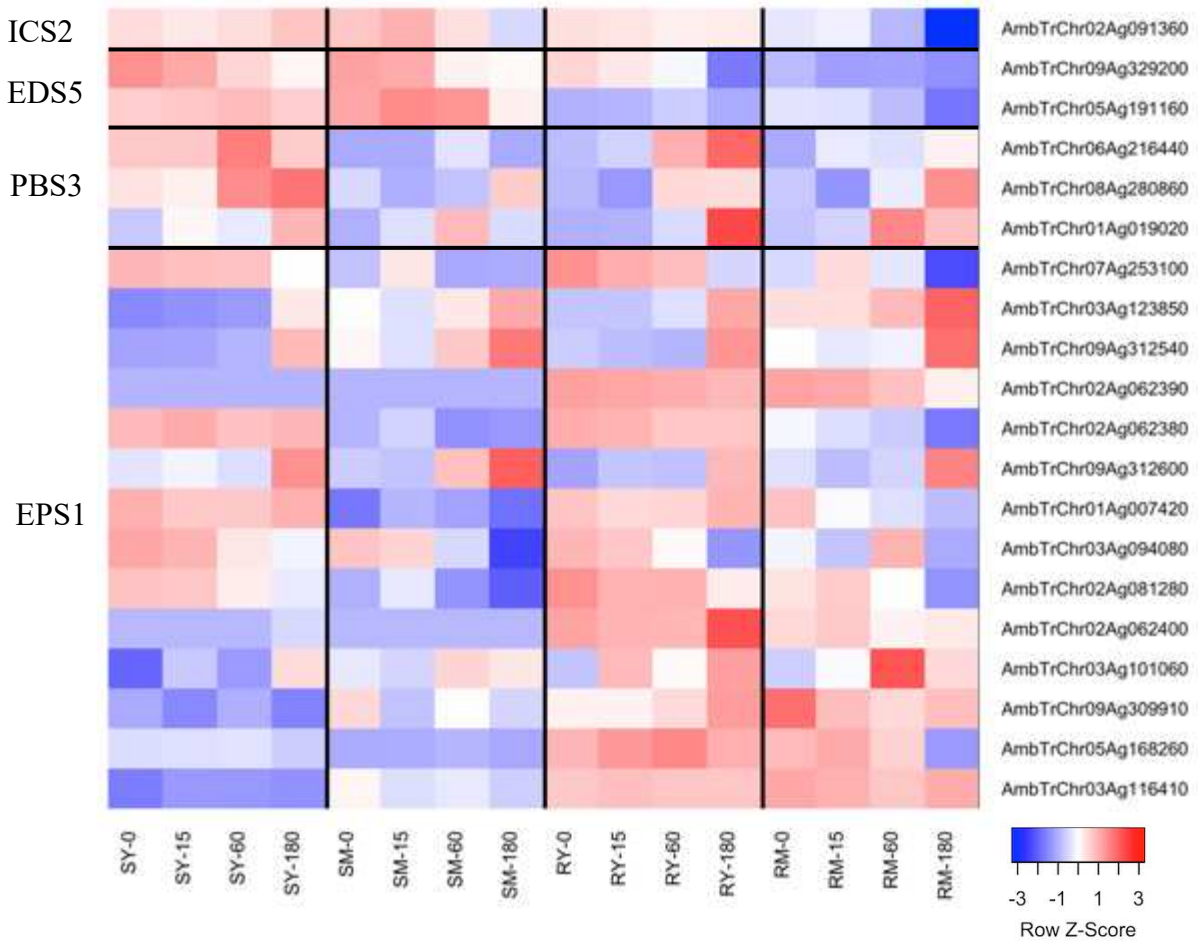

Figure 2.8. Heat map of log transformed TMM scaled CPM values for steps of the isochorismate synthase pathway of salicylic biosynthesis: isochorismate synthase 2 (ICS2), enhanced disease susceptibility 5 (EDS5), avrPphB susceptible (PBS3), ENHANCED PSEUDOMONAS SUSCEPTIBILITY 1 (EPS1), averaged across biological replicates in all samples.

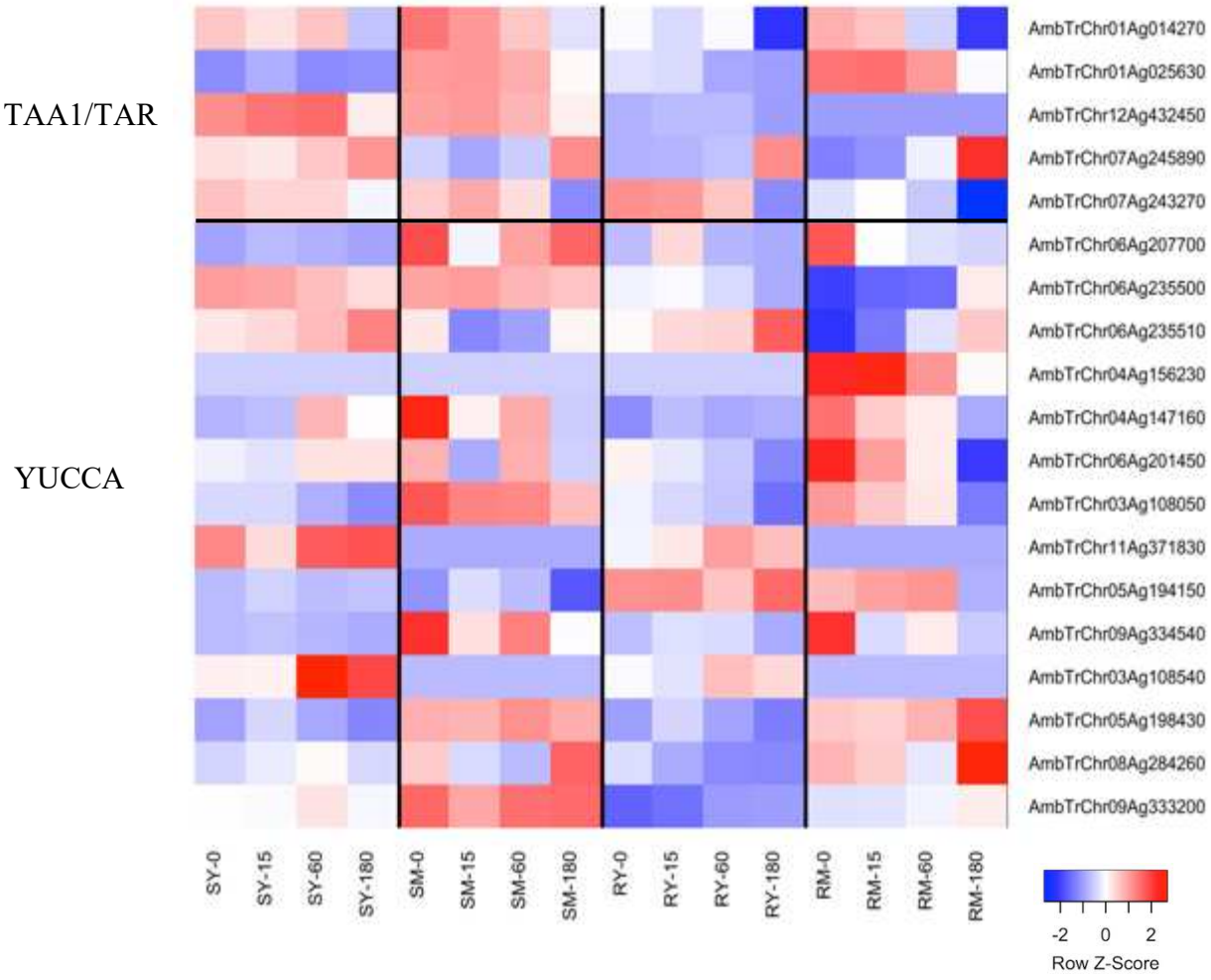

Figure 2.9. Heat map of log transformed TMM scaled CPM values for steps of indole-3-acetic acid: TRYPTOPHAN AMINOTRANSFERASE OF ARABIDOPIS (TAA/TAR), flavin monooxygenase-like enzyme (YUCCA), averaged across biological replicates in all samples.

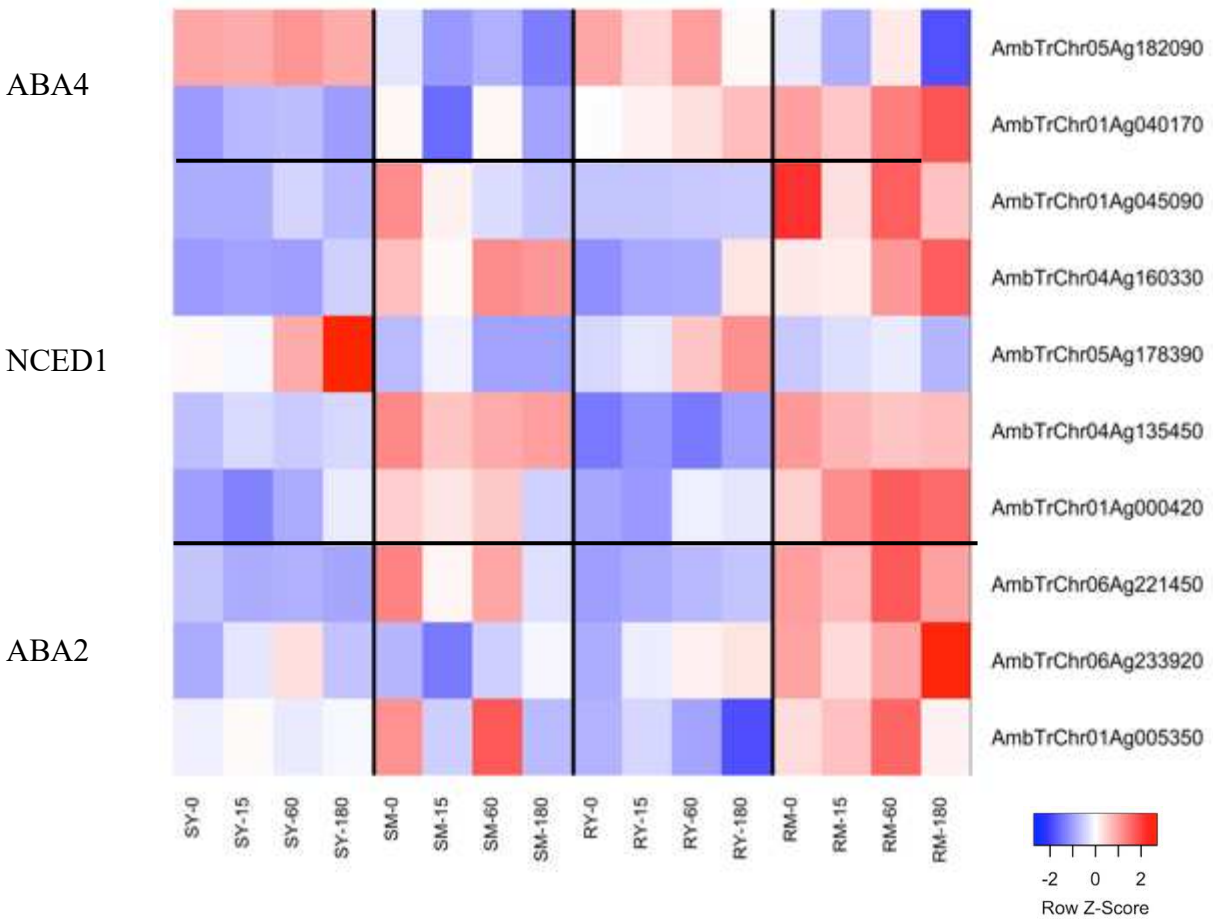

Figure 2.10. Heat map of log transformed TMM scaled CPM values for steps of abscisic acid: ABSCISIC ACID-DEFICIENT 4 (ABA4), 9-cis-epoxycarotenoid dioxygenase (NCED1), ABSCISIC ACID-DEFICIENT 2 (ABA2), averaged across biological replicates in all samples.

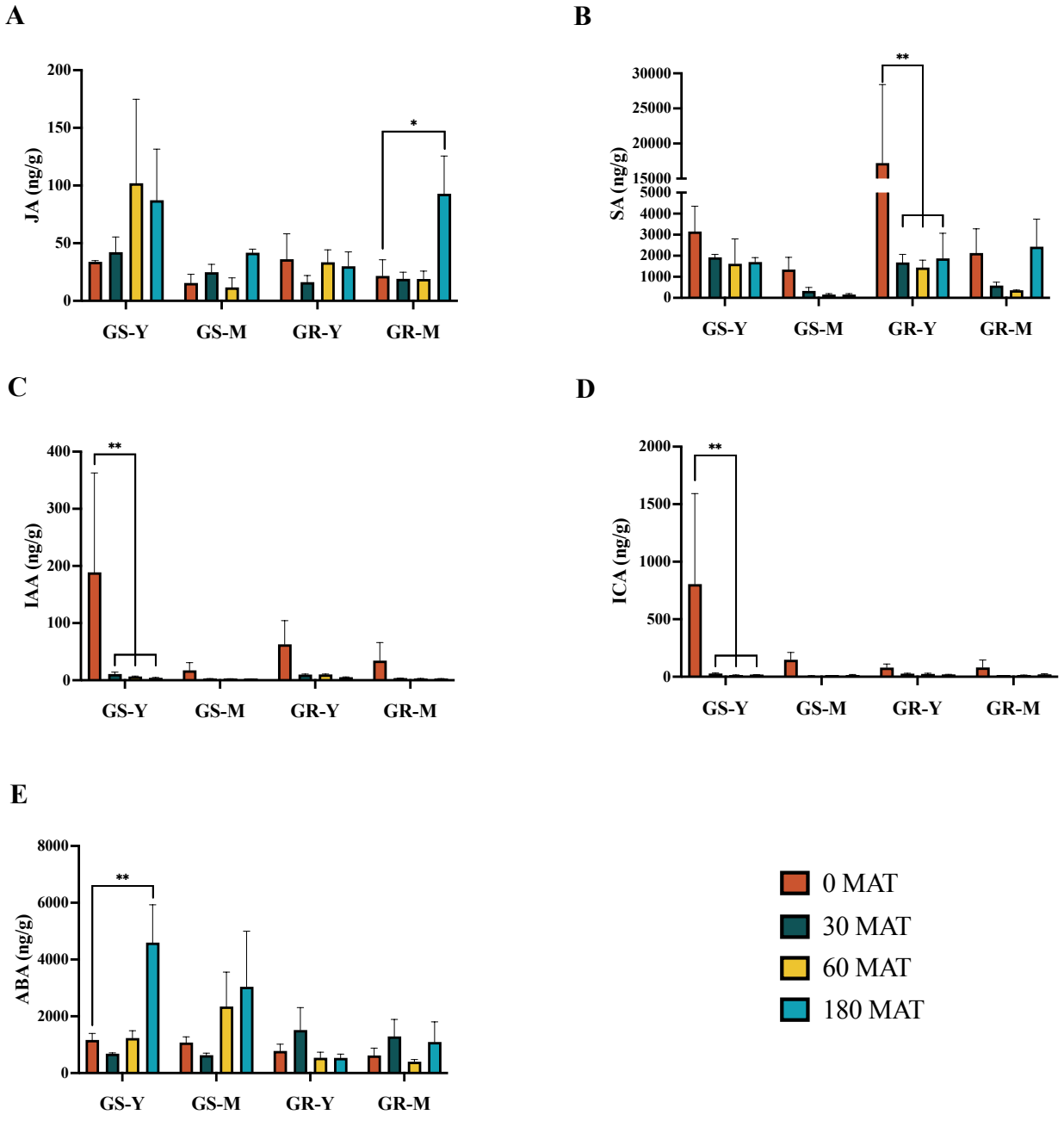

Figure 2.11. Means and standard errors of nanograms of phytohormone per gram of lyophilized leaf tissue, A. jasmonic acid, B. salicylic acid C. indole-3-acetic acid, D. indole-3-carboxylic acid and E. abscisic acid, at each time point 0, 30, 60, and 180 minutes after treatment. Single asterisk (*) indicates p value > 0.05, double asterisk ** indicates p value > 0.01.

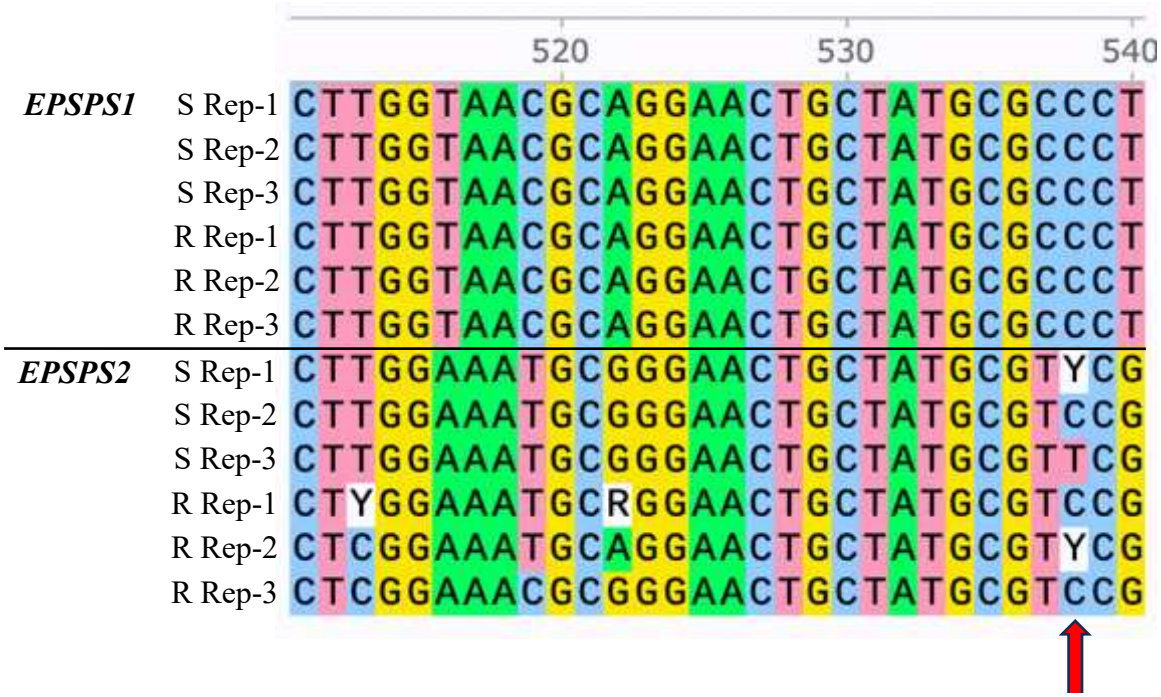

Figure 2.12. Alignment of nucleotide sequences of EPSPS1 and EPSPS2 in all RNAseq samples. Red arrow indicates location of Pro106Ser C to T single nucleotide polymorphism.

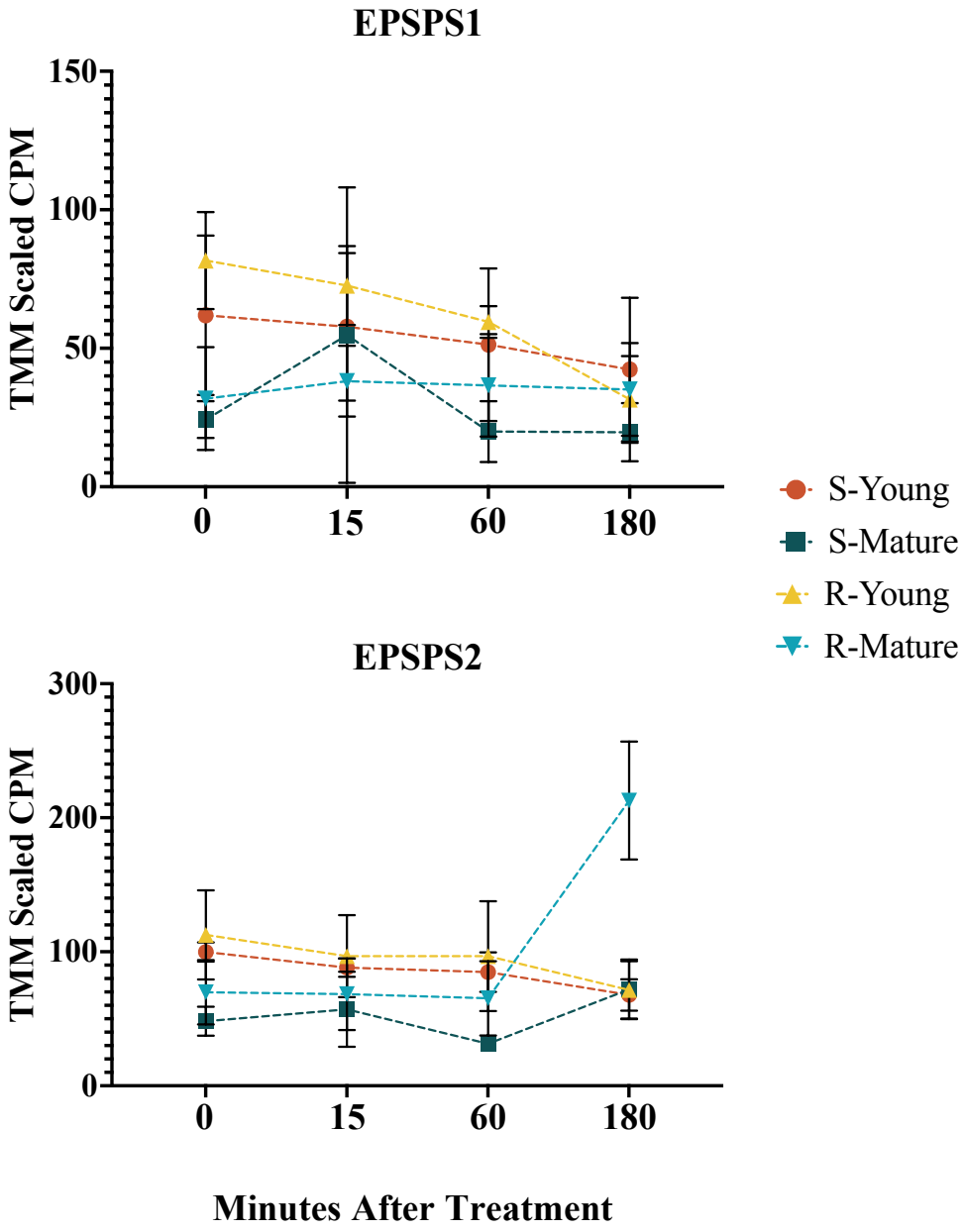

Figure 2.13. Mean TMM scaled CPM of EPSPS1 and EPSPS2 in each sample across the time course from 0 to 180 minutes after treatment. Asterisk showing EPSPS2 in resistant mature (RM) tissue 180 minutes after treatment is significantly higher than other tissues at 180 minutes, and RM at earlier time points.

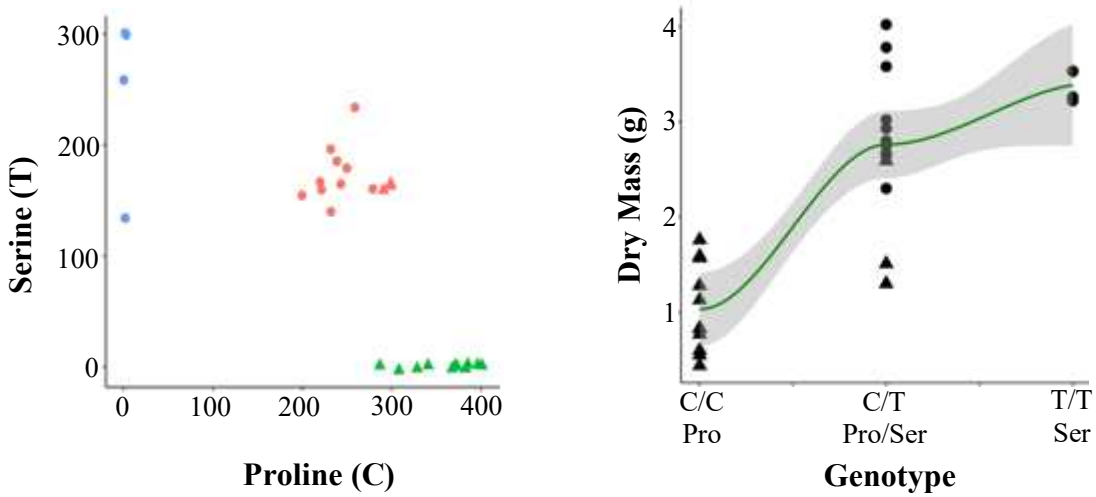

Figure 2.14. Allelic discrimination for *EPSPS2* using relative fluorescent units associated with the alleles for proline or serine (left) and linear regression of dry mass and genotype (right), both plots indicate glyphosate susceptible individuals by a triangle and glyphosate-resistant individuals with a circle.

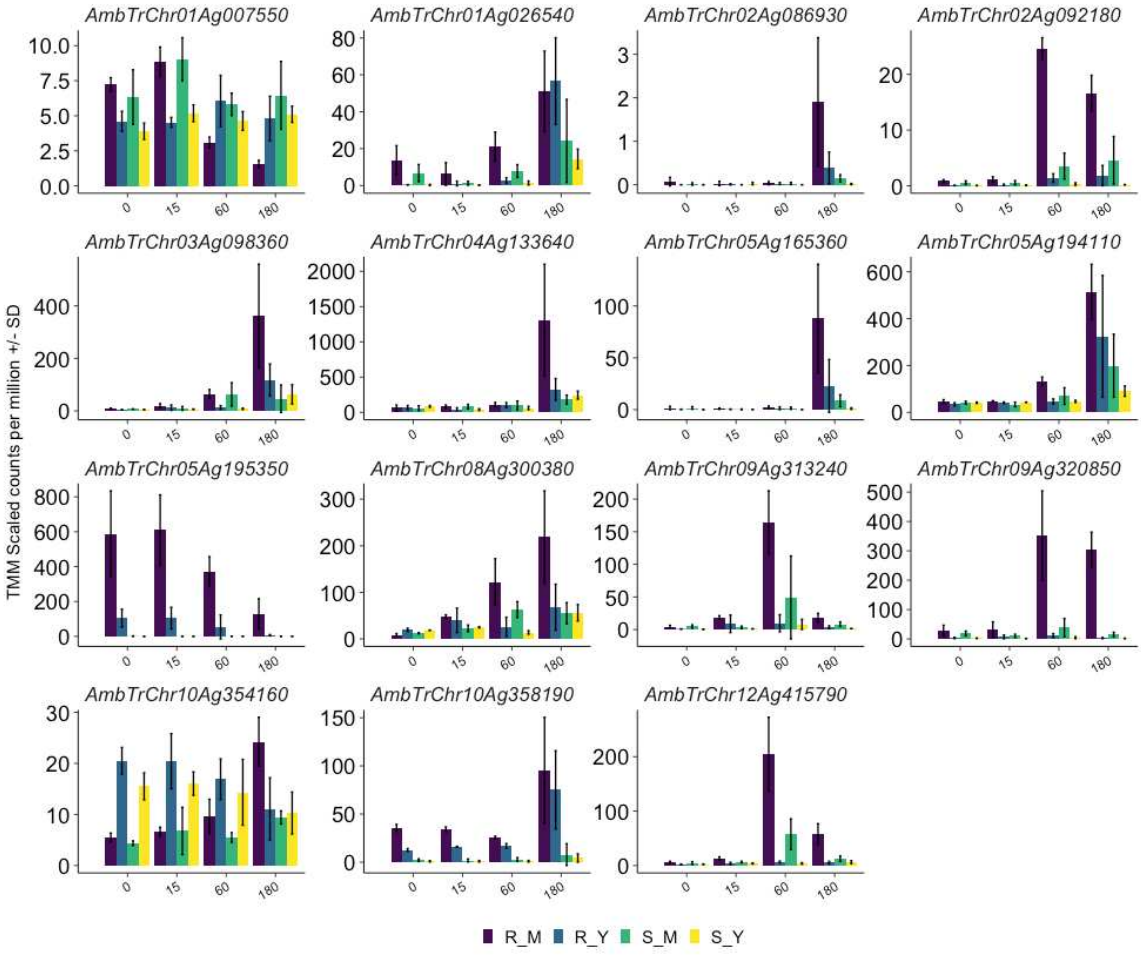

Figure 2.15. Plots of mean TMM scaled CPM for candidate genes of interest listed in Table 2.5, with treatment time along the x-axis and each sample type indicated by bar color.

CHAPTER THREE: MAPPING GLYPHOSATE RESISTANCE AND RAPID RESPONSE IN *AMBROSIA TRIFIDA*

3.1 INTRODUCTION

Over one and half centuries has passed since Gregor Mendel was inspired to describe the principles of inheritance he observed in his garden. Advances in the 20th century such as unraveling the structure and function of deoxyribonucleic acid (Küpper et al.) and development of innovative techniques such as sanger sequencing and polymerase chain reaction (PCR), allowing replication of DNA in vitro. These discoveries and many others laid the foundation for the vastly growing fields of molecular biology and genomics. The mechanisms underlying the code of life were being unraveled, leading to the development of many new questions along with methods and technologies to help address them. As the new millennium approached so did the next generation of sequencing technology. Over the past two decades a genomic renaissance brought the exponential advancement and utilization of next generation sequencing (NGS) and experimental techniques around the data it generates. Sequencing approaches became a staple of forward genetics studies seeking to reveal the genetic basis of phenotypic traits and over time the technology has become more accessible, affordable, and specialized. Increased availability of genomic resources for a variety of species are available largely through collaborative efforts of industry and academia (Montgomery et al. 2023). This rapid expansion of technology and resources is allowing research in many fields to quickly pinpoint the genetic basis of important phenotypes or alleles useful to population genetics and conservation. The technology has been echoing into everyday facets of human society for several decades now. Processes that require years of laborious trial and error such as crop development and drug discovery can be expedited by using targeted methods driven by genomic studies. There may always be hurdles to overcome,

but our knowledge and utility of the DNA and inheritance has increased exponentially in a relatively short span of our history.

Trait mapping techniques using next generation sequencing technologies have expedited the discovery of alleles associated with important traits. There has always been a need for crop cultivars that can produce in the presence of environmental stresses and pathogens but workflows to quickly identify and introduce alleles with these benefits is growing more important with the looming concern of increased instances of flooding, drought, and fluctuations in pathogen and pest patterns, efficient crop development can bring advantages to growers, consumers, and the environment (Majeed et al. 2022). Genes involved in yield, size, or flavor of desirable part of a plant can also been identified to guide enhancement of these traits through gene editing or marker assisted breeding.

Trait mapping can also be used to investigate the genetic, evolutionary, and geographic origins of traits that are undesirable or disruptive in plants (Bharamappanavara et al. 2020). We can learn about how some weeds are able to quickly adapt and invade climates that contrast their native range while accumulating alleles conferring resistance to multiple herbicide groups (Leon et al. 2021). Through this understanding we can develop practices to prevent selection pressure from human behavior that may select or spread for these alleles. It has been understood that repeated application of a herbicides with the same mode of action can select for resistance alleles. Understanding the presence and frequency of such alleles can inform strategic decisions and improve the success of measures to prevent resistance such chemical rotation and tank mixes.

While problematic traits in weeds can be mapped to understand weediness and competition, they are also a potential source of beneficial traits. Some populations of weedy rice in the US have evolved resistance to blast disease (*Magnaporthe oryzae*), a global threat to rice production. Trait mapping uncovered a quantitative trait locus (QTL) with five candidate genes for blast disease which could be introduced to cultivated rice (Liu et al. 2015).

Multiple approaches to trait mapping using NGS have been developed with distinctions in sample prep and analysis that make each more appropriate for different experimental questions or systems. Quantitative trait loci (QTL) mapping uses whole genome sequence to identify regions of a genome that segregate with a trait of interest. Bulk segregant analysis (BSA) follows this same principle but multiple individuals with a phenotype are bulked together and the entire pool of DNA is sequenced. The term bulk segregant analysis pre-dates NGS, referring to the process of pooling individuals together for subsequent analysis with methods such as southern blot or RFLP to identify molecular markers that segregate with a trait (Quarrie et al. 1999; Ruas et al. 1998). Utilizing NGS techniques with BSA approach provides an economical method to carry out whole genome sequencing and map QTLs. This method has been used to identify genomic regions associated with herbicide resistance in *Amaranthus tuberculatus* (waterhemp) populations resistant to the HPPD inhibitor tembotrione (Murphy et al. 2021).

Though glyphosate resistance in *Ambrosia trifida* was first reported fifteen years ago no mechanisms of resistance have been validated in either of two distinct biotypes, characterized by the presence or absence of a rapid cell rapid response in the mature leaves. Initial studies did not identify any changes to the glyphosate target site (Van Horn et al. 2018). It was recently reported that the *A. trifida* genome contains a second EPSPS locus that sometimes contains a $Pro^{106}Ser$ mutation associated with glyphosate resistance ((Page et al. 2024). The contribution of the

mutation to resistance must be further characterized as the resistance allele was also observed in RNAseq reads of susceptible individuals. Previous work in *A. trifida* revealed that significant reduction of translocation begins by 24 hours and continues through 96 hours after treatment in the rapid response biotype, this was concluded to be a consequence of the rapid cell death (Moretti et al. 2018). In recent years the International Weed Genomic Consortium has generated genomic resources for many of the most problematic weed species, making genome wide mapping and association studies a powerful option for researchers working with non-model species (Montgomery et al. 2023). Through his effort a high-quality reference genome for *A. trifida* was sequenced and assembled.

3.2 MATERIALS AND METHODS

Generation of F_2 population

A segregating F_2 mapping population was generated from parental lines of *A. trifida* from Ontario Canada, previously reported by Van Horn et. al., 2018. Both the glyphosate-resistant rapid response (GR-RR) and glyphosate-susceptible nonrapid response (GS-NR) lines were inbred two generations by single seed descent. The parental lines were planted in Magenta® boxes in 2-4 cm of moistened soil (Fafard Custom Mix, Sun Gro Horticulture), and cold stratified at 4 °C for 6 weeks to break dormancy. Seedlings were grown under a photoperiod of 14 h light, 25 °C/10h dark, 20 °C. When the plants reached the flowering stage one individual was emasculated by removal of developing male flowers and placed into a pollination bag with another individual with intact male flowers. Seeds were collected from the emasculated individual and considered to be the F_1 generation. These seeds were cultivated as previously described and 50 F_1 individuals were self-pollinated to produce F_2 lines.

Treatment and phenotypic rating

The F_2 seeds were cultivated as previously described. When healthy seedlings reached 10-20 cm height, 96 individuals were treated with glyphosate (Roundup PowerMAX®) at 0.84 kg ae ha^{-1}, using a laboratory track sprayer calibrated at 187·L ha^{-1} spray volume with an 8002EVS single even flat-fan nozzle. Phenotypic ratings were collected over the following 35 days to place each plant into a pool for bulk segregant analysis. For the rapid response phenotype, death of the mature leaves was scored at 24, 48 and 72 hours after treatment. A score of 1 indicated no injury to the old leaves, and thus no rapid response. A score of 2 of 3 indicated either small or medium lesions dispersed across the mature leaves, respectively. A score 4 indicated that up to three quarters of the mature leaf was dead and curling but some areas of living tissue was visible. A rating of 5 meant that a strong rapid response was observed as the entire mature leaf was dead and curled at the ends. Resistance rating focused on damage to the apical meristem and newest growth at 7, 14, 28, and 35 days after treatment. A score of 1 indicated no damage to the growth points, 2 indicated some blackening of the tips of the newest growth, 3 indicated that at least half of the newest growth was black, chlorotic or had slight epinasty, 4 meant the regrowth was over three quarters discolored or had moderate epinasty, and a rating of 5 meant the apical meristem was completely dead. Regrowth at 35 days was rated where a score of 1 indicated no new regrowth, 2 meant little growth and leaves had some abnormalities such as epinasty or misshapen leaves, 3 indicated moderate regrowth with some abnormality, 4 indicated moderate regrowth of healthy leaves, and 5 meant abundant regrowth of healthy leaves and dry mass were measured. The whole plant was collected for dry mass and dried in a commercial drying oven at 50 C until weight did not change over 48 hours.

DNA extraction and sequencing

DNA was extracted from all 96 plants using a CTAB based protocol and normalized to 20 ng/µl (Aboul-Maaty and Oraby 2019). The DNA was pooled into four bulks for sequencing based on the phenotypic data. The bulks consisted of glyphosate-resistant rapid response (GR-RR), glyphosate-resistant nonrapid response (GR-NR), glyphosate-susceptible rapid response (GS-RR), and glyphosate-susceptible nonrapid response (GS-NR). The four bulked DNA samples were shipped to Novogene, Sacramento CA, for Illumina paired-end sequencing.

QTL mapping

The Fastp package was used to remove Illumina sequencing adapters, reads with phred quality of score less than 20, and assess the overall quality scores of the reads (Chen et al. 2018). The processed reads were aligned to the *A. trifida* reference genome provided by the International Weed Genomics Consortium, using Burrows-Wheeler Alignment Tool (Li 2013; Montgomery et al. 2023). Duplicate reads were marked in the alignment files using Picard tools (Institute). GATK was used to call variants on the mapped reads (Van der Auwera and O'Connor 2020). Single nucleotide polymorphisms (SNPs) were selected and filtered based on GATK best practice recommendations. A table of the SNPs that passed filtering was loaded into R-studio. The QTLseqR package (version 0.7.5.2) was used to run a DeltaSNP Index and G-prime analysis on pairs of bulks to isolate QTLs associated with resistance and rapid response (Mansfeld and Grumet 2018). Prior to analysis input SNPs were filtered based on a reference allele frequency of 0.20, a minimum total depth of 40 reads, a maximum total depth of 400 reads, a minimum sample depth of 20 reads, and Phred-scaled probability of 99 (Dong et al.). A window size of 3 megabases (Mb) was selected for the analyses. QTL intervals within a 90% or greater confidence interval from the DeltaSNP index analysis, or adjusted p-value of less than 0.05 from the G-prime analysis were selected as candidate QTLs. Some additional intervals that did not meet

these significance requirements, but exceeding background noise were also selected as intervals of interest. All variants from the selected QTL regions were annotated using SNPeff (version 5.2) (Cingolani et al. 2012).

Marker design for trait association and fine mapping

Marker regions were selected along each of the candidate QTLs to confirm association with resistance or rapid response and narrow the size of the intervals toward causative genes. This consisted of Kompetitive Allele Specific PCR (KASP) genotyping primers designed at 10 positions approximately evenly spaced throughout the interval (He et al. 2014). Genotyping markers were designed on SNPs that were homozygous in susceptible or slow-response bulks, had a minimum read depth of 30, and no other variants near the marker that would interfere with hybridization to the DNA. A phred scaled probability of 99 was preferred but lower GQ was considered if read depth was higher an all other criteria were met, including the primer having a melting temperature 60° C +/- 4° C, a delta G sufficiently high enough that dimerization to self or other primers was not likely, possible hairpins had a melt temperature 10° C or more below the annealing temperature of the marker set, and GC content was between 40-60% . To explore association of other intervals to either resistance or rapid response, a single KASP genotyping marker was designed near the center of the interval using the same criteria previously described.

Phenotype and marker validation

To further validate QTL markers and phenotypic ratio of resistance and rapid response traits, a total of 160 additional F_2 individuals were grown, treated, and rated as previously described. A Chi-squared Goodness of Fit test was used to calculate the probability of the null hypotheses that resistance and rapid response are single gene dominant traits using expected ratio

of 9:3:3:1 for the combined phenotypes, or 3:1 for the individual phenotypes. The individuals with the most extreme phenotype scores for resistance or rapid response were selected for initial marker validation and DNA was extracted as previously described.

3.3 RESULTS AND DISCUSSION

The phenotypic rating of the original 96 F2 plants revealed some phenotypic ambiguity, where 82 and 78 plants were considered more confident for resistance and rapid response, respectively. These plants were selected based on the extreme ends of the damage ratings, as well as holistic consideration of regrowth and dry mass at 35 days (Figure 3.1). Interestingly, resistance and rapid response did not always co-segregate. Some previous postulations about these populations assumed that resistance and rapid response were one in the same, or that they are genetically linked. Only 66 plants received confident scores for both traits simultaneously. These were ultimately sorted into the four DNA bulks for sequencing. A chi-square goodness of fit test using all plants failed to reject that either trait followed an inheritance pattern of 3:1, indicating each is a single gene dominant trait (Table 3.1). However, the test did reject that the two traits together followed a 9:3:3:1 ratio. Further, a chi-squared test using only the confident calls rejected that resistance followed the 3:1 ratio but failed to reject the null hypothesis for the rapid response (Table 3.2).

An additional 160 F_2 plants were grown, treated, and scored to validate the bulk segregant ratios and QTL mappings. While there is some variation across the population these individuals had more discernable phenotypes than the original set of plants scored for sequencing. Resistant plants were clearly distinct from susceptible within three weeks of treatment, and the rapid response occurred as early as 6 hours after treatment with most plants showing either a strong

rapid response or no rapid response by 24 hours. This was more obvious than the first set of F_2 plants which showed either no symptoms or a weak response by 24 hours and the full response by 48-72 hours after treatment. Chi-squared statistics for the validation set were similar to the confidently called individuals from the original set. The null hypothesis that resistance is a single gene dominant trait was rejected but failed to reject that the rapid response follows an inheritance pattern of 3:1 (Table 3.3). The reason for the ambiguity in the initial 96 plants compared to the later 160 was likely due to multiple factors. The original set was treated in early spring when temperatures can remain low in Northern Colorado. These plants were transported to an unattached greenhouse following the re-entry interval of four hours for glyphosate, requiring a brief period outside in lower temperatures. The second set was treated in autumn, on notably warm days, and kept in a greenhouse attached to the treatment area. The two greenhouses were managed by different groups on campus, and though temperature and light settings were identical, there are likely variations between the two based on placement of light ballast, spacing from cooling pads and air vents, and maintenance status of these features. Past studies show that temperature effects absorption and translocation in *A. trifida*, indicating that the difference in seasons and greenhouse environment following treatment could affect the efficacy of glyphosate uptake and translocation to the target site as (Boheemen et al.).

The Illumina reads from the four bulks had sufficient quality and a high mapping rate to the reference genome (Table 3.4). Analysis using the deltaSNP index and G-prime methods revealed that resistance may be associated with three separate intervals on chromosomes one, six, and eleven (Table 3.5, Figure 3.2), while rapid response was associated with one large segment of chromosome ten (Table 3.5, Figure 3.3). The results of QTL mapping support the findings chi-square goodness of fit tests on the phenotypic ratios observed only the confident

scores of the original set of plants, and the whole set of plants for validation. This further indicates that the two traits are not linked, that resistance is multigenic, and that rapid response is likely from a single dominant gene. The four previously mentioned intervals were selected as putative QTLs for resistance or rapid response and 5 additional regions were selected as regions of interest (Table 3.5)

A variable quantity of SNPs and genes are within each interval (Table 3.5). The finding of three QTLs significantly associated with resistance indicates a multigenic form of resistance. Four genes within the QTL1 were annotated as ABC transporters, one type C and three type G found consecutively along the chromosome. The ABC transporter type C contained a combination of variants in the upstream region, missense mutations, and high effect frameshift in the coding sequence. This family of ABC transporter has been previously associated with glyphosate resistance, typically from upregulation believed to sequester glyphosate away from the target site (Pan et al. 2021). If this ABC type C transporter is a carrier of glyphosate perhaps it is involved in systemic transport to sink tissues, or transport into the chloroplasts, therefore loss of function would prevent glyphosate from reaching its target site. The other three ABC transporters are the G type, which has not been identified in glyphosate resistance but is associated with multidrug resistance and has a variety of natural substrates (Kerr et al. 2011). Transcriptomic analysis in *A. trifida* determined that the first of these ABC transporters is downregulated in resistant young tissue but upregulated in matures leaves after glyphosate treatment, the second is constitutively down in resistant young tissue, and the third is constitutively down in both resistant mature and young tissue compared to susceptible plants. Most of the variants associated with these gene are in the sequence region upstream to the gene. Variations in upstream regions could be associated with promotor motifs and alter interaction of

transcription factors. The coding sequence of one of the three ABC transporters contained a missense variation, potentially changing substrate affinity and altering substrate affinity. More work is needed to determine if these transporters interact with glyphosate and if mutations in the promotors or coding sequences negatively affect the ability of glyphosate systemically translocated throughout the plant to sufficiently inhibit its target enzyme, EPSPS.

A total of 46 genes were annotated within QTL2, located on chromosome 6. This included a solute carrier family 35 gene with multiple variants in the upstream region and one missense mutation in the coding sequence. This gene was previously found to be down regulated in resistant leaves of *A. trifida* after glyphosate treatment. Some members of this gene family transport various forms of phosphate into the chloroplast. Like other putative carriers of glyphosate, downregulation of such a transporter may prevent glyphosate from reaching its target site in the chloroplast.

While none of the 33 genes annotated in the third resistance QTL, on chromosome 11, are associated with glyphosate resistance they could be associated with a novel mechanism that has yet to be characterized. Additionally, another adjacent region of chromosome 11 is included in the regions of interest. It is possible that the two regions form one larger region that appeared as two separate peaks in the deltaSNP Index plot, without further analysis it is difficult to determine if such regions are part of a nearby peak, a separate peak, or noise in the dataset. The annotation of genes containing variants should be expanded into this interval to further look for candidates for resistance candidates.

It has been previously hypothesized that the rapid response in *A. trifida* is mediated by pathways involved in immune signaling due to parallels to the hypersensitive response. Rapid response being a single gene dominant trait could support this idea considering the gene for gene

resistance model. Given that the rapid response also displays a rapid burst of ROS it is possible that a pathogen response is somehow bridged to the abiotic stress of herbicide response through a sequence variant in this QTL. Multiple genes located within the rapid response associated QTL4 are associated with pathogen perception and signal transduction that leads to cell death. Several segments of the QTL contain clusters of genes annotated as putative disease resistance proteins containing NB-LRR domains. Some genes in these regions are annotated as RPP13-like (*recognition of Peronospora parasitica*), an NLR resistance gene from *Arabidopsis thaliana* (Leonelli et al. 2011). Another gene present in this region *LRRAC1*, is involved in resistance to some bacteria and fungi (Bianchet et al. 2019). Other genes clustered in the interval include TIR-NLR proteins *RPV1* (resistance to *Plasmopara viticola*), *RUN1,* and *TMV resistance protein N-like* which sufficiently mediate cell death in *Vitis vinifera* (grape), *Muscadinia rotundifolia* (muscadine), and *Nicotiana tabacum* (tobacco) (Williams et al. 2016; Massonnet et al. 2022). Each of these NLR-LRR domains have multiple sequence variations compared to the *A. trifida* reference genome. Some variants were in intergenic regions which could be associated with promotors and gene regulation. Others were associated with missense variations coding for alternative amino acids, and some where higher impact variants leading to frame shifts. Another type of gene associated with the hypersensitive response form of programmed cell death, *metacaspase1*, was found in this QTL and had many upstream variants, several missense mutations, and a few potential frameshifts compared to the reference genome. A transcription factor in the *NAC* (*No apical meristem*) family as located within the rapid response interval. Some members of this family have also been associated with hypersensitive response and programmed cell death (Lee et al. 2017). Another identified in the rapid response interval was *EDS1* (*Enhanced disease susceptibility1*), a lipase-like gene associated with programmed cell

death in the hypersensitive response and has essential roles in R-gene-mediated pathogen response. *EDS1* had many upstream sequence variants and some missense mutations compared to the reference genome.

The QTLs for resistance on chromosomes one, six and eleven contain transporters that could potentially carry glyphosate to or away from its target site, as well as other genes that may be related to a novel resistance mechanism. Chromosome ten, associated with rapid response, contains variants in multiple genes associated with cell death in response to pathogen defense, particularly during the hypersensitive response. This supports results of previous transcriptomic analysis that showed these genes to be differentially expressed in resistant tissues along with other genes that are associated with the hypersensitive response. It is likely that the rapid cell death observed in the rapid response biotype of A. *trifida* is associated with variation in one of these genes. To determine which genes are causative to resistance or rapid response phenotypes, association to the phenotypes should be further assessed by quantifying alleles specific to the resistant or rapid response bulks using KASP genotyping markers or other methods such as RFLP or sanger sequencing. A final selection of candidates can be used for functional validation. If variation in the coding sequence is suspected then transformation of the mutant version can be expressed in a heterologous system to assess resistance or the rapid response, or if possible, into susceptible non-rapid response A. trifida individuals.

While rapid response was not directly linked to resistance in this bulk segregant analysis it is believed to be the causative factor in reduced translocation of glyphosate by 24 hours after treatment (Moretti et al. 2018). In some conditions this could provide a tipping point toward survival, allowing plants with alleles for low level resistance to survive and produce progeny that accumulate multiple resistance alleles. While hypothetical, in this way the rapid response could

lend a hand in evolution of resistance and may explain why the two traits are found together while not directly linked.

3.4 TABLES

Table 3.1. Observed frequencies of glyphosate resistance and rapid response phenotypes in the initial 96 F2 individuals treated and rated for sequencing. The expected frequencies in the F2 progeny under the null hypothesis that each trait is inherited through a single dominant gene and Chi squared value, degrees of freedom and p-values determined from each test.

Phenotype		Observed	Expected	Chi square tests of goodness of fit
Glyphosate Resistance				
Resistant		72	72	$X^2 = 0$
Susceptible		24	24	$df = 1$
	Total	96		$p = 1$
Rapid Response				
Rapid		76	72	$X^2 = 0.89$
Nonrapid		20	24	$df = 1$
	Total	96		$p = 0.346$
Resistance and Rapid Response				
Res. Rapid		62	54	$X^2 = 8.23$
Res. Nonrapid		14	18	$df = 3$
Sus. Rapid		10	18	$p = 0.040$
Sus. Nonrapid		10	6	
	Total	96		

X^2 = Chi square of observed and expected phenotypic frequencies; *df* = degrees of freedom for each test equal to n – 1 with n being number of phenotypes.
p = P-value determined by Chi square test

Table 3.2. Observed frequencies of glyphosate resistance and rapid response phenotypes in a subset of the initial 96 F2 individuals having the least ambiguous phenotypes. The expected frequencies in the F2 progeny under the null hypothesis that each trait is inherited through a single dominant gene, Chi squared value, degrees of freedom and p-values from each test.

Phenotype		Observed	Expected	Chi square tests of goodness of fit
Glyphosate Resistance				
Resistant		61.5	61.5	$X^2 = 5.87$
Susceptible		20.5	20.5	$df = 1$
	Total	61.5		$p = 0.02$
Rapid Response				
Rapid		59	58.5	$X^2 = 0.02$
Nonrapid		19	19.5	$df = 1$
	Total	78		$p = 0.896$
Resistance and Rapid Response				
Res. Rapid		50	37.125	
Res. Nonrapid		3	12.375	$X^2 = 13.30$
Sus. Rapid		8	12.375	$df = 3$
Sus. Nonrapid		5	4.125	$p = 0.004$
	Total	66		

X^2 = Chi square of observed and expected phenotypic frequencies; *df* = degrees of freedom for each test equal to n – 1 with n being number of phenotypes.
p = P-value determined by Chi square test

Table 3.3. Observed frequencies of glyphosate resistance and rapid response phenotypes in the second set of 160 F2 individuals for further validation of phenotypic ratios and mapping markers. The expected frequencies in the F2 progeny under the null hypothesis that each trait is inherited through a single dominant gene and Chi squared value, degrees of freedom and p-values determined from each test.

Phenotype		Observed	Expected	Chi square tests of goodness of fit
Glyphosate Resistance				
Resistant		137	120	$X^2 = 9.63$
Susceptible		23	40	$df = 1$
	Total	160		$p = 0.002$
Rapid Response				
Rapid		129	120	$X^2 = 2.70$
Nonrapid		31	40	$df = 1$
	Total	160		$p = 0.44$
Resistance and Rapid Response				
Res. Rapid		117	90	
Res. Nonrapid		20	30	$X^2 = 21.87$
Sus. Rapid		13	30	$df = 3$
Sus. Nonrapid		10	10	$p = 6.953E\text{-}5$
	Total	160		

X^2 = Chi square of observed and expected phenotypic frequencies; *df* = degrees of freedom for each test equal to n – 1 with n being number of phenotypes.
p = P-value determined by Chi square test

Table 3.4. Number if reads before and after trimming Illumina reads to remove adapters and low-quality base scores (phred < 20), quality scores, and alignment rate to the reference genome of A. trifida. All bulks had 37% GC content.

Bulk ID	Raw Reads	Trimmed Reads	Fwd Q20 (%)	Rev Q20 (%)	Fwd Q30 (%)	Rev Q30 (%)	Mapped Reads (%)
GR-RR	812091365	806795392	98.20	97.79	94.65	93.56	98.94
GR-NR	807860390	802181697	98.47	97.53	95.30	92.68	98.93
GS-RR	770532577	765693565	98.49	97.71	95.37	93.07	96.54
GS-NR	760549568	755556157	98.25	97.61	94.44	92.79	98.81

Table 3.5. Candidate QTL associated with either glyphosate resistance or rapid response, the chromosome where each is located and the start and stop position (bp), the number of SNPs and genes located in that interval. QTLs 1-4 passed significance thresholds of either the Delta SNPindex or G prime analysis. QTLs 5-9 were not significant in this analysis but were selected as putative intervals of interest.

QTL	Trait	Chromosome	Start	End	SNPs	Genes
1	Resistance	Chr01	51462683	64220104	38249	374
2	Resistance	Chr06	70142213	75199983	3910	46
3	Resistance	Chr11	59951184	62262046	1657	33
4	Rapid Response	Chr10	528568	120122181	234524	2988
5	Resistance	Chr01	109096633	117690888	17350	165
6	Resistance	Chr06	19502	39074950	117146	1518
7	Resistance	Chr11	54489590	57730308	2367	79
8	Rapid Response	Chr04	68636297	70378852	2014	19
9	Rapid Response	Chr09	65594674	66017129	1000	12

3.5 FIGURES

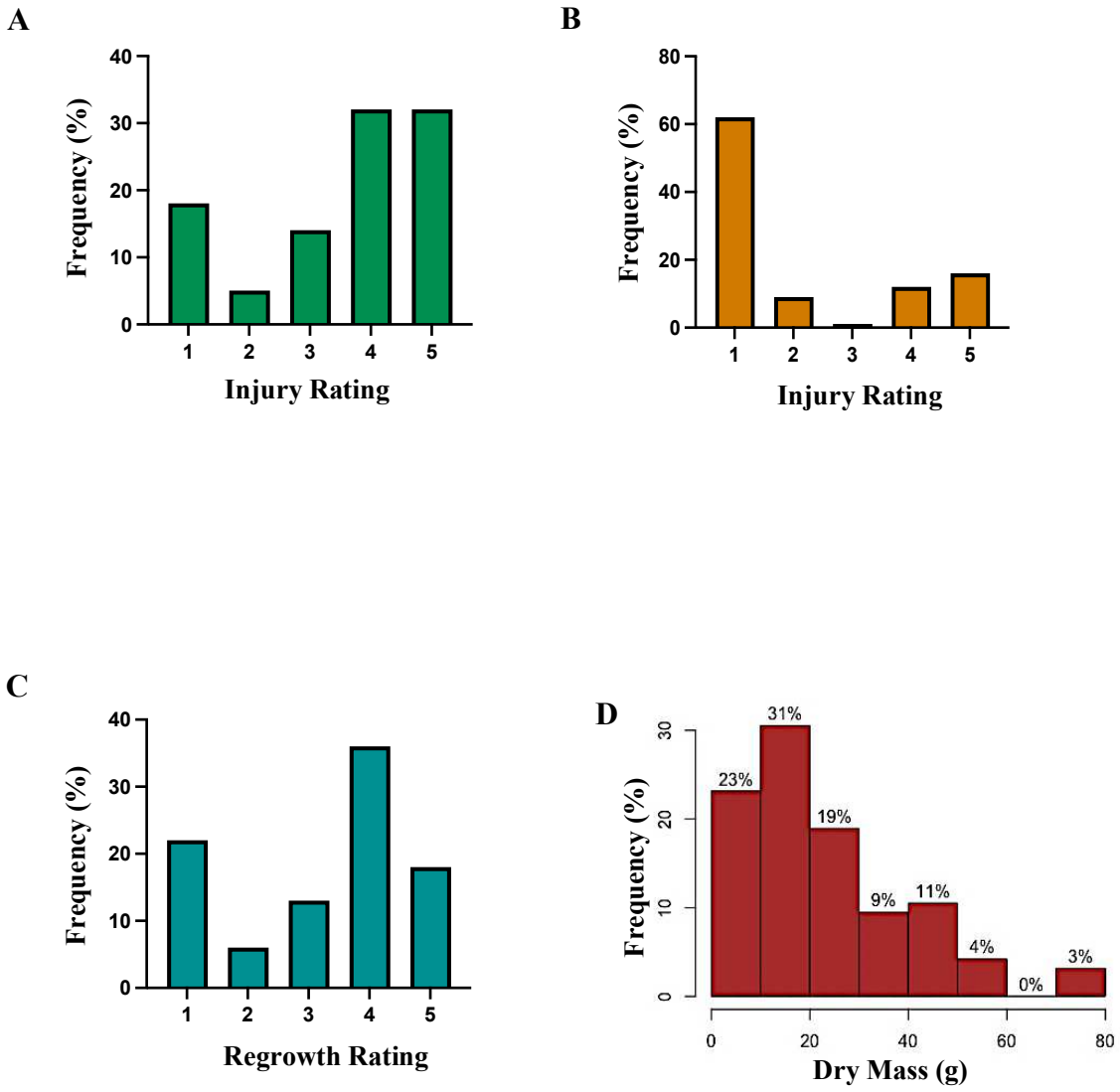

Figure 3.1. Distribution of phenotypic ratings A. Injury of mature leaves at 72 hours after treatment, B. Injury of growth points at 35 days after treatment, C. Regrowth at 35 days after treatment, D. Dry mass at 35 days after treatment.

A

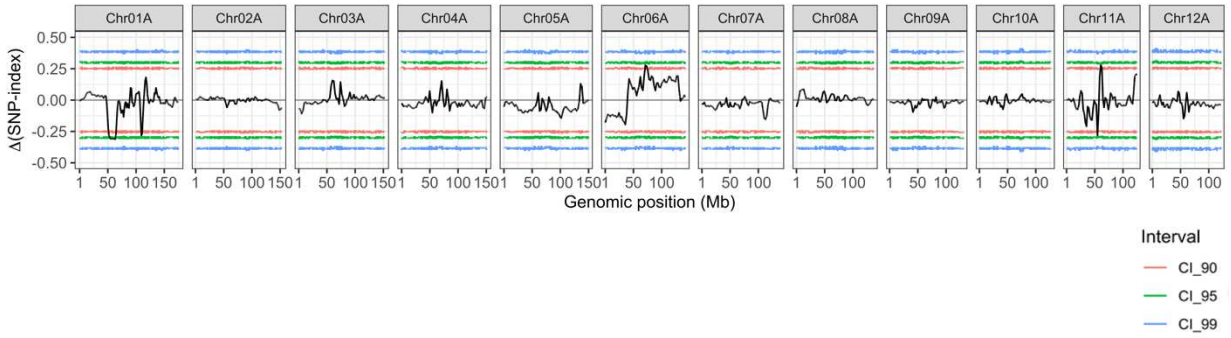

B

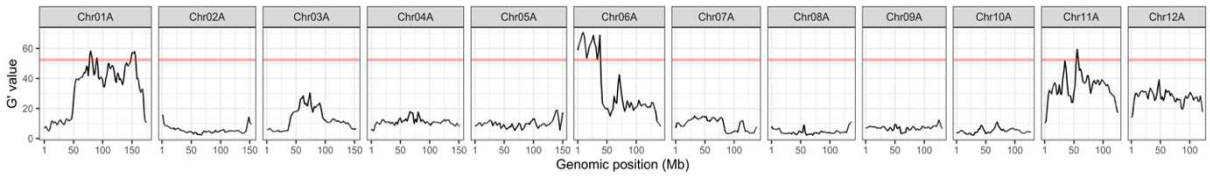

Figure 3.2. Delta SNP index (A) or G prime (B) analysis plots when the low bulk contains the susceptible samples, and the high bulk consists of resistant samples. Confidence intervals of 90, 95, and 95 are indicated on the Delta SNP index plots by blue, green, and red lines. An adjusted p-value of 0.05 is indicated by the red line on G prime plot.

A

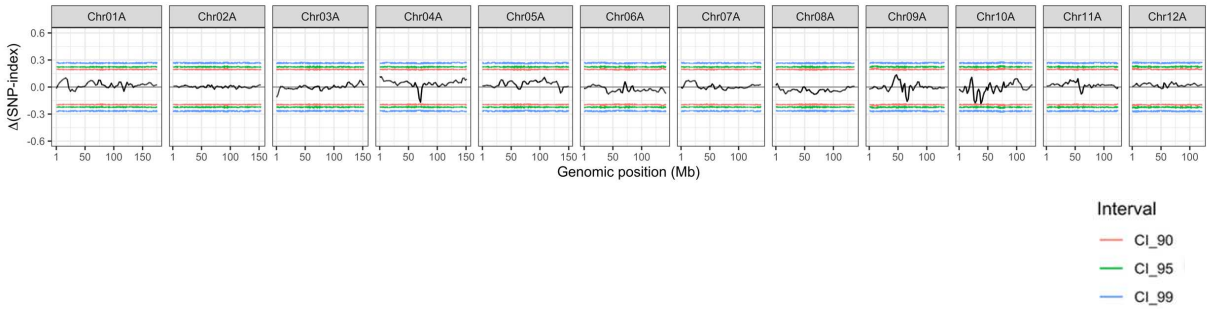

B

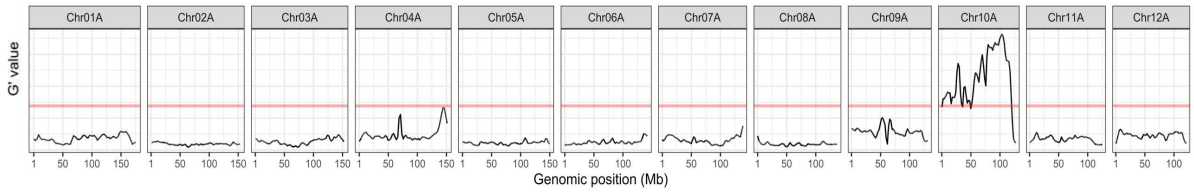

Figure 3.3 Delta SNP index (A) or G prime (B) analysis plots when the low bulk contains the nonrapid response samples, and the high bulk consists of rapid response samples. Confidence intervals of 90, 95, and 95 are indicated on the Delta SNP index plots by blue, green, and red lines. An adjusted p-value of 0.05 is indicated by the red line on G prime plot.

CHAPTER 4 - CONCLUSIONS

A single nucleotide polymorphism in the sequence of a second locus of the glyphosate target site 5-enolpyruvylshikimate-3-phosphate (*EPSPS*) was characterized from the RNAseq reads of an accession of glyphosate-resistant rapid response biotype and an accession of glyphosate susceptible nonrapid response biotype. The change of C to T endowed a Pro106Ser missense mutation and was associated with the glyphosate resistance phenotype in an F_2 progeny of the sequenced accessions.

It was determined that the rapid cell death observed in mature leaves of the rapid response resistant biotypes did not always co-segregate with resistance. Phenotypic ratios and quantitative trait loci (QTL) mapping of an F2 population also revealed that the rapid response is likely controlled by a single gene, located on chromosome 10, and that resistance is likely a multigenic trait with QTLs on chromosomes 1, 6, and 11.

A set of candidate genes of interest for glyphosate resistance or the rapid response were suggested for further validation. Two ABCC transporters were upregulated in mature glyphosate-resistant leaves. Another transporter from the MATE family was significantly up regulated in both young and mature tissue of resistant leaves. The upregulation of these transporters may be involved in sequestering glyphosate away from the target site in some or all tissues, preventing systemic inhibition of the target site enzyme and plant death (Pan et al. 2021; Moretti et al. 2017; Tani et al. 2015; Lv et al. 2021). An aldo-keto reductase was identified with significant upregulation in resistant tissue by 180 minutes after treatment. Previous work in *Echinochloa colona* validated that members of this gene family can metabolize glyphosate in plants (Pan et al. 2019b).

Genes such as these, in addition to the *EPSPS2* Pro106Ser mutation, likely work synergistically or additively to confer glyphosate resistance. The *EPSPS2* Pro106Ser mutation reduces the ratio of sensitive to insensitive glyphosate target site enzyme. ABC or MATE transporters and aldo-keto reductases simultaneously reduce the amount of glyphosate reaching the remaining sensitive target site, culminating in overall plant resistance.

Several genes related to biotic stress response were differentially expressed in resistant leaves. Gene families involved in perception of a pathogen or wounding by herbivory such as NB-LRRs were differentially expressed in resistant tissue and found within the candidate QTLs. Resistance to *Plasmopara viticola* (RPV1) is one such gene that is upregulated in resistant tissue by 180 MAT after treatment. Variation in this gene compared to non-rapid response populations may allow perception of glyphosate treatment similar to damage associated molecular patterns (DAMPs) in other forms of stress response. Several genes associated with signaling the hypersensitive response (HR) cell death were identified, some steps were selected as genes of interest such as rapid alkalinization factor-like 33 (RALF33-like) and its receptor kinase FERONIA, ethylene responsive factor (AP2/ERF), metacaspase-1, and HR-like lesion inducer.

Jasmonic acid (JA) was significantly higher in resistant mature leaves by 180 minutes after treatment, and though salicylic acid (SA) quantity was similar to before treatment in resistant mature leaves, this differs from susceptible mature leaves where it decreased. These phytohormones are associated with HR-like cell death signaling. Due to the overlap of response to glyphosate and HR-like cell death, it is proposed that the rapid response is an HR-like response being signaled through perception of damage caused by glyphosate treatment, such as lipid peroxidation.

Several limitations to this study should be acknowledged and potentially bridged by future studies. The short time course of the RNAseq and phytohormone metabolomic analyses was intended to capture the rapid response. Knowing that that resistance and rapid response are not one in the same, and that differential expression of genes associated with resistance has been significant beginning at later time points, this study may not capture changes in transcription that are causative of resistance.

Measurement of phytohormone quantities in response to glyphosate treatment only included non-conjugated forms of the hormones. To obtain the full spectrum of phytohormone shifts, it may be important to include conjugated forms of SA and JA.

A major factor limiting the design and analysis of all experiments reported in this work is the issue of genetically impure seed lines. Though inbreeding through single seed descent was attempted to generate the resistant rapid response and susceptible non-rapid response lines used in these studies, both phenotypic and genetic evidence of crossing has been observed. This likely produced noisier datasets than what would be expected in more pure lines.

REFERENCES:

Aboul-Maaty NA-F, Oraby HA-S (2019) Extraction of high-quality genomic DNA from different plant orders applying a modified CTAB-based method. Bulletin of the National Research Centre 43 (1):25. doi:10.1186/s42269-019-0066-1

Ahsan N, Lee D-G, Lee K-W, Alam I, Lee S-H, Bahk JD, Lee B-H (2008) Glyphosate-induced oxidative stress in rice leaves revealed by proteomic approach. Plant Physiology and Biochemistry 46 (12):1062-1070. doi:https://doi.org/10.1016/j.plaphy.2008.07.002

Alexa A, Rahnenführer J, Lengauer T (2006) Improved scoring of functional groups from gene expression data by decorrelating GO graph structure. Bioinformatics 22 (13):1600-1607. doi:10.1093/bioinformatics/btl140

Andrews S (2010) FastQC: A Quality Control Tool for High Throughput Sequence Data [Online]. Available online at: http://wwwbioinformaticsbabrahamacuk/projects/fastqc/

Anil Kumar S, Hima Kumari P, Shravan Kumar G, Mohanalatha C, Kavi Kishor PB (2015) Osmotin: a plant sentinel and a possible agonist of mammalian adiponectin. Frontiers in Plant Science 6. doi:10.3389/fpls.2015.00163

Baillie AC, Corbett JR, Dowsett JR, McCloskey P (1972) Inhibitors of shikimate dehydrogenase as potential herbicides. Pesticide Science 3 (2):113-120. doi:https://doi.org/10.1002/ps.2780030202

Beckie HJ (2020) Herbicide Resistance in Plants. Plants 9 (4):435. doi:10.3390/plants9040435

Bharamappanavara M, Siddaiah AM, Ponnuvel S, Ramappa L, Patil B, Appaiah M, Maganti SM, Sundaram RM, Shankarappa SK, Tuti MD, Banugu S, Parmar B, Rathod S, Barbadikar KM, Kota S, Subbarao LV, Mondal TK, Channappa G (2020) Mapping QTL hotspots associated with weed competitive traits in backcross population derived from Oryza sativa L. and O. glaberrima Steud. Scientific Reports 10 (1):22103. doi:10.1038/s41598-020-78675-7

Bianchet C, Wong A, Quaglia M, Alqurashi M, Gehring C, Ntoukakis V, Pasqualini S (2019) An Arabidopsis thaliana leucine-rich repeat protein harbors an adenylyl cyclase catalytic center and affects responses to pathogens. Journal of Plant Physiology 232:12-22. doi:10.1016/j.jplph.2018.10.025

Blighe K, Lun A (2019) PCAtools: PCAtools: Everything Principal Components Analysis.

Boheemen LA, Lombaert E, Nurkowski KA, Gauffre B, Rieseberg LH, Hodgins KA (2017) Multiple introductions, admixture and bridgehead invasion characterize the introduction history of Ambrosia artemisiifolia in Europe and Australia. Molecular ecology 26 (20):5421-5434. doi:10.1111/mec.14293

Bradshaw LD, Padgette SR, Kimball SL, Wells BH (1997) Perspectives on Glyphosate Resistance. Weed Technology 11 (1):189-198

Brecke B, J. , Duke WB (1980) Effect of Glyphosate on Intact Bean Plants (Phaseolus vulgaris L.) and Isolated Cells. Plant Physiology 66 (4):656-659

Bromilow RH, Chamberlain K (2000) The herbicide glyphosate and related molecules: physicochemical and structural factors determining their mobility in phloem. Pest Management Science 56 (4):368-373. doi:https://doi.org/10.1002/(SICI)1526-4998(200004)56:4<368::AID-PS153>3.0.CO;2-V

Brumos J, Robles LM, Yun J, Vu TC, Jackson S, Alonso JM, Stepanova AN (2018) Local Auxin Biosynthesis Is a Key Regulator of Plant Development. Developmental Cell 47 (3):306-318.e305. doi:https://doi.org/10.1016/j.devcel.2018.09.022

Caarls L, Pieterse CMJ, Van Wees SCM (2015) How salicylic acid takes transcriptional control over jasmonic acid signaling. Frontiers in Plant Science 6. doi:10.3389/fpls.2015.00170

Cakmak I, Yazici A, Tutus Y, Ozturk L (2009) Glyphosate reduced seed and leaf concentrations of calcium, manganese, magnesium, and iron in non-glyphosate resistant soybean. European Journal of Agronomy 31 (3):114-119. doi:https://doi.org/10.1016/j.eja.2009.07.001

Chen S, Zhou Y, Chen Y, Gu J (2018) fastp: an ultra-fast all-in-one FASTQ preprocessor. Bioinformatics 34 (17):i884-i890. doi:10.1093/bioinformatics/bty560

Cingolani P, Platts A, Wang LL, Coon M, Nguyen T, Wang L, Land SJ, Lu X, Ruden DM (2012) A program for annotating and predicting the effects of single nucleotide polymorphisms, SnpEff. Fly 6 (2):80-92. doi:10.4161/fly.19695

Conte SS, Lloyd AM (2011) Exploring multiple drug and herbicide resistance in plants—Spotlight on transporter proteins. Plant Science 180 (2):196-203. doi:https://doi.org/10.1016/j.plantsci.2010.10.015

de Freitas-Silva L, Rodríguez-Ruiz M, Houmani H, da Silva LC, Palma JM, Corpas FJ (2017) Glyphosate-induced oxidative stress in Arabidopsis thaliana affecting peroxisomal metabolism and triggers activity in the oxidative phase of the pentose phosphate pathway (OxPPP) involved in NADPH generation. Journal of Plant Physiology 218:196-205. doi:https://doi.org/10.1016/j.jplph.2017.08.007

Dill GM, CaJacob CA, Padgette SR (2008) Glyphosate-resistant crops: adoption, use and future considerations. Pest Management Science 64 (4):326-331. doi:https://doi.org/10.1002/ps.1501

Dobin A, Davis CA, Schlesinger F, Drenkow J, Zaleski C, Jha S, Batut P, Chaisson M, Gingeras TR (2013) STAR: ultrafast universal RNA-seq aligner. Bioinformatics 29 (1)

Dong H, Song Z, Liu T, Liu Z, Liu Y, Chen B, Ma Q, Li Z (2020) Causes of differences in the distribution of the invasive plants Ambrosia artemisiifolia and Ambrosia trifida in the Yili Valley, China. Ecology and Evolution 10 (23):13122-13133. doi:10.1002/ece3.6902

Duke SO (2011) Glyphosate Degradation in Glyphosate-Resistant and -Susceptible Crops and Weeds. Journal of Agricultural and Food Chemistry 59 (11):5835-5841. doi:10.1021/jf102704x

Duke SO, Powles SB (2008) Glyphosate: a once-in-a-century herbicide. Pest Management Science 64 (4):319-325. doi:https://doi.org/10.1002/ps.1518

Edgar RC (2004) MUSCLE: multiple sequence alignment with high accuracy and high throughput. Nucleic Acids Res 32 (5):1792-1797. doi:10.1093/nar/gkh340

Faus I, Zabalza A, Santiago J, Nebauer SG, Royuela M, Serrano R, Gadea J (2015) Protein kinase GCN2 mediates responses to glyphosate in Arabidopsis. BMC Plant Biology 15 (1):14. doi:10.1186/s12870-014-0378-0

Feng PCC, Chiu T, Douglas Sammons R (2003) Glyphosate efficacy is contributed by its tissue concentration and sensitivity in velvetleaf (Abutilon theophrasti). Pesticide Biochemistry and Physiology 77 (3):83-91. doi:https://doi.org/10.1016/j.pestbp.2003.08.005

Foyer CH (2018) Reactive oxygen species, oxidative signaling and the regulation of photosynthesis. Environ Exp Bot 154:134-142. doi:10.1016/j.envexpbot.2018.05.003

Franck CM, Westermann J, Boisson-Dernier A (2018) Plant Malectin-Like Receptor Kinases: From Cell Wall Integrity to Immunity and Beyond. Annual Review of Plant Biology 69 (1):301-328. doi:10.1146/annurev-arplant-042817-040557

Fuchs B, Saikkonen K, Helander M (2021) Glyphosate-Modulated Biosynthesis Driving Plant Defense and Species Interactions. Trends in Plant Science 26 (4):312-323. doi:10.1016/j.tplants.2020.11.004

Funke T, Han H, Healy-Fried ML, Fischer M, Schönbrunn E (2006) Molecular basis for the herbicide resistance of Roundup Ready crops. Proceedings of the National Academy of Sciences 103 (35):13010-13015. doi:10.1073/pnas.0603638103

Funke T, Yang Y, Han H, Healy-Fried M, Olesen S, Becker A, Schönbrunn E (2009) Structural Basis of Glyphosate Resistance Resulting from the Double Mutation Thr97 → Ile and Pro101 → Ser in 5-Enolpyruvylshikimate-3-phosphate Synthase from Escherichia coli. Journal of Biological Chemistry 284 (15):9854-9860. doi:10.1074/jbc.m809771200

Gaines TA, Duke SO, Morran S, Rigon CAG, Tranel PJ, Küpper A, Dayan FE (2020) Mechanisms of evolved herbicide resistance. Journal of Biological Chemistry 295 (30):10307-10330. doi:10.1074/jbc.rev120.013572

Gaines TA, Zhang W, Wang D, Bukun B, Chisholm ST, Shaner DL, Nissen SJ, Patzoldt WL, Tranel PJ, Culpepper AS, Grey TL, Webster TM, Vencill WK, Sammons RD, Jiang J,

Preston C, Leach JE, Westra P (2010) Gene amplification confers glyphosate resistance in Amaranthus palmeri. Proceedings of the National Academy of Sciences 107 (3):1029-1034. doi:10.1073/pnas.0906649107

Ge X, d'Avignon A, Ackerman J, Ostrander E, Sammons R (2013) Application of 31P-NMR Spectroscopy to Glyphosate Studies in Plants: Insights into Cellular Uptake and Vacuole Sequestration Correlated to Herbicide Resistance. In.

Geiger DR, Shieh W-J, Fuchs MA (1999) Causes of Self-Limited Translocation of Glyphosate in Beta vulgaris Plants. Pesticide Biochemistry and Physiology 64 (2):124-133. doi:https://doi.org/10.1006/pest.1999.2419

George Thompson AM, Iancu CV, Neet KE, Dean JV, Choe J-Y (2017) Differences in salicylic acid glucose conjugations by UGT74F1 and UGT74F2 from Arabidopsis thaliana. Scientific Reports 7 (1):46629. doi:10.1038/srep46629

Gomes MP, Juneau P (2016) Oxidative stress in duckweed (Lemna minor L.) induced by glyphosate: Is the mitochondrial electron transport chain a target of this herbicide? Environmental Pollution 218:402-409. doi:https://doi.org/10.1016/j.envpol.2016.07.019

Gomes MP, Le Manac'h SG, Maccario S, Labrecque M, Lucotte M, Juneau P (2016) Differential effects of glyphosate and aminomethylphosphonic acid (AMPA) on photosynthesis and chlorophyll metabolism in willow plants. Pesticide Biochemistry and Physiology 130:65-70. doi:https://doi.org/10.1016/j.pestbp.2015.11.010

Gomes MP, Le Manac'H SG, Hénault-Ethier L, Labrecque M, Lucotte M, Juneau P (2017) Glyphosate-Dependent Inhibition of Photosynthesis in Willow. Frontiers in Plant Science 8. doi:10.3389/fpls.2017.00207

Gomes MP, Smedbol E, Chalifour A, Hénault-Ethier L, Labrecque M, Lepage L, Lucotte M, Juneau P (2014) Alteration of plant physiology by glyphosate and its by-product aminomethylphosphonic acid: an overview. Journal of Experimental Botany 65 (17):4691-4703. doi:10.1093/jxb/eru269

Gougler JA, Geiger DR (1981) Uptake and Distribution of N-Phosphonomethylglycine in Sugar Beet Plants. Plant Physiology 68 (3):668-672. doi:10.1104/pp.68.3.668

Grabherr MG, Haas BJ, Yassour M, Levin JZ, Thompson DA, Amit I, Adiconis X, Fan L, Raychowdhury R, Zeng Q, Chen Z, Mauceli E, Hacohen N, Gnirke A, Rhind N, Di Palma F, Birren BW, Nusbaum C, Lindblad-Toh K, Friedman N, Regev A (2011) Full-length transcriptome assembly from RNA-Seq data without a reference genome. Nature Biotechnology 29 (7):644-652. doi:10.1038/nbt.1883

Griffiths G (2020) Jasmonates: biosynthesis, perception and signal transduction. Essays in Biochemistry 64 (3):501-512. doi:10.1042/ebc20190085

Harre NT, Johnson WG, Nie H, Robertson RR, Weller SC, Young BG (2017) Distribution of Herbicide-Resistant Giant Ragweed (Ambrosia trifida) in Indiana and Characterization of

Distinct Glyphosate-Resistant Biotypes. Weed Science 65 (6):699-709. doi:10.1017/wsc.2017.56

He C, Holme J, Anthony J (2014) SNP genotyping: the KASP assay. Methods Mol Biol 1145:75-86. doi:10.1007/978-1-4939-0446-4_7

Healy-Fried ML, Funke T, Priestman MA, Han H, Schönbrunn E (2007) Structural Basis of Glyphosate Tolerance Resulting from Mutations of Pro101 in Escherichia coli 5-Enolpyruvylshikimate-3-phosphate Synthase. Journal of Biological Chemistry 282 (45):32949-32955. doi:10.1074/jbc.m705624200

Heap I (2023) The International Survey of Herbicide Resistant Weeds. Accessed 10/17/2023

Herrmann KM, Weaver LM (1999) THE SHIKIMATE PATHWAY. Annual Review of Plant Physiology and Plant Molecular Biology 50 (1):473-503. doi:10.1146/annurev.arplant.50.1.473

Holländer H, Amrhein N (1980) The Site of the Inhibition of the Shikimate Pathway by Glyphosate: I. Inhibition by Glyphosate of Phenylpropanoid Synthesis in Buckwheat (Fagopyrum esculentum Moench). Plant Physiology 66 (5):823-829

Hong G, Zhang W, Li H, Shen X, Guo Z (2014) Separate enrichment analysis of pathways for up- and downregulated genes. Journal of The Royal Society Interface 11 (92):20130950. doi:10.1098/rsif.2013.0950

Huang S, Van Aken O, Schwarzländer M, Belt K, Millar AH (2016) The Roles of Mitochondrial Reactive Oxygen Species in Cellular Signaling and Stress Response in Plants. Plant Physiology 171 (3):1551-1559. doi:10.1104/pp.16.00166

Institute B Picard Tools. http://broadinstitute.github.io/picard/.

Ivanov B, Borisova-Mubarakshina M, Vilyanen D, Vetoshkina D, Kozuleva M (2022) Cooperative pathway of O(2) reduction to H(2)O(2) in chloroplast thylakoid membrane: new insight into the Mehler reaction. Biophys Rev 14 (4):857-869. doi:10.1007/s12551-022-00980-4

Janků, Luhová, Petřivalský (2019) On the Origin and Fate of Reactive Oxygen Species in Plant Cell Compartments. Antioxidants 8 (4):105. doi:10.3390/antiox8040105

Jaworski EG (1972) Mode of action of N-phosphonomethylglycine. Inhibition of aromatic amino acid biosynthsis. Journal of Agricultural and Food Chemistry 20 (6):1195-1198. doi:10.1021/jf60184a057

Jugulam M, Niehues K, Godar AS, Koo DH, Danilova T, Friebe B, Sehgal S, Varanasi VK, Wiersma A, Westra P, Stahlman PW, Gill BS (2014) Tandem Amplification of a Chromosomal Segment Harboring 5-Enolpyruvylshikimate-3-Phosphate Synthase Locus Confers Glyphosate Resistance in Kochia scoparia. PLANT PHYSIOLOGY 166 (3):1200-1207. doi:10.1104/pp.114.242826

Kanissery R, Gairhe B, Kadyampakeni D, Batuman O, Alferez F (2019) Glyphosate: Its Environmental Persistence and Impact on Crop Health and Nutrition. Plants 8 (11):499. doi:10.3390/plants8110499

Kerr ID, Haider AJ, Gelissen IC (2011) The ABCG family of membrane-associated transporters: you don't have to be big to be mighty. British Journal of Pharmacology 164 (7):1767-1779. doi:10.1111/j.1476-5381.2010.01177.x

Kim D, Paggi JM, Park C, Bennett C, Salzberg SL (2019) Graph-based genome alignment and genotyping with HISAT2 and HISAT-genotype. Nature Biotechnology 37 (8):907-915. doi:10.1038/s41587-019-0201-4

Kitchen LM, Witt WW, Rieck CE (1981) Inhibition of δ-Aminolevulinic Acid Synthesis by Glyphosate. Weed Science 29 (5):571-577. doi:10.1017/S004317450006375X

Kolde R (2019) pheatmap: Pretty Heatmaps. R package version 1.0.12

Koo D-H, Sathishraj R, Nakka S, Ju Y, Nandula VK, Jugulam M, Friebe B, Gill BS (2023) Extrachromosomal circular DNA–mediated spread of herbicide resistance in interspecific hybrids of pigweed. Plant Physiology 193 (1):229-233. doi:10.1093/plphys/kiad281

Küpper A, Borgato E, Patterson E, Netto A, Nicolai M, de Carvalho S, Nissen S, Gaines T, Christoffoleti P (2017) Multiple Resistance to Glyphosate and Acetolactate Synthase Inhibitors in Palmer Amaranth (Amaranthus palmeri) Identified in Brazil. Weed Science 65 (3):317-326. doi:10.1017/wsc.2017.1

Law CW, Chen Y, Shi W, Smyth GK (2014) voom: precision weights unlock linear model analysis tools for RNA-seq read counts. Genome Biology 15 (2):R29. doi:10.1186/gb-2014-15-2-r29

Lee MH, Jeon HS, Kim HG, Park OK (2017) An Arabidopsis NAC transcription factor NAC4 promotes pathogen-induced cell death under negative regulation by microRNA164. New Phytologist 214 (1):343-360. doi:10.1111/nph.14371

Leon RG, Dunne JC, Gould F (2021) The role of population and quantitative genetics and modern sequencing technologies to understand evolved herbicide resistance and weed fitness. Pest Management Science 77 (1):12-21. doi:10.1002/ps.5988

Leonelli L, Pelton J, Schoeffler A, Dahlbeck D, Berger J, Wemmer DE, Staskawicz B (2011) Structural Elucidation and Functional Characterization of the Hyaloperonospora arabidopsidis Effector Protein ATR13. PLoS Pathogens 7 (12):e1002428. doi:10.1371/journal.ppat.1002428

Lespérance MA (2015) Programmed cell death and altered translocation cause glyphosate resistance in giant ragweed (Ambrosia trifida L.). University of Guelph

Li H (2013) Aligning sequence reads, clone sequences and assembly contigs with BWA-MEM. arXiv:13033997v2

Li H, Handsaker B, Wysoker A, Fennell T, Ruan J, Homer N, Marth G, Abecasis G, Durbin R (2009) The Sequence Alignment/Map format and SAMtools. Bioinformatics 25 (16):2078-2079. doi:10.1093/bioinformatics/btp352

Liao Y, Smyth GK, Shi W (2013) featureCounts: an efficient general purpose program for assigning sequence reads to genomic features. Bioinformatics 30 (7):923-930. doi:10.1093/bioinformatics/btt656

Liu H, Ravichandran S, Teh O-K, McVey S, Lilley C, Teresinski HJ, Gonzalez-Ferrer C, Mullen RT, Hofius D, Prithiviraj B, Stone SL (2017) The RING-Type E3 Ligase XBAT35.2 Is Involved in Cell Death Induction and Pathogen Response. Plant Physiology 175 (3):1469-1483. doi:10.1104/pp.17.01071

Liu L, Sonbol F-M, Huot B, Gu Y, Withers J, Mwimba M, Yao J, He SY, Dong X (2016) Salicylic acid receptors activate jasmonic acid signalling through a non-canonical pathway to promote effector-triggered immunity. Nature Communications 7 (1):13099. doi:10.1038/ncomms13099

Liu Y, Qi X, Gealy DR, Olsen KM, Caicedo AL, Jia Y (2015) QTL Analysis for Resistance to Blast Disease in U.S. Weedy Rice. Molecular Plant-Microbe Interactions® 28 (7):834-844. doi:10.1094/mpmi-12-14-0386-r

Lu L, Liu JB, Wang JQ, Lian CY, Wang ZY, Wang L (2022) Glyphosate-induced mitochondrial reactive oxygen species overproduction activates parkin-dependent mitophagy to inhibit testosterone synthesis in mouse leydig cells. Environ Pollut 314:120314. doi:10.1016/j.envpol.2022.120314

Lv Z, Zhao M, Wang W, Wang Q, Huang M, Li C, Lian Q, Xia J, Qi J, Xiang C (2021) Changing Gly311 to an acidic amino acid in the MATE family protein DTX6 enhances Arabidopsis resistance to the dihydropyridine herbicides. Molecular Plant 14 (12):2115-2125

Majeed A, Johar P, Raina A, Salgotra RK, Feng X, Bhat JA (2022) Harnessing the potential of bulk segregant analysis sequencing and its related approaches in crop breeding. Front Genet 13:944501. doi:10.3389/fgene.2022.944501

Mansfeld BN, Grumet R (2018) QTLseqr: An R Package for Bulk Segregant Analysis with Next-Generation Sequencing. The Plant Genome 11 (2):180006. doi:https://doi.org/10.3835/plantgenome2018.01.0006

Massonnet M, Vondras AM, Cochetel N, Riaz S, Pap D, Minio A, Figueroa-Balderas R, Walker MA, Cantu D (2022) Haplotype-resolved powdery mildew resistance loci reveal the impact of heterozygous structural variation on NLR genes in Muscadinia rotundifolia. G3 Genes|Genomes|Genetics 12 (8). doi:10.1093/g3journal/jkac148

McElroy JS, Hall ND (2020) *Echinochloa colona* with reported resistance to glyphosate conferred by aldo-keto reductase also contains a Pro-106-Thr *EPSPS* target-site mutation. Plant Physiol 183:447-450

Mittler R (2017) ROS Are Good. Trends Plant Sci 22 (1):11-19. doi:10.1016/j.tplants.2016.08.002

Moeder W, Ung H, Mosher S, Yoshioka K (2010) SA-ABA antagonism in defense responses. Plant Signaling & Behavior 5 (10):1231-1233. doi:10.4161/psb.5.10.12836

Molin WT, Wright AA, Lawton-Rauh A, Saski CA (2017) The unique genomic landscape surrounding the EPSPS gene in glyphosate resistant Amaranthus palmeri: a repetitive path to resistance. BMC Genomics 18 (1). doi:10.1186/s12864-016-3336-4

Molin WT, Yaguchi A, Blenner M, Saski CA (2020) The EccDNA Replicon: A Heritable, Extranuclear Vehicle That Enables Gene Amplification and Glyphosate Resistance in Amaranthus palmeri[OPEN]. The Plant cell 32 (7):2132-2140. doi:10.1105/tpc.20.00099

Montgomery JS, Morran S, MacGregor DR, McElroy JS, Neve P, Neto C, Vila-Aiub MM, Sandoval MV, Menéndez AI, Kreiner JM, Fan L, Caicedo AL, Maughan PJ, Martins BAB, Mika J, Collavo A, Aldo Merotto J, Subramanian NK, Bagavathiannan MV, Cutti L, Islam MM, Gill BS, Cicchillo R, Gast R, Soni N, Wright TR, Zastrow-Hayes G, May G, Malone JM, Sehgal D, Kaundun SS, Dale RP, Vorster BJ, Peters B, Lerchl J, Tranel PJ, Beffa R, Jugulam M, Fengler K, Llaca V, Patterson EL, Gaines T (2023) The International Weed Genomics Consortium: Community Resources for Weed Genomics Research. bioRxiv:2023.2007.2019.549613. doi:10.1101/2023.07.19.549613

Moretti ML, Alárcon-Reverte R, Pearce S, Morran S, Hanson BD (2017) Transcription of putative tonoplast transporters in response to glyphosate and paraquat stress in Conyza bonariensis and Conyza canadensis and selection of reference genes for qRT-PCR. PLOS ONE 12 (7):e0180794. doi:10.1371/journal.pone.0180794

Moretti ML, Van Horn CR, Robertson R, Segobye K, Weller SC, Young BG, Johnson WG, Douglas Sammons R, Wang D, Ge X, d' Avignon A, Gaines TA, Westra P, Green AC, Jeffery T, Lespérance MA, Tardif FJ, Sikkema PH, Christopher Hall J, McLean MD, Lawton MB, Schulz B (2018) Glyphosate resistance in Ambrosia trifida: Part 2. Rapid response physiology and non-target-site resistance: Glyphosate resistance in Ambrosia trifida: Part 2. Pest management science 74 (5):1079-1088. doi:10.1002/ps.4569

Muñoz-Rueda A, Gonzalez-Murua C, Becerril JM, Sánchez-Díaz MF (1986) Effects of glyphosate [N-(phosphonomethyl)glycine] on photosynthetic pigments, stomatal response and photosynthetic electron transport in Medicago sativa and Trifolium pratense. Physiologia Plantarum 66 (1):63-68. doi:https://doi.org/10.1111/j.1399-3054.1986.tb01234.x

Murphy BP, Beffa R, Tranel PJ (2021) Genetic architecture underlying HPPD-inhibitor resistance in a Nebraska Amaranthus tuberculatus population. Pest Manag Sci 77 (11):4884-4891. doi:10.1002/ps.6560

Norma Francenia S-S, Raúl S-C, Beatriz H-C, Claudia V-C (2019) Shikimic Acid Pathway in Biosynthesis of Phenolic Compounds. In: Marcos S-H, Rosario G-M, Mariana P-T (eds)

Plant Physiological Aspects of Phenolic Compounds. IntechOpen, Rijeka, p Ch. 3. doi:10.5772/intechopen.83815

Oliveros JC (2015) Venny. An interactive tool for comparing lists with Venn's diagrams. https://bioinfogp.cnb.csic.es/tools/venny/index.html.

Orcaray L, Zulet A, Zabalza A, Royuela M (2012) Impairment of carbon metabolism induced by the herbicide glyphosate. Journal of Plant Physiology 169 (1):27-33. doi:10.1016/j.jplph.2011.08.009

Page ER, Martin S, Meloche S, Thibodeau A, Nurse RE, Sikkema PH, Tardif FJ, Cowbrough MJ, Laforest M (2024) Revisiting the origins of glyphosate-resistant giant ragweed (Ambrosia trifida L.) in Canada. Canadian Journal of Plant Science 0 (0):null. doi:10.1139/cjps-2023-0145

Pan L, Yu Q, Han H, Mao L, Nyporko A, Fan L, Bai L, Powles S (2019a) Aldo-keto Reductase Metabolizes Glyphosate and Confers Glyphosate Resistance in Echinochloa colona. Plant Physiology 181 (4):1519-1534. doi:10.1104/pp.19.00979

Pan L, Yu Q, Han H, Mao L, Nyporko A, Fan L, Bai L, Powles S (2019b) Aldo-keto Reductase Metabolizes Glyphosate and Confers Glyphosate Resistance in Echinochloa colona. Plant Physiology 181 (4):1519-1534. doi:10.1104/pp.19.00979

Pan L, Yu Q, Wang J, Han H, Mao L, Nyporko A, Maguza A, Fan L, Bai L, Powles S (2021) An ABCC-type transporter endowing glyphosate resistance in plants. Proceedings of the National Academy of Sciences 118 (16):e2100136118. doi:10.1073/pnas.2100136118

Patterson EL, Pettinga DJ, Ravet K, Neve P, Gaines TA (2018) Glyphosate Resistance and EPSPS Gene Duplication: Convergent Evolution in Multiple Plant Species. Journal of Heredity 109 (2):117-125. doi:10.1093/jhered/esx087

Patterson EL, Saski CA, Sloan DB, Tranel PJ, Westra P, Gaines TA (2019) The Draft Genome of Kochia scoparia and the Mechanism of Glyphosate Resistance via Transposon-Mediated EPSPS Tandem Gene Duplication. Genome Biology and Evolution 11 (10):2927-2940. doi:10.1093/gbe/evz198

Pearson K (1901) LIII. On lines and planes of closest fit to systems of points in space. The London, Edinburgh, and Dublin Philosophical Magazine and Journal of Science 2 (11):559-572. doi:10.1080/14786440109462720

Penning TM (2015) The aldo-keto reductases (AKRs): Overview. Chemico-Biological Interactions 234:236-246. doi:10.1016/j.cbi.2014.09.024

Pereira FCM, Tayengwa R, Alves PLDCA, Peer WA (2019) Phosphate Status Affects Phosphate Transporter Expression and Glyphosate Uptake and Transport in Grand Eucalyptus (Eucalyptus grandis). Weed Science 67 (1):29-40. doi:10.1017/wsc.2018.58

Piasecki C, Yang Y, Benemann DP, Kremer FS, Galli V, Millwood RJ, Cechin J, Agostinetto D, Maia LC, Vargas L, Stewart CN (2019) Transcriptomic Analysis Identifies New Non-Target Site Glyphosate-Resistance Genes in Conyza bonariensis. Plants 8 (6):157. doi:10.3390/plants8060157

Pizzul L, Castillo MdP, Stenström J (2009) Degradation of glyphosate and other pesticides by ligninolytic enzymes. Biodegradation 20 (6):751-759. doi:10.1007/s10532-009-9263-1

Pospíšil P (2016) Production of Reactive Oxygen Species by Photosystem II as a Response to Light and Temperature Stress. Frontiers in Plant Science 7. doi:10.3389/fpls.2016.01950

Powles SB (2008) Evolved glyphosate-resistant weeds around the world: lessons to be learnt. Pest Management Science 64 (4):360-365. doi:https://doi.org/10.1002/ps.1525

Powles SB, Debrah FL-C, James JD, Preston C (1998) Evolved Resistance to Glyphosate in Rigid Ryegrass (Lolium rigidum) in Australia. Weed Science 46 (5):604-607

Quarrie SA, Lazić-Jančić V, Kovačević D, Steed A, Pekić S (1999) Bulk segregant analysis with molecular markers and its use for improving drought resistance in maize. Journal of Experimental Botany 50 (337):1299-1306

Reddy KN, Rimando AM, Duke SO, Nandula VK (2008) Aminomethylphosphonic Acid Accumulation in Plant Species Treated with Glyphosate. Journal of Agricultural and Food Chemistry 56 (6):2125-2130. doi:10.1021/jf072954f

Rhoads DM, Umbach AL, Subbaiah CC, Siedow JN (2006) Mitochondrial Reactive Oxygen Species. Contribution to Oxidative Stress and Interorganellar Signaling. Plant Physiology 141 (2):357-366. doi:10.1104/pp.106.079129

Richard EP, Goss JR, Arntzen CJ (1979) Glyphosate Does Not Inhibit Photosynthetic Electron Transport and Phosphorylation in Pea (Pisum sativum) Chloroplasts. Weed Science 27 (6):684-688

Ritchie ME, Phipson B, Wu D, Hu Y, Law CW, Shi W, Smyth GK (2015) limma powers differential expression analyses for RNA-sequencing and microarray studies. Nucleic Acids Research 43 (7):e47-e47. doi:10.1093/nar/gkv007

Robinson MD, Oshlack A (2010) A scaling normalization method for differential expression analysis of RNA-seq data. Genome Biology 11 (3):R25. doi:10.1186/gb-2010-11-3-r25

Ruas CF, Fairbanks DJ, Evans RP, Stutz HC, Andersen WR, Ruas PM (1998) Male-Specific DNA in the Dioecious Species Atriplex garrettii (Chenopodiaceae). American Journal of Botany 85 (2):162-167. doi:10.2307/2446304

Sammons RD, Gaines TA (2014) Glyphosate resistance: state of knowledge. Pest Management Science 70 (9):1367-1377. doi:10.1002/ps.3743

Sandmann G, Römer S, Fraser PD (2006) Understanding carotenoid metabolism as a necessity for genetic engineering of crop plants. Metabolic Engineering 8 (4):291-302. doi:https://doi.org/10.1016/j.ymben.2006.01.005

Santner A, Estelle M (2007) The JAZ Proteins Link Jasmonate Perception with Transcriptional Changes. The Plant Cell 19 (12):3839-3842. doi:10.1105/tpc.107.056960

Schönbrunn E, Eschenburg S, Shuttleworth WA, Schloss JV, Amrhein N, Evans JNS, Kabsch W (2001) Interaction of the herbicide glyphosate with its target enzyme 5-enolpyruvylshikimate 3-phosphate synthase in atomic detail. Proceedings of the National Academy of Sciences 98 (4):1376-1380. doi:10.1073/pnas.98.4.1376

Servaites JC, Tucci MA, Geiger DR (1987) Glyphosate Effects on Carbon Assimilation, Ribulose Bisphosphate Carboxylase Activity, and Metabolite Levels in Sugar Beet Leaves. Plant Physiology 85 (2):370-374. doi:10.1104/pp.85.2.370

Shaner DL (2009) Role of Translocation as A Mechanism of Resistance to Glyphosate. Weed Science 57 (1):118-123. doi:10.1614/WS-08-050.1

Shaner DL, Lyon JL (1979) Somatal cycling in Phaseolus vulgaris L. In response to glyphosate. Plant Science Letters 15 (1):83-87. doi:https://doi.org/10.1016/0304-4211(79)90098-1

Siehl D (1997) Inhibitors of EPSP synthase, glutamine synthetase and histidine synthesis. 1:37-67

Simpson PJ, Tantitadapitak C, Reed AM, Mather OC, Bunce CM, White SA, Ride JP (2009) Characterization of Two Novel Aldo–Keto Reductases from Arabidopsis: Expression Patterns, Broad Substrate Specificity, and an Open Active-Site Structure Suggest a Role in Toxicant Metabolism Following Stress. Journal of Molecular Biology 392 (2):465-480. doi:https://doi.org/10.1016/j.jmb.2009.07.023

Sprankle P, F. Meggitt W, Penner D (1975) Absorption, Action, and Translocation of Glyphosate. Weed Science 23 (3):235-240

Steinrücken HC, Amrhein N (1980) The herbicide glyphosate is a potent inhibitor of 5-enolpyruvylshikimic acid-3-phosphate synthase. Biochemical and Biophysical Research Communications 94 (4):1207-1212. doi:https://doi.org/10.1016/0006-291X(80)90547-1

Steinrücken HC, Amrhein N (1984) 5-Enolpyruvylshikimate-3-phosphate synthase of Klebsiella pneumoniae. European Journal of Biochemistry 143 (2):351-357. doi:10.1111/j.1432-1033.1984.tb08379.x

Stone SL (2022) Ubiquitin ligases at the nexus of plant responses to biotic and abiotic stresses. Essays Biochem 66 (2):123-133. doi:10.1042/ebc20210070

Takano HK, Patterson EL, Nissen SJ, Dayan FE, Gaines TA (2019) Predicting herbicide movement across semi-permeable membranes using three phase partitioning. Pestic Biochem Physiol 159:22-26. doi:10.1016/j.pestbp.2019.05.009

Tani E, Chachalis D, Travlos IS (2015) A Glyphosate Resistance Mechanism in Conyza canadensis Involves Synchronization of EPSPS and ABC-transporter Genes. Plant Molecular Biology Reporter 33 (6):1721-1730. doi:10.1007/s11105-015-0868-8

Team R (2020) RStudio: Integrated Development for R. RStudio, PBC, Boston, MA

Tola AJ, Jaballi A, Missihoun TD (2021) Protein Carbonylation: Emerging Roles in Plant Redox Biology and Future Prospects. Plants 10 (7):1451. doi:10.3390/plants10071451

Traxler C, Gaines TA, Küpper A, Luemmen P, Dayan FE (2023) The nexus between reactive oxygen species and the mechanism of action of herbicides. Journal of Biological Chemistry 299 (11):105267. doi:10.1016/j.jbc.2023.105267

Tzin V, Galili G (2010) New Insights into the Shikimate and Aromatic Amino Acids Biosynthesis Pathways in Plants. Molecular Plant 3 (6):956-972. doi:https://doi.org/10.1093/mp/ssq048

Ullah C, Chen Y-H, Ortega MA, Tsai C-J (2023) The diversity of salicylic acid biosynthesis and defense signaling in plants: Knowledge gaps and future opportunities. Current Opinion in Plant Biology 72:102349. doi:https://doi.org/10.1016/j.pbi.2023.102349

Van der Auwera GA, O'Connor BD (2020) Genomics in the Cloud: Using Docker, GATK, and WDL in Terra (1st Edition). O'Reilly Media,

Van Horn CR, Moretti ML, Robertson RR, Segobye K, Weller SC, Young BG, Johnson WG, Schulz B, Green AC, Jeffery T, Lesperance M, Tardif F, Sikkema P, Hall JC, McLean M, Lawton M, Sammons RD, Gaines T (2018) Glyphosate resistance in *Ambrosia trifida*: Part 1. Novel rapid cell death response to glyphosate. Pest Manage Sci 74:1071-1078

Van Rensen JJS (1974) Effects of N-(phosphonomethyl)glycine on photosynthetic reactions in Scenedesmus and in isolated spinach chIoroplast. M Avron, ed Proceedings of the Third International Congress on Photosynthesis Elsevier Scientific Pub Co, Amsterdam:683-687

Vivancos PD, Driscoll SP, Bulman CA, Ying L, Emami K, Treumann A, Mauve C, Noctor G, Foyer CH (2011) Perturbations of Amino Acid Metabolism Associated with Glyphosate-Dependent Inhibition of Shikimic Acid Metabolism Affect Cellular Redox Homeostasis and Alter the Abundance of Proteins Involved in Photosynthesis and Photorespiration. Plant Physiology 157 (1):256-268. doi:10.1104/pp.111.181024

Westwood J, Biesboer D (1985) The influence of glyphosate on endogenous levels of free IAA and phenolic compounds in leafy spurge. Leafy Spurge Symposium Bozeman, MT, pp 5–13

Williams SJ, Yin L, Foley G, Casey LW, Outram MA, Ericsson DJ, Lu J, Boden M, Dry IB, Kobe B (2016) Structure and Function of the TIR Domain from the Grape NLR Protein RPV1. Frontiers in Plant Science 7. doi:10.3389/fpls.2016.01850

Wright AA, Rodriguez-Carres M, Sasidharan R, Koski L, Peterson DG, Nandula VK, Ray JD, Bond JA, Shaw DR (2018) Multiple Herbicide–Resistant Junglerice (Echinochloa colona): Identification of Genes Potentially Involved in Resistance through Differential Gene Expression Analysis. Weed Science 66 (3):347-354. doi:10.1017/wsc.2018.10

Wu J, Zhu W, Zhao Q (2023) Salicylic acid biosynthesis is not from phenylalanine in Arabidopsis. Journal of Integrative Plant Biology 65 (4):881-887. doi:10.1111/jipb.13410

Xie Z, Nolan TM, Jiang H, Yin Y (2019) AP2/ERF Transcription Factor Regulatory Networks in Hormone and Abiotic Stress Responses in Arabidopsis. Frontiers in Plant Science 10. doi:10.3389/fpls.2019.00228

Yan J, Yao R, Chen L, Li S, Gu M, Nan F, Xie D (2018) Dynamic Perception of Jasmonates by the F-Box Protein COI1. Molecular Plant 11 (10):1237-1247. doi:10.1016/j.molp.2018.07.007

Yang Y, Gardner C, Gupta P, Peng Y, Piasecki C, Millwood RJ, Ahn T-H, Stewart CN (2021) Novel Candidate Genes Differentially Expressed in Glyphosate-Treated Horseweed (Conyza canadensis). Genes 12 (10):1616. doi:10.3390/genes12101616

Yuan P, Tanaka K, Poovaiah BW (2022) Calcium/Calmodulin-Mediated Defense Signaling: What Is Looming on the Horizon for AtSR1/CAMTA3-Mediated Signaling in Plant Immunity. Frontiers in Plant Science 12. doi:10.3389/fpls.2021.795353

Zhang C, Feng L, He T-t, Yang C-h, Chen G-q, Tian X-s (2015) Investigating the mechanisms of glyphosate resistance in goosegrass (Eleusine indica) population from South China. Journal of Integrative Agriculture 14 (5):909-918. doi:https://doi.org/10.1016/S2095-3119(14)60890-X

Zhang C, Feng L, Tian XS (2018) Alterations in the 5' untranslated region of the 5-enolpyruvylshikimate-3-phosphate synthase (EPSPS) gene influence EPSPS overexpression in glyphosate-resistant Eleusine indica. Pest Manag Sci 74 (11):2561-2568. doi:10.1002/ps.5042

Zhang C, Yu C-j, Zhang T-j, Guo W-l, Tian X-s (2021) Transcriptomic analysis reveals the transcription factors involved in regulating the expression of EPSPS gene, which confers glyphosate resistance of goosegrass (Eleusine indica). Journal of Integrative Agriculture 20 (8):2180-2194. doi:https://doi.org/10.1016/S2095-3119(21)63682-1